

Aus dem Lehrstuhl für Zellbiologie (Anatomie III)
am Biomedizinischen Centrum (BMC) München
Leitung: Prof. Dr. rer. nat. Michael Kiebler

**The role of the RNA-binding protein Staufen2 and the effects
of physical activity on adult hippocampal neurogenesis**

Dissertation
zum Erwerb des Doktorgrades der Medizin
an der Medizinischen Fakultät der
Ludwig-Maximilians-Universität zu München

vorgelegt von
Surina Alisha Louisa Frey

aus
München
2021

Mit Genehmigung der Medizinischen Fakultät
der Universität München

Berichterstatter: Prof. Dr. rer. nat. Michael A. Kiebler

Mitberichterstatter: Prof. Dr. Dominik Paquet

PD Dr. Svetlana Sirko

Mitbetreuung durch den
promovierten Mitarbeiter: Dr. med. vet. Bastian Popper

Dekan: Prof. Dr. med. dent. Reinhard Hickel

Tag der mündlichen Prüfung: 22.04.2021

Teilergebnisse der vorliegenden Arbeit wurden veröffentlicht in:

Frey S*, Schieweck R*, Forné I, Imhof A, Straub T, Popper B, Kiebler MA.

Physical Activity Dynamically Regulates the Hippocampal Proteome along the

Dorso-Ventral Axis. *International Journal of Molecular Sciences*. 2020;

21(10):3501. <https://www.mdpi.com/1422-0067/21/10/3501>

*These authors contributed equally to this work.

Copyright Notice: Open access article distributed under the Creative Commons

Attribution (CCBY) License (<https://creativecommons.org/licenses/by/4.0/>)

Table of Content

1	Summary	1
2	Zusammenfassung	3
3	Introduction	5
3.1	RNA-binding proteins.....	5
3.1.1	Overview	5
3.1.2	Pumilio2.....	5
3.1.3	Staufen2.....	6
3.2	Adult neurogenesis in mice.....	7
3.2.1	Localization and process.....	7
3.2.2	New neurons with new characteristics	9
3.2.3	The functional role of the dentate gyrus and adult-born neurons	10
3.2.4	Involvement of glial cells	10
3.2.5	Adult neurogenesis in the human hippocampus	11
3.3	Involvement of adult neurogenesis in neuropsychiatric disorders	12
4	Statement of purpose	13
5	Material and Methods	14
5.1	Materials	14
5.1.1	Buffers and solutions	14
5.1.2	Antibodies for immunohistochemistry	14
5.1.3	Equipment for microdissection.....	15
5.1.4	Mass spectrometry preparation kit.....	15
5.2	Animals.....	16
5.2.1	Wild-type mice	16
5.2.2	Glia-labeled mice.....	16
5.2.3	Stau2 ^{GT} mice	16
5.3	Activity-dependent neurogenesis	16
5.4	Immunohistochemistry.....	19
5.4.1	Tissue preparation.....	19
5.4.2	Selection of representative slices.....	19
5.4.3	Immunostaining	20
5.4.3.1	Marker for Staufen2	20
5.4.3.2	Proliferation markers.....	20
5.4.3.3	Glial markers.....	20
5.4.3.4	Neuronal markers	20
5.4.4	Confocal microscopy	21
5.4.5	Quantification of DCX-stained cell bodies and dendrites	22
5.5	Microdissection.....	22
5.5.1	Tissue preparation.....	22
5.5.2	Dissection using stereo microscopy.....	23
5.6	LC Mass spectrometry	24

5.6.1	Tissue preparation and processing.....	24
5.6.2	Data analysis.....	25
5.7	Statistical analysis.....	26
6	Results.....	27
6.1	Cell proliferation and astrocytes in naive WT and Stau2 ^{GT} mice	27
6.2	Enhanced physical activity selectively impacts neurogenesis in the hippocampus	29
6.2.1	Activity-enhanced neurogenesis is limited in dorsal hippocampus	30
6.2.2	Activity-enhanced neurogenesis is increased in ventral hippocampus.....	33
6.3	The role of Stau2 in activity-dependent adult neurogenesis	37
6.3.1	Expression of Stau2 in glial-labeled hippocampus.....	37
6.3.2	No effects on activity-enhanced neurogenesis in dorsal hippocampus of Stau2 ^{GT} mice	39
6.3.3	Limited effects on activity-enhanced neurogenesis in ventral hippocampus of Stau2 ^{GT} mice.....	41
6.4	Enhanced physical activity conveys proteomic alterations in the hippocampus.....	44
6.4.1	Hippocampal proteome analysis.....	44
6.4.1.1	Upregulated proteins	46
6.4.1.2	Downregulated proteins	47
6.4.1.3	Upregulated proteins with role in either neuronal, apoptotic or proliferative processes or locomotory behavior	48
6.4.2	Hippocampal subregion proteome analysis	50
6.4.2.1	Changes in the dorsal hippocampus	50
6.4.2.2	Subregion-specific proteome in the dorsal hippocampus.....	51
6.4.2.3	Changes in the ventral hippocampus.....	55
6.4.2.4	Subregion-specific proteome in the ventral hippocampus	56
7	Discussion	60
7.1	Differential effects of enhanced physical activity on dorsal and ventral hippocampus.....	60
7.2	Metabolic enzymes as main drivers of activity-enhanced alterations in the hippocampal proteome.....	63
7.3	Actin cytoskeleton as a crucial process during EPA.....	65
7.4	Stau2 is necessary for activity-enhanced adult neurogenesis.....	66
7.5	Activity-enhanced adult neurogenesis and neurodegenerative diseases – an outlook	67
	References.....	69
	List of abbreviations.....	89
	List of figures	90
	List of tables	94
	Danksagung.....	95
	Eidesstattliche Erklärung	96

1 Summary

Adult neurogenesis is a complex process, describing the generation of newly born, immature neurons in the mature, adult brain and has yet only been described in two specific brain regions: the subventricular zone and the dentate gyrus (DG) of hippocampus. This neuronal process is currently in the limelight of molecular research, as adult hippocampal neurogenesis has been associated with cognition and its impairment with the appearance of neurodegenerative disorders. Staufen2 (Stau2) is a RNA-binding protein, required for the differentiation of neurons during embryonal neurogenesis. In mice, adult hippocampal neurogenesis can be induced by voluntary physical activity through the use of running wheels. As the hippocampus represents a highly complex brain structure, it remains unclear to what extent the hippocampus possesses distinct functional regions. Recent studies postulate that the dorsal and ventral parts of the hippocampus are involved in different pathways for spatial learning and emotional behavior and furthermore the hippocampal subregions express different transcriptomes.

This research project investigates, whether enhanced physical activity induces adult neurogenesis, and whether there are differences between dorsal and ventral hippocampus. Here, the absolute number of immature neurons and its dendritic arborization was evaluated. As Stau2 plays a role during embryonic neurogenesis, the question whether the process of activity-dependent adult neurogenesis is impaired in Stau2-deficient mice has also been evaluated. Lastly, this project explored if the hippocampal proteome changes upon enhanced physical activity, and if there are differences in the dorsal and ventral hippocampus and in their different subregions, the DG, CA3- and CA1-region.

These scientific issues were explored using two distinct experimental setups: an immunohistochemical approach followed by quantification, and micro-dissection and consecutive label-free mass spectrometry.

Two different mice types were used for the immunohistochemical experiments: wild-type (WT) and Stau2^{GT} mice. The control groups contained adult, 10-week-old mice. The test groups were adult 13 weeks old, as they were additionally exposed to running wheels over a period of three weeks for voluntary use. The newly-born hippocampal neurons were stained with Doublecortin (DCX), a valid marker for immature neurons. Here, the absolute number of DCX-positive cell bodies, the number of primary and secondary dendrites, as well as their mean length were manually quantified. The dorsal and ventral parts of the hippocampus were separately investigated.

The micro-dissection and consecutive mass spectrometric protein analysis were conducted using only WT mice. The same aforementioned experimental setup was applied with a 10-week-old control group without running wheels and a 13-week-old test group with access to running wheels for voluntary use over a period of three weeks. The dorsal and ventral parts of the hippocampus, as well as their subregions (DG, CA3 and CA1) were analyzed

separately. Therefore 10 mice with each 2 hippocampal parts and each 3 sub-regions were distinctly manually dissected, leading to 60 samples in total that were further processed in mass spectrometry. Subsequently, the extensive proteome data set of the test group was compared to the control group and additionally, their dorsal to ventral parts and its subregions to each other. The proteins were further researched by studying their molecular functions, biological processes and pathways in which the proteins are implicated.

The DCX quantification of WT mice revealed that the dorsal and ventral hippocampus react differently upon enhanced physical activity (EPA). Only in the ventral DG the number of immature neurons as well as their primary and secondary dendrites increased upon EPA. The mean length of primary and secondary dendrites was augmented in both dorsal and ventral regions.

In *Stau2*-deficient mice neither the dorsal nor the ventral hippocampus showed a significant change in the number of newly-generated neurons and dendrites. The mean dendritic length was only augmented in ventral DG upon EPA.

The protein analysis by mass spectrometry demonstrated that upon activity-dependent adult neurogenesis, there was a significant shift in the proteomic compilation of the entire hippocampus. The majority of proteins were significantly upregulated upon EPA with metabolic enzymes as main drivers, cytoskeleton remodeling and localization to mitochondria. These upregulated proteins have important implications for disease-related pathways too, e.g. Alzheimer's disease. Furthermore, some of the detected proteins possess established roles in locomotion, neurogenesis, growth and apoptotic processes. Moreover, a target protein of *Stau2*, namely RhoA, which has a known role in the growth and differentiation of neurites, was also upregulated upon physical activity. Not only in the entire hippocampus, but also in the dorsal and ventral parts and their subregions the enriched proteins differed from each other and are involved in different molecular pathways.

These results advance current scientific knowledge, according to which the hippocampus contains different parts that interact through distinct but thus far unknown neuronal conduits. These findings provide evidence that activity-dependent adult neurogenesis affects the dorsal and ventral hippocampus differentially. Additionally, this process is strongly impaired under *Stau2*-deficiency. Furthermore, under voluntary physical activity, the proteome of the hippocampus, its dorsal and ventral parts, and their different subregions are significantly altered. Alongside existing research, these results add to our understanding of the functional structure of the hippocampus, the proteomic changes upon EPA and the role of *Stau2* in adult neurogenesis. Future studies should use these findings to gain a better understanding of the molecular mechanisms in neurodegenerative diseases, laying the foundation for new therapeutic approaches.

2 Zusammenfassung

Adulte Neurogenese ist ein komplexer Prozess, der die Entstehung von neuen, unreifen Neuronen im ausgereiften Gehirn beschreibt und bisher ausschließlich in zwei Regionen des Gehirns bestätigt werden konnte, der Subventrikulären Zone und dem hippocampalen Gyrus Dentatus. Dieser neuronale Vorgang liegt aktuell im Fokus der Grundlagenforschung, da adulte hippocampale Neurogenese mit kognitiven Fähigkeiten assoziiert wird und dessen Defekt in der Entstehung von neurodegenerativen Erkrankungen eine bislang unklare Rolle spielt. Stau2 (Stau2) ist ein RNA-Bindeprotein, welches in der Differenzierung von Neuronen in der embryonalen Neurogenese eine wichtige Rolle spielt. Durch freiwillige körperliche Aktivität mittels Laufrädern kann adulte Neurogenese im Hippocampus von Mäusen induziert werden. Inwieweit der Hippocampus als komplexe Hirnstruktur, in seinen Anteilen getrennte Funktionen besitzt, ist weitestgehend unklar. Aktuelle Studien postulieren, dass die dorsalen und ventralen Anteile des Hippocampus in unterschiedlichen funktionellen Signalwegen eingebunden sind und sich die Expression von mRNAs im Hippocampus lokoregional stark unterscheidet.

In dieser experimentellen Studie wurde untersucht, ob freiwillige körperliche Aktivität adulte Neurogenese im Hippocampus induziert, und ob es hierbei Unterschiede in den dorsalen und ventralen Anteilen gibt. Hierbei wurden neben der Anzahl der Neuronen, auch ihre dendritische Verzweigung untersucht. Da Stau2 eine Rolle in der embryonalen Neurogenese spielt, betrachtete diese Arbeit zusätzlich die Frage, ob bei Stau2-defizienten Mäusen der Prozess der adulten Neurogenese beeinträchtigt ist. Des Weiteren wurde erforscht, ob auch das Proteom nach verstärkter körperlicher Aktivität verändert ist, und ob es hierbei Unterschiede im dorsalen und ventralen Hippocampus, sowie deren einzelnen Subregionen, Gyrus Dentatus (GD), CA3- und CA1- Region gibt.

Die Fragestellungen wurden mittels zwei verschiedener experimenteller Ansätze bearbeitet: Immunhistochemie mit anschließender Quantifizierung und Mikrodissektion mit label-freier Massenspektrometrie. Für die immunhistochemischen Versuche wurden zwei verschiedene Maustypen untersucht: Wildtypen (WT) und Stau2-defiziente Mäuse. Die jeweiligen Kontrollgruppen beinhalteten 10 Wochen alte, adulte Mäuse. Die Testgruppen waren 13 Wochen alt, da sie zusätzlich über einen Zeitraum von 3 Wochen Zugang zu Laufrädern hatten, welche sie freiwillig nutzen konnten. Die neu gebildeten hippocampalen Neurone wurden mittels Doublecortin (DCX), einem validen Marker für unreife Neuronen, angefärbt. Zur Quantifizierung wurde die absolute Anzahl der DCX-positiven Zellkörper, ihrer primären und sekundären Dendriten und deren durchschnittliche Länge analysiert. Die dorsalen und ventralen Anteile des Hippocampus wurden hierbei getrennt untersucht.

Die Mikrodissektion und konsekutive massenspektrometrische Proteinanalyse wurden ausschließlich an o.g. WT vorgenommen. Hier bestand der gleiche Versuchsaufbau mit

einer Kontrollgruppe ohne Laufräder (n=5) und einer Testgruppe mit zusätzlichen 3 Wochen Zugang zu Laufrädern (n=5). Die dorsalen und ventralen Anteile des Hippocampus, sowie ihre Subregionen wurden getrennt untersucht. Somit wurden 10 Mäuse, mit je 2 Anteilen und je 3 Subregionen, einzeln manuell präpariert und die daraus resultierenden 60 Proben getrennt massenspektrometrisch bearbeitet. Anschließend wurde der Proteom-Datensatz der Test- und Kontrollgruppe und zusätzlich die einzelnen Subregionen miteinander verglichen. Es wurde analysiert, welche Funktionen die Proteine besitzen und in welche biologischen Prozesse und Signalwege sie implementiert sind.

Die DCX-Quantifizierung der WT zeigte, dass der dorsale und ventrale Hippocampus unterschiedlich auf körperliche Aktivität reagieren. Nur im ventralen GD war die Anzahl unreifer Neuronen, sowie die Anzahl ihrer primären und sekundären Dendriten nach körperlicher Aktivität gesteigert. In beiden Regionen zeigte sich ein Zuwachs in der durchschnittlichen Länge der primären und sekundären Dendriten.

Bei *Stau2*-defizienten Mäusen zeigte sich weder in den dorsalen, noch in den ventralen Anteilen ein signifikanter Anstieg in der Anzahl neuer Neuronen und ihrer Dendriten. Die Dendritenlänge war nur im ventralen GD erhöht.

Die massenspektrometrische Proteinanalyse zeigte unter körperlicher Aktivität eine signifikante Verschiebung des Proteoms im gesamten Hippocampus. Der Großteil der Proteine war signifikant hochreguliert, lokalisiert zu Mitochondrien und involviert in metabolische Vorgänge, der Regulation des Zytoskeletts, sowie auch krankheitsbezogenen Regelkreisen, u. a. von Morbus Alzheimer. Einige der detektierten Proteine besitzen nachweislich eine Funktion in Fortbewegung, Neurogenese, Wachstums-, oder Apoptose-Prozessen. Auch ein Zielprotein von *Stau2*, *RhoA*, welches eine bedeutende Rolle in dem Wachstum und der Differenzierung von Neuriten besitzt, war nach Aktivität hochreguliert. Nicht nur im gesamten Hippocampus, auch in den dorsalen und ventralen Anteilen, sowie den Subregionen unterschieden sich die angereicherten Proteine, die in verschiedenen Regelkreisen eingebunden sind.

Diese Ergebnisse fügen sich gut in den aktuellen wissenschaftlichen Kontext ein, wonach der Hippocampus unterschiedliche Anteile besitzt, die über getrennte, bislang unklare, Signalwege fungieren. Dieses Forschungsprojekt liefert Belege, dass aktivitätsabhängige adulte Neurogenese im dorsalen und ventralen Hippocampus unterschiedlich stark ausgeprägt ist, dieser Prozess bei *Stau2*-Defizienz zusätzlich beeinträchtigt ist und zudem das Proteom des Hippocampus im Gesamten, seinen dorsalen und ventralen Anteilen, sowie deren einzelnen Subregionen nach körperlicher Aktivität signifikant verändert ist. Diese Ergebnisse stellen gemeinsam mit bisherigen Daten eine Grundlage dar, den funktionalen Aufbau des Hippocampus genauer zu verstehen, mittels der erforschten Proteine Signalwege unter adulter Neurogenese weiter aufzuklären und zudem einige Proteintargets für Pathomechanismen und daraus resultierende Therapieansätze für neurodegenerative Erkrankungen weiter zu erforschen.

3 Introduction

3.1 RNA-binding proteins

3.1.1 Overview

During brain development as well as in the mature brain, local translation of mRNAs in axonal growth cones or synapses enables neurons to respond to environmental signals and remodel, critically contributing to synaptic development and plasticity (A. C. Lin et al., 2007; Martin et al., 2006). Upon neuronal stimulation, RNA-binding proteins (RBPs) control the local expression of localized mRNAs (Jung et al., 2014). Hereby, RBPs bind preferentially to the 3'-untranslated region of mRNAs and, together with other proteins, build heterogeneous complexes, so called ribonucleoparticles (RNPs). These are assembled in the cell nucleus and then transported in an inactivate state – thereby preventing premature translation – to specific subcellular sites. For that, they require motor proteins that transport them via the cytoskeleton towards their final destination in dendrites or axons near synapses, where translation can be triggered upon synaptic activation (Holt et al., 2009; Jung et al., 2014; Martin et al., 2009).

To time, there are only a few RBPs in neurons and in the brain that have been well-studied. Most of the neuronal RBPs observed in vertebrates have been initially identified through studies in *Drosophila* oocytes and neuroblasts, for example, the two RBPs Staufen and Pumilio. The importance of these RBPs has risen, as they have been recently linked to crucial neuronal processes like for instance long-term memory formation (Dubnau et al., 2003; Kiebler et al., 2006).

3.1.2 Pumilio2

In mammals, two orthologs Pumilio1 (Pum1) and Pumilio2 (Pum2) exist. Both present widespread and similar expression patterns in humans (Spasov et al., 2002). Pum1 is expressed in various brain regions in mice and its deficiency is associated with motor dysfunction and neuronal degeneration in cerebellum (Gennarino et al., 2015a). Pum2 is expressed in neurons in the mammalian brain, more precisely in cell bodies and dendrites, and plays a role in dendritic RNP complexes. When its translation is silenced, the outgrowth of dendrites is stimulated (Fiore et al., 2009). Pum2 is involved in mRNA transport and plays a function in translation repression (Vessey et al., 2006). Furthermore, Pum2 is critical for the regulation of neuronal excitability in mice and is associated with late-onset epilepsy (Follwaczny et al., 2017). Importantly, Pum2 co-localizes with another neuronal RBP, Stau2, and subsequently forms RNA complexes that target neuronal mRNAs (Vessey et al., 2012).

3.1.3 Staufen2

The Staufen family is a group of double-stranded RBPs that has an important role in mRNA localization. In mammals, there are two orthologs of Staufen, Staufen1 (Stau1) and Staufen2 (Stau2), followed by several splice isoforms. Stau1 is ubiquitously expressed, whereas Stau2 is mainly expressed in brain tissue and in testis. The two orthologues are not co-localizing and have widely distinct functions, although both participate in dendritic spine morphogenesis (Duchaîne et al., 2002; Vessey et al., 2008). In neurons, Stau2 has its somatodendritic localization and is found in dendritic RNPs, similar to Pum2 (Kiebler et al., 1999). As the RBP binds its target mRNAs, it assembles into large protein complexes and undergoes microtubule-dependent transport into neuronal dendrites (Kiebler et al., 2006). It has shown to be important for RNA localization in neuronal dendrites (Sharangdhar et al., 2017; Tang et al., 2001), as well as for RNA transport in neurons (Bauer et al., 2019). Previous studies have shown that Stau2 interacts with ribosomes, suggesting an additional function in translation. (Duchaîne et al., 2002; Wickham et al., 1999).

During the process of brain development, Stau2 seems to be important for cell fate determination. It directly regulates localization and expression of neurogenic RNA targets, such as *Prox1* and is enriched in radial glial cells (RGCs), which are neuronal precursor cells in the embryonic cortex (Vessey et al., 2012). During neurogenesis, when RGCs divide asymmetrically into another RGC and an intermediate progenitor cell (IPC) or a neuron, Stau2 is distributed asymmetrically into the differentiating cell. Knockdown of Stau2 leads to an increase of these IPCs and a reduction of RGCs, thereby enhancing neurogenesis (Kusek et al., 2012; Vessey et al., 2012). Through their regulatory function and localization, this RBP controls the balance between maintenance and differentiation of neuronal precursors and is therefore crucial for adequate embryonic neuronal development.

In the mature brain, knockdown of Stau2 in mammalian hippocampal neurons leads to decreased dendritic arborization and reduced number of synapses (Goetze et al., 2006). Stau2 is supposed to play a role during axon guidance, as it co-localizes with *RhoA* mRNA at the growth cone during axonal development (Wu et al., 2005). In *Drosophila*, one Staufen protein exists, which is involved in activity-dependent synaptic plasticity and is required for long-term memory formation (Dubnau et al., 2003). Furthermore, in hippocampal slice cultures, Stau2 is not required for protein synthesis-dependent long-term potentiation (LTP), but is necessary for long-term depression (Lebeau et al., 2011). In rats, both processes – LTP and long-term depression (LTD) – are influenced by Stau2 deficiency: LTP is augmented, whereas LTD is reduced (Berger et al., 2017). Overall, these findings demonstrate that Stau2 is essential during neuronal development in the embryonic brain but is also required for dendritic spine morphogenesis and synaptic function in the mature brain of flies and mammals. A recent study in our laboratory investigated the role of Stau2 in the context of hippocampus-dependent learning and

memory in mice, and revealed that *Stau2* affects their novelty preference and explorative behavior, both of which are important features of spatial learning (Popper et al., 2018). Therefore, *Stau2* in mammals contributes to the complex processes of learning and memory, mediated by the hippocampus, a region where adult neurogenesis is currently in the limelight.

3.2 Adult neurogenesis in mice

Adult neurogenesis is a complex process that relies on versatile molecular pathways. Over fifty years ago, Altman discovered that neurogenesis persists in the hippocampus beyond embryonic development and into adulthood, and is thus regarded as the founder of adult hippocampal neurogenesis (Altman, 1962; Altman et al., 1965). Verified by many following studies, it is generally accepted that adult neurogenesis takes place in most mammals and the human brain (Spalding et al., 2013). Adult neurogenesis occurs under normal physiological conditions only in two distinct regions in the mouse brain: the subventricular zone (SVZ) along the lateral ventricles and the subgranular zone (SGZ) in the dentate gyrus (DG) of the hippocampus (Gage, 2000; Lim et al., 2014). In the SGZ, newly generated neurons are originating from neuronal precursor cells that are localized in the SGZ of the DG and integrate into the regional neuronal network. Through the establishment of new immunohistochemical methods, immature newly generated granule cells could be labeled and the field revived in the 1990s (Cameron et al., 1993). Due to the increasing variety of molecular methods, research has increasingly focused on the characteristics and functional implications of these newly generated neurons within the hippocampal network. In mice experiments, the commonly known methods on generating newborn adult neurons in a short period of time are behaviorally induced experiments or physical-activity-dependent models. To induce neurogenesis in adult mice, enhanced physical activity (EPA) through voluntary wheel running was applied over a period of three weeks as described previously (Clark et al., 2011; Van Praag et al., 1999; Vivar et al., 2016). In 1999, van Praag *et al.* compared different models to induce adult neurogenesis and indicated that the activity dependent model leads to an increase in the number of newborn neurons.

3.2.1 Localization and process

In the SVZ, adult neural stem cells (NSCs) generate neuroblasts that transfer through the rostral migratory stream to the olfactory bulb and transform into interneurons (Gage, 2000; Lim et al., 2014). In the SGZ, the newly generated neurons rise from NSCs, namely type 1 radial glia-like cells. They proliferate and produce intermediate progenitor cells, that subsequently generate neuroblasts. They migrate into the granular layer and differentiate into dentate granule cells (**Figure 1**) (Goncalves et al., 2016).

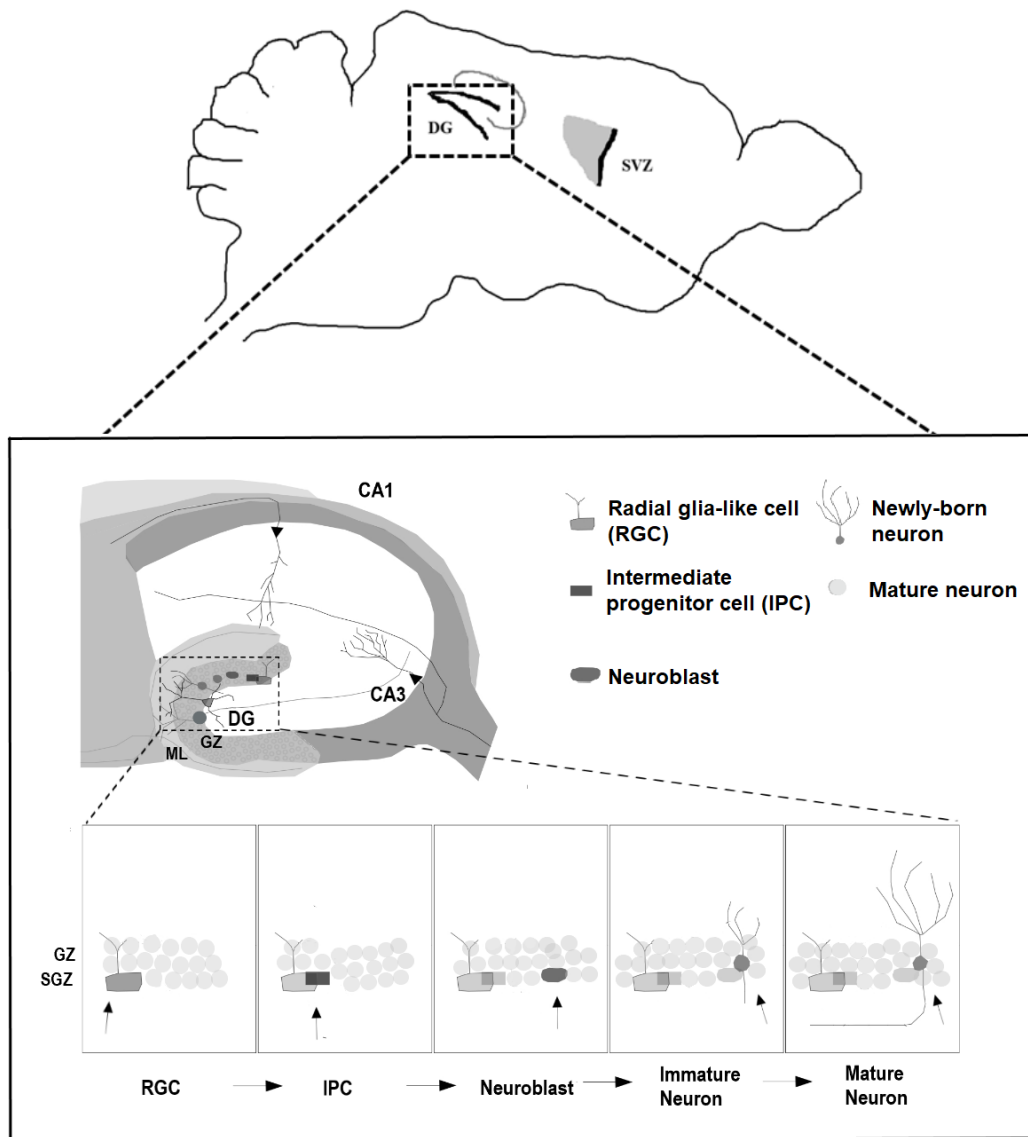


Figure 1: Adult neurogenesis in mice. Sagittal sections showing a mouse brain including two regions with adult neurogenesis: the dentate gyrus (DG) and the subventricular zone (SVZ). Upper part: magnification of the DG; lower part: five distinct stages of adult hippocampal neurogenesis (see text for details). Abbreviations: ML, molecular layer; GZ, granular zone; SGZ, subgranular zone; CA, cornu ammonis. Own illustration, figure inset based on Ming et al., 2011.

In the first week, they extend limited processes. In the following week, these immature neurons mature and grow dendrites reaching towards the molecular layer and axons enter the hippocampal subregion CA3. During the third week, these dendrites of newborn neurons begin to form efferent and afferent synapses towards regional structures: spines grow and connect to axon fibres from the entorhinal cortex and axonal boutons, later represented as mossy fibres, reach the CA3 pyramidal cells (Zhao et al., 2006). Interestingly, the afferent as well as the efferent structures of adult-born neurons target preferably mature synaptic partners with already existing synapses during neuronal development, suggesting a competitive process between immature and mature neurons (Toni et al., 2007, 2008). At around four weeks, the newly generated cells are fully

integrated into the neuronal network of the hippocampus. Interestingly, however, these adult-born neurons differ from those that were generated during embryonic development.

3.2.2 New neurons with new characteristics

At week four of adult neurogenesis, the newly generated cells present different electrophysiological properties, such as a lower resting membrane potential and a higher input resistance, which renders them more excitable (Mongiat et al., 2009). On top of that, they transiently show stronger synaptic plasticity, with lower LTP induction thresholds and augmented LTP amplitudes (Ge et al., 2007). A recent study by Danielson *et al.*, (2016) using *in vivo* two photon imaging in mice also revealed that while adult-born DGCs are more excitable, they are less spatially coordinated in comparison to the other DGCs. The different physiological properties in excitability and synaptic plasticity happen in a transient period during maturation and are crucial for understanding the potential functions of adult-born DGCs (**Figure 2**). When the newly generated neurons mature during the following stages of adult neurogenesis, they receive stronger inhibitory input, show decreased activity and finally resemble mature DGCs (Marín-Burgin et al., 2012).

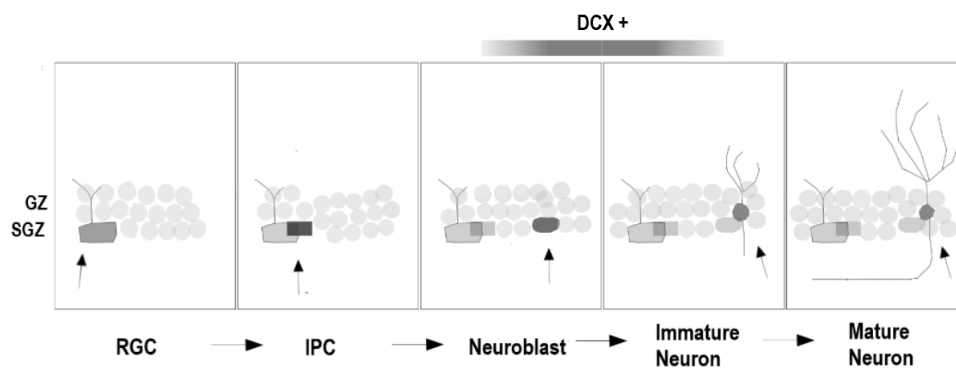


Figure 2: Five stages of adult hippocampal neurogenesis including DCX + stages (see text for details). Abbrev.: GZ, granular zone; SGZ, subgranular zone; DCX, doublecortin. Own illustration, based on Ming et al., 2011.

During development, differentiation, and maturation, adult-born DGCs express stage-specific markers that are transient and therefore allow precise characterization and identification of neurons and enable to distinguish neuronal precursors from mature neurons.

Doublecortin (DCX) is a neuronal marker during differentiation in adult neurogenesis (**Figure 2**). DCX is a microtubule-associated protein that is involved in neuronal migration (Gleeson et al., 1999). In the adult brain, it is almost only expressed in the two areas with persistent neurogenesis, the SVZ and the hippocampal dentate gyrus. During adult neurogenesis in mice, the expression of DCX starts in neuroblasts, persists in immature neurons for approximately three weeks, and then declines parallel to the

maturation of new neurons until it disappears completely (Brown et al., 2003; Kempermann et al., 2003; Snyder et al., 2009). DCX is present in the soma as well as dendrites of neurons (Rao et al., 2004). Due to its localization within the cell, its local and transient expression pattern, DCX is a specific and appropriate marker for quantification of newly generated and immature neurons.

3.2.3 The functional role of the dentate gyrus and adult-born neurons

The hippocampus presents a complex circuit with the DG as the major input region. The DG receives input from various regions, namely the limbic system, primarily the entorhinal cortex via the perforant pathway, the perirhinal cortex, the medial septum and midbrain structures, as well as intra-hippocampal inputs from CA3, inhibitory interneurons, mossy cells and the contralateral hippocampus. This has been proven for mature granule cells, but also adult-born neurons in mice (Du et al., 2016; Vivar et al., 2012). Additionally, pathways with the hypothalamic-pituitary-adrenal (HPA) axis and amygdala exist. The DG sends its efferent structures mainly to the pyramidal cells of the CA3 hippocampal subregion, but also to mossy cells and interneurons in the DG itself. Its broad but particular synaptic connectivity reflects its importance in higher brain functions such as episodic memory, spatial learning, pattern separation and emotional behavior. Adult-born neurons pass a hyperexcitable period during maturation, enhance plasticity in the DG and are directly connected to brain regions that are major in learning, memory, pattern separation and behavior (Clelland et al., 2009; Danielson et al., 2016; Kheirbek et al., 2012; Nakashiba et al., 2012; Snyder et al., 2011; Zhao et al., 2006). All these findings make the adult born granule cells central components in memory.

The hippocampus of rodents, especially well-studied in rats, contains a dorso-ventral axis with differences in both input and output (Kheirbek et al., 2013). It has been demonstrated that restricted dorsal hippocampal lesions led to impaired spatial function, concluding that dorsal parts mediate preferably spatial memory and learning (Moser et al., 1993; Pothuizen et al., 2004). By contrast, ventral hippocampal neurons are in contact with the amygdala, the nucleus accumbens and the HPA axis, and thus are particularly associated with emotional behavior and stress response (Henke, 1990; Shah et al., 2016). Isolated lesions in the ventral HC resulted in reduced unconditioned fear behavior and decreased locomotor activity (Bast et al., 2001; Kjelstrup et al., 2002).

Thus, the hippocampus along its dorso-ventral axis contributes to different functional pathways. This is supported by the fact that connected brain regions show a topographical gradient towards the hippocampus, too, like the entorhinal cortex (Dolorfo & Amaral, 1998; Kishi et al., 2006; Li et al., 1994).

3.2.4 Involvement of glial cells

Apart from the NSC and radial glia population, there are other glial cells that support and

control adult neurogenesis in the dentate gyrus. Studies revealed that astrocytes regulate the development as well as survival of adult-born neurons. They significantly influence the proliferation of precursors as well as their fate determination into neurons (Song et al., 2002). These findings were unexpected since in embryonal neurogenesis, neurons are mainly generated before glial cells, wherefore mature glia mainly seem to play a supportive role in neuronal development. Furthermore, astrocytes in the direct environment of newborn neurons regulate dendritic spine formation and synaptic maturation through vesicle exocytosis, such as release of D-serine. D-serine is known to be a co-agonist of NMDA receptors, which in turn mediate signal transmission in maturing adult born neurons (Sultan et al., 2015). Thus, apart from neuronal proliferation, glia, especially astrocytes, are crucial for functional integration of newly-generated, immature neurons within the hippocampal circuitry.

3.2.5 Adult neurogenesis in the human hippocampus

Adult neurogenesis occurs in rodents, but what about the human brain? The same process in rats and mice has been described for the human adult hippocampus, through specific labeling of immature neurons (Eriksson et al., 1998). Recently, the extent of adult neurogenesis in human is under debate and actively investigated by using various experimental approaches: While many reports focus on BrdU and DCX labeling, one study researched neurogenesis by assessing the ^{14}C concentration in DNA of hippocampal post-mortem tissue and concluded a persistent neuronal turnover throughout adulthood despite a decrease with age (Spalding et al., 2013). However, the occurrence of adult neurogenesis in the human dentate gyrus is currently still under debate. When observed, adult-born neurons are interpreted to maintain cognitive function, and the decline could reflect cognitive and emotional changes in elderly people (Boldrini et al., 2018; Sorrells et al., 2018).

It is difficult to generalize findings on post-mortem or unhealthy brain tissue to the healthy brain. Undoubtedly, more *in vivo* diagnostics in humans would greatly improve our knowledge. Clinical diagnostics such as MRI data, PET imaging and cognitive testing propose a relation between adult neurogenesis and behavioral pattern separation. MRI studies researched possible biomarkers or correlated regional cerebral blood volume with angiogenesis, that coupled with neurogenesis for monitoring adult neurogenesis in humans (Manganas et al., 2007; Pereira et al., 2007). These methods aim to work on the functional implication of adult-born neurons during our lifetime, but their reliability is still limited as the diagnostics are inaccurate and not highly validated (Ho et al., 2013). Currently, interests arise not only on the existence but moreover on the functional implication of newly-generated neurons in the DG.

3.3 Involvement of adult neurogenesis in neuropsychiatric disorders

In the last decade, there is an increased interest in the role of RBPs in the context of neurological and psychiatric diseases. In this context, it is interesting to note that both Pum2 and Stau2 deficiency in rodents contributes to impaired behavior and memory testing and additionally, Pum2-deficient mice play a critical role in epileptogenesis (Follwaczny et al., 2017; Popper et al., 2018; Siemen et al., 2011). Parallel to these findings on RBPs, adult neurogenesis has recently gained high interest in the context of neurodegenerative and psychiatric disorders. The most common neurodegenerative diseases linked to altered adult neurogenesis are Parkinson's (PD), Huntington's (HD) and Alzheimer's disease (AD). In rodents with PD or HD, cell apoptosis is enhanced, cell proliferation reduced, and furthermore the number of newly generated neurons is decreased (Höglinger et al., 2004; Lazic et al., 2004; Winner et al., 2012). In AD, links to altered neurogenesis vary and depend on the AD transgenic animal models, whereas the majority detected decreased proliferation and correlation with β -amyloid plaques (Donovan et al., 2006; Rodríguez et al., 2008). In humans suffering from AD, adult neurogenesis is altered compared to healthy controls (Moreno-Jiménez et al., 2019).

Furthermore, adult neurogenesis plays an emerging role in psychiatric disorders like depression, cognitive impairment and anxiety. Regarding major depression, several studies proposed a link to deficits in adult neurogenesis in the DG. The number of newly-generated neurons in the SGZ was found to be reduced and moreover, chronic treatment with antidepressants can normalize or even improve neurogenesis in affected mammals (Malberg et al., 2000; Van Bokhoven et al., 2011). On top of that, adult hippocampal neurogenesis seems to be directly necessary for the anxiolytic effects of antidepressive agents tested in mice (Santarelli et al., 2003). In humans, changes in progenitor proliferation of depressed patients and subsequent antidepressant therapy could not be observed (Lazic et al., 2006). However, several other studies confirmed a reduction in NSCs and proliferation in the HC, as well as an increase in DG volume and enhanced neurogenesis after treatment with antidepressants (Boldrini et al., 2009, 2013; Lucassen et al., 2010).

Thus, there is rising evidence in animal models as well as in research on human brain that alterations in the process of adult neurogenesis are linked to major neurodegenerative and psychiatric disorders – but whether this is a cause or consequence is still under debate.

4 Statement of purpose

The aim of the present study was to investigate the effects of enhanced physical activity (EPA) on the hippocampus and the process of adult neurogenesis. Moreover, we aimed to characterize the role of the RBP Stau2 in the context of adult hippocampal neurogenesis, as Stau2 plays an essential role during embryonal neurogenesis, and also in the adult brain. But what about its role during the process of adult hippocampal neurogenesis? Therefore, in this study we decided to investigate two different existing mouse lines: male Stau2^{GT} mice and age-matched male wild-type mice. Both groups comprised each one control group of naïve adult mice and one test group with free access to running wheels. Voluntary running presents a well-established experimental model to investigate effects of EPA on neurogenesis in the adult mouse brain and was performed over a time period of three weeks. Subsequently, these brains were subjected to immunohistochemistry and the amount of adult-born immature neurons and their arborization, in particular their primary and secondary dendrites, were then quantified. Here, we aimed to clarify, whether the number of newly-generated neurons and dendrites in the dentate gyrus change upon EPA-dependent adult neurogenesis, whether the effects of EPA differ in dorsal and ventral hippocampus and moreover, whether there is a difference when Stau2 is deficient.

Up to now, fundamental research mainly focusses on alterations in the transcriptome when investigating the process of adult hippocampal neurogenesis. However, changes on the mRNA level give less insight into the actual cellular processes than alterations on the protein level. For that, mass spectrometry was applied to identify changes in the hippocampal proteome of adult WT mice upon voluntary running and compared to their naïve counterparts. Then, we aimed to identify whether upon EPA, the up- and downregulated proteins in the hippocampus can be clustered to specific cellular localizations, biological processes or pathways. There is little evidence how exactly newborn neurons contribute to learning and memory formation in the hippocampus and whether these processes affect the entire hippocampus or localized regions. We therefore distinguished between dorsal and ventral parts of the hippocampus and examined them separately. Furthermore, we examined the dorsal and ventral parts of the hippocampus more precisely by dividing them into their different functional subregions, namely the dentate gyrus, CA3 region and CA1 region.

This study aims to uncode the functional role of the hippocampus itself, but also the contribution of RBPs such as Stau2 in the context of adult hippocampal neurogenesis and to reveal proteomic changes upon EPA. New insights in these fields contribute to understanding normal neuronal function, the processes of brain plasticity and the molecular mechanisms in neuropsychiatric diseases and therefore could provide grounds for new therapeutic approaches.

5 Material and Methods

Some of the subsections of this chapter have been previously published in Frey et al.,2020 and have been adopted in a slightly modified form.

5.1 Materials

5.1.1 Buffers and solutions

Table 1: List of buffers and solutions.

Name	Components
Storing Solution	30% glycerol, 30% ethylene glycol, 10% Phosphate buffer pH 7.3 out of 0,1425% Sodium dihydrogen phosphate (NaH_2PO_4) and 0,375% Sodium hydroxide (NaOH), in ddH ₂ O pH 7,4
Blocking Solution	0,5% Triton, 1% (w/v) BSA in 40ml PBS
Phosphate buffered saline (PBS)	0,8% sodium chloride (NaCl), 0,21% potassium chloride (KCl), 0,144% sodium dihydrogen phosphate (NaH_2PO_4), 0,24% potassium dihydrogen phosphate (KH_2PO_4) in ddH ₂ O pH 7,4
Mounting Medium	Cryomount Tissue-Tek® O.C.T. compound
Milli Q H ₂ O	Purified water using the Merck MilliQ Ultrapure Water System
EtOH 70	Ethanol 70%
EtOH 96	Ethanol 96%
EtOH 100	Ethanol 100%

5.1.2 Antibodies for immunohistochemistry

Table 2: List of primary and secondary antibodies and nuclear staining used for immunohistochemistry, Abbrev.: AF, Alexa Fluor.

Primary Antibodies			
Antibody	Species	Company/Laboratory	Dilution
Anti-DCX	Guinea pig	Millipore	1:400
Anti-DCX	Rabbit	Abcam	1:1000
Anti-GFAP	Mouse	Sigma-Aldrich	1:500
Anti-Ki-67	Rabbit	Life Technologies	1:100
Anti-GFP	Chicken	Götz Laboratory BMC	1:500

Anti-Stau2	Rabbit	Kiebler Laboratory BMC	1:500	
Anti-NeuN	Chicken	Millipore	1:500	
Anti-MAP2	Mouse	Sigma-Aldrich	1:1000	
Secondary Antibodies				
Antibody	Species	Company/Laboratory	Dye	Dilution
Anti-Guinea Pig	Goat	Jackson Immuno Research	Cy 3	1:500
Anti-Mouse, Anti-Rabbit	Donkey	Life Technologies	AF 488	1:500
Anti-Rabbit	Donkey	Molecular Probes (Life Technologies)	AF 647	1:500
Anti-Chicken	Goat	Molecular Probes (Life Technologies)	AF 647	1:500
Anti-Chicken		Götz Laboratory	AF 488	1:500
Anti-Goat	Calf	Dianova	Cy 3	1:500
Anti-Rabbit	Donkey	Molecular Probes (Life Technologies)	AF 555	1:250
Anti-Mouse	Donkey	Molecular Probes (Life Technologies)	AF 647	1:500
Nuclear staining				
DAPI		Thermo Fisher and Carl Roth		1:500

5.1.3 Equipment for microdissection

For proteome analysis, mice brain slices were manually dissected using a stereo microscope (Wild, Germany). The materials included: ethanol 70%, injection-cannulas sized 0.40 x 20mm (Sterican, B.Braun, Germany), scalpels, 1.5ml tubes (Product 4182.1, Carl Roth, Germany) containing the samples (60 tubes in total), polystyrene box with ice for cooling the samples and a stereo microscope. During microdissection, personal protective wear such as gloves and laboratory coat were used.

5.1.4 Mass spectrometry preparation kit

The Sample Preparation Kit by PREOMICS (PreOmics GmbH, Germany) is divided into three steps: Lysis, Digestion and Purification. The involved materials contain protease reconstitution buffer, trypsin-mix for digestion, washing and eluting buffers. The exact preparation protocol can be accessed via the following link (https://preomics.com/resources/protocols/PreOmics_iST_SamplePrepKit_Protocol_In_D_Cartridge_8x_Mammalian_Tissue_v1_0.pdf).

5.2 Animals

5.2.1 Wild-type mice

This subsection has been previously published in Frey et al.,2020.

The experiments performed were authorized by the authors' institutional committee on animal care and were conducted according to the German Animal Protection Law, conforming to international guidelines on the ethical use of animals (Az. 5.1-5682/LMU/BMC/CAM 2019-0007) (Frey et al., 2020).

For experiments, male wild-type mice (genetic background: C57Bl6/JRj Janvier laboratories, France) aged 10 weeks (control group) and 13 weeks (test group) were investigated. Test group mice had free access to a low-profile running table (Product ENV-047, Med Associates, VT, USA) in their home cages over a period of three weeks for voluntary use and were sacrificed at the age of 13 weeks to investigate the effect of enhanced physical activity (EPA) on the hippocampus. Naïve adult mice without access to running wheels represent the control group and were sacrificed at the age of 10 weeks. All mice were held in groups of two to three animals under specified pathogen-free conditions in filter-top cages with a 12/12-hour light/dark cycle. All animals had free access to water (acidified and desalinated) and standard rodent chow (Altromin, 1310M).

5.2.2 Glia-labeled mice

Transgenic mice expressing glia cell type specific reporters were provided by Prof. Magdalena Götz (BMC Munich, Germany). The following transgenic mice were used to label glial precursor cells *NG2-YFP* (Nishiyama et al., 2005), oligodendrocytes *SOX10-GFP* (Stolt et al., 2002) and astrocytes *Aldh1l1-GFP* (Cahoy et al., 2008).

5.2.3 *Stau2*^{GT} mice

The transgenic *Stau2*^{Gt(RRG396)Byg} mouse line (termed *Stau2*^{GT} mice in the remainder) was provided by Prof. Sally Temple (Neural Stem Cell Institute, Rensselaer, NY). The *Stau2*^{GT} mice show a deficiency of 40% at the protein level compared to wild-type littermates (Popper et al., 2018). *Stau2*^{GT} mice were divided into two groups: the control group consists of three male adult mice aged 10 weeks and the test group consists of five male adult mice aged 13 weeks after additional three weeks of voluntary running when compared to their 10-week old counterparts. These mice were kept under the identical housing conditions as their wild-type littermates.

5.3 Activity-dependent neurogenesis

To induce neurogenesis in adult mice, voluntary wheel running was applied over a period of three weeks as described previously (**Figure 3**) (Clark et al., 2011; Van Praag et al.,

1999; Vivar et al., 2016). This method is considered to be more robust to behavioral experiments and similar to enriched environment conditions. On top of that, it is more reproducible and thus can be set and analyzed by using exact parameters. We used wireless, battery-powered running tables (Product ENV-047, Med Associates, VT, USA) in a time frame of three weeks. Every cage with two to three mice contained one wheel and their functionality were checked every day. As mentioned above, adult neurogenesis in mice is undergoing different differentiation stages (**Figure 2**). At around three weeks of differentiation, the adult-born DGCs present their peak in spine growth (Zhao et al., 2006) and neurons build first connections to the CA3 hippocampal subregion. The total number of rotations per day was recorded over a period of three weeks.

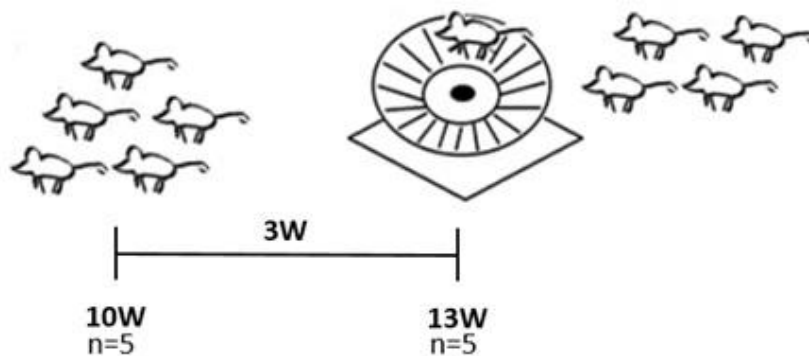


Figure 3: Experimental outline. Mice without (10W, n=5) or with (13W, n=5) exposure to running wheel. Abbrev.: W, weeks; (Figure modified from Frey et al., 2020).

The following two work schemes represent the different experimental set-ups for immunohistochemistry and mass spectrometry (**Figure 4** and **5**).

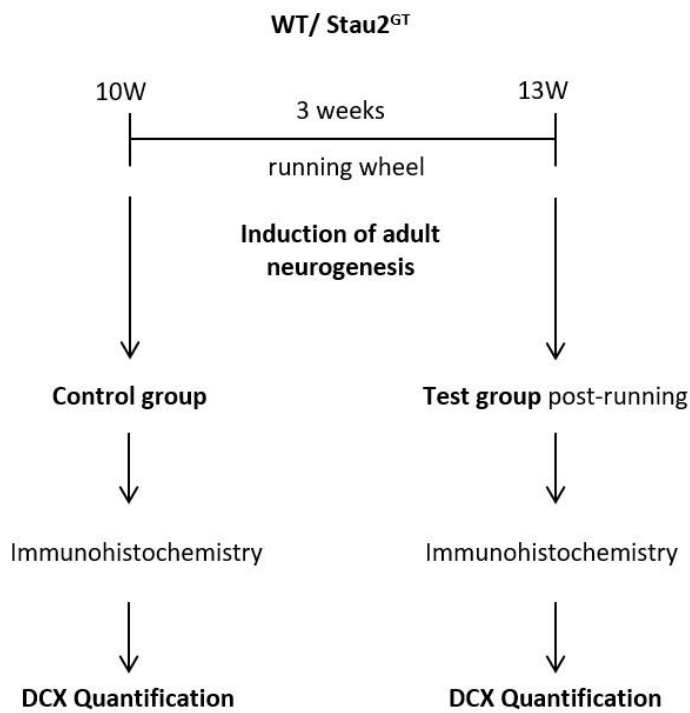


Figure 4: Schematic representation showing the experimental workflow for immunohistochemistry performed on WT and Stau2^{GT} mice. Abbrev.: W, weeks.

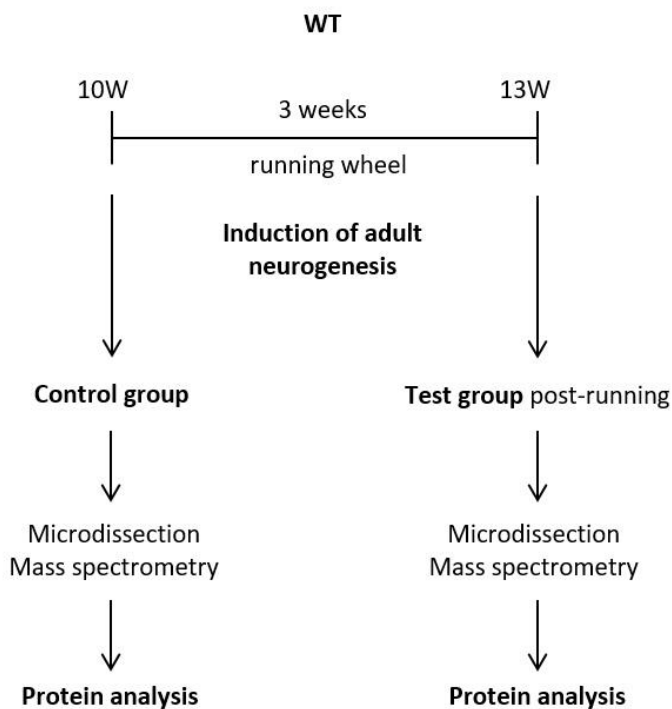


Figure 5: Schematic representation showing the experimental workflow for microdissection followed by mass spectrometry performed on WT mice. Abbrev.: W, weeks.

5.4 Immunohistochemistry

5.4.1 Tissue preparation

This subsection has been previously published in Frey et al.,2020.

Mice were deeply anaesthetized with CO₂ and instantly prepared for tissue preservation. They were intracardially perfused with PBS and afterwards with 4% paraformaldehyde (PFA) (pH 7; Roti®-Histofix, Germany) for ~ 12 min (Vivar et al., 2012). Brains were carefully removed and post-fixed in 4% PFA for 12-72 hours at 4°C. After that brains were dehydrated in 30% sucrose in ddH₂O at 4°C for 1-2 days. Brains were sliced into 40 µm coronal sections with a Leica cryotome (Product CM1850, Leica Microsystems, Germany) and stored free-floating in storing solution at -20°C until use for immunohistochemistry.

5.4.2 Selection of representative slices

For differentiating between dorsal and ventral parts of the hippocampus, one representative slice from both regions was selected for immunohistochemical experiments (**Figure 6**). The representative sections of one dorsal and one ventral hippocampal slice were transferred on glass slides for staining and subsequent imaging. Through depicting one section per dorsal and ventral part of the hippocampus, we could compare our parameters more precisely within a group and especially in between the control and test group. The understanding of more anterior parts as dorsal and posterior parts as ventral along the dorso-ventral axis of the HC has previously been applied (Kheirbek et al., 2013).

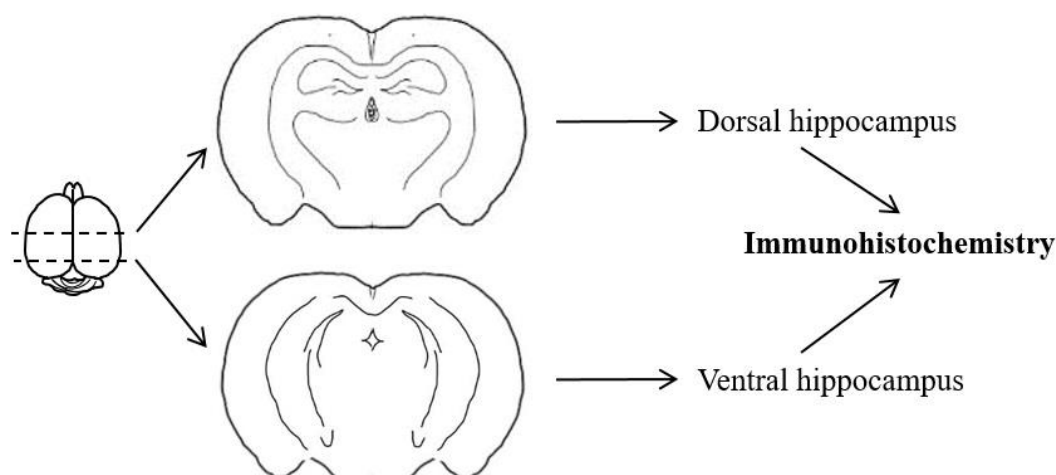


Figure 6: Experimental scheme indicating the chosen subdivision of the hippocampus into dorsal and ventral sections.

5.4.3 Immunostaining

This subsection has been previously published in Frey et al., 2020.

Coronal brain sections were first washed three times for 10 min in PBS, blocked in blocking solution (see Table 1) for 45 min at room temperature (RT) and subsequently incubated with primary antibodies in blocking solution at 4°C overnight. After that, free-floating sections were washed three times for 10 min in PBS and incubated with secondary antibodies (see Table 2) diluted in blocking solution for 2h at RT. Sections were incubated with 4',6-diamidino-2-phenylindole (DAPI, 2 µg/ml) for nuclear staining for 5 min at RT and washed three times for 10 min in PBS. After washing, the sections were mounted on Superfrost glass slides (Carl Roth, Germany) with Cryomount (Tissue-Tek® O.C.T. Compound, Sakura® Finetek, Japan), (**Figure 7**). Slides were stored at 4°C before imaging.

5.4.3.1 Marker for Staufen2

For immunostaining of Staufen2 appearance in the glial-labeled transgenic mice, polyclonal rabbit anti-Stau2 antibody was used. This RBP marker was co-stained with GFP to label whether Stau2 is present in the different glial cell types in mice.

5.4.3.2 Proliferation markers

To get insight into the ongoing proliferative processes in control and test mice, I used anti-Ki-67 antibodies. Ki-67 is a nuclear protein that is ubiquitously expressed, but only present in proliferating cells (Weigel et al., 2010). The dilution of Ki-67 was previously tested (Vallejo et al., 2017) and provided by the company.

5.4.3.3 Glial markers

In the transgenic mice expressing GFP, staining for the glial cell types was performed using anti-GFP antibodies. In the main research project, regarding WT and Stau2^{GT} mice we used anti-GFAP to mark glial cells, but also early neuronal progenitors (McCall et al., 1996).

5.4.3.4 Neuronal markers

As mentioned above, Doublecortin (DCX) is a representative marker of newborn neurons in the adult dentate gyrus (Couillard-Despres et al., 2005; Rao et al., 2004). To distinguish these cells from mature neurons, DCX was combined with anti-NeuN antibody (Mullen et al., 1992). This combination was used for the quantitative analysis of DCX+ neurons and their dendrites (representing immature neurons).



Figure 7: Ventral and dorsal mice brain slices mounted on one microscope slide for immunostaining. Abbrev.: DH, dorsal hippocampus; VH, ventral hippocampus (Figure modified from Frey et al., 2020).

5.4.4 Confocal microscopy

This subsection has been previously published in Frey et al.,2020.

Confocal microscopy was realized using an inverted Leica SP8 microscope (Leica Microsystems, Germany, provided by the Bioimaging Facility at the BMC) with lasers for 405, 488, 552 and 638 nm excitation, respectively. Images were taken with a 40×1.3 oil objective for DCX quantification. AF488, Cy3, AF555 and AF647 were recorded with hybrid photo detectors and DAPI with a photomultiplier tube. (Follwaczny et al., 2017; Frey et al., 2020). Overview images with high resolution were obtained with a 20×1.3 oil objective. For comparison of the DG between different animals, the same number of tile scans for each dentate gyrus was chosen (6 tiles for the dorsal, 7 tiles for the ventral hippocampus, each at 290,71x290,71 μm , (**Figure 8**). As the dendrites don't sprout in a planar level, the dentate gyrus was imaged with a depth of around 10 μm (9,98 μm) for every tile scan . Therefore, the dendrites in different layers could be traced, overlapping cells could be distinguished and the manual quantification was more precisely.

Additionally, the entire granule cell layer of each dentate gyrus was analyzed, as the number of cells vary within the axes of the dentate gyrus itself and furthermore, we wanted to avoid pre-selection of areas. Overall, two entire dentate gyrus per mouse, one dorsal and one ventral, were analyzed.

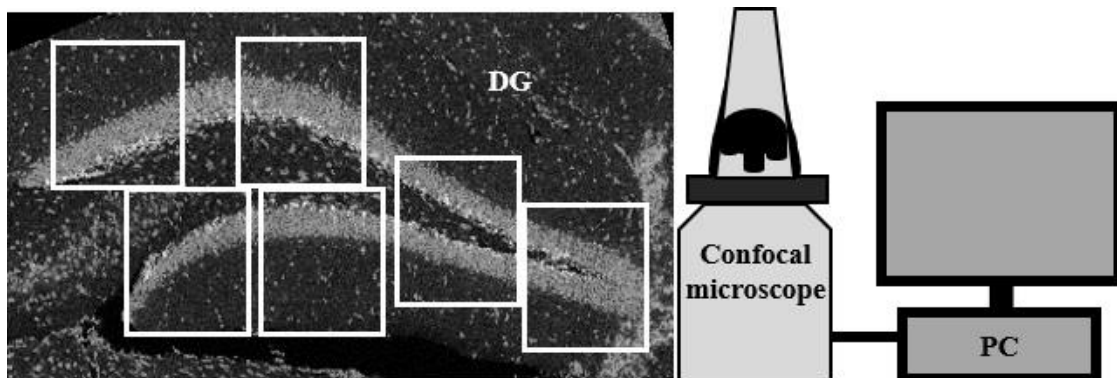


Figure 8: Confocal microscopy imaging an entire dorsal dentate gyrus by selecting each time six tile scans. Abbrev.: DG, dentate gyrus. (Figure modified from Frey et al., 2020).

5.4.5 Quantification of DCX-stained cell bodies and dendrites

In the subsequent quantification, the following parameters were investigated: the total number of DCX-positive (DCX+) cell bodies, and the total number and length of DCX+ primary, as well as secondary dendrites. The quantification was performed manually and required looking into the entire imaged dentate gyrus (x-, y-axes) including its depth (9,98 μm) to search the DCX-stained newborn neurons and their dendrites.

The criteria for including the immature neuronal cell bodies into the analysis were (i) positive DCX-staining of the cell body, together with (ii) a simultaneous DAPI-staining of its cell nucleus and a localization in the subgranular or granular zone of the DG. The dendrites were counted in, when they had direct contact to the DCX+ cell body from whom they arose and if no interruption of the staining along the dendrite was observed. The differentiation between primary and secondary dendrites was made at the first branching point of dendrites (**Figure 9**). Besides the absolute number of primary and secondary dendrites, their length was analyzed too (in μm).

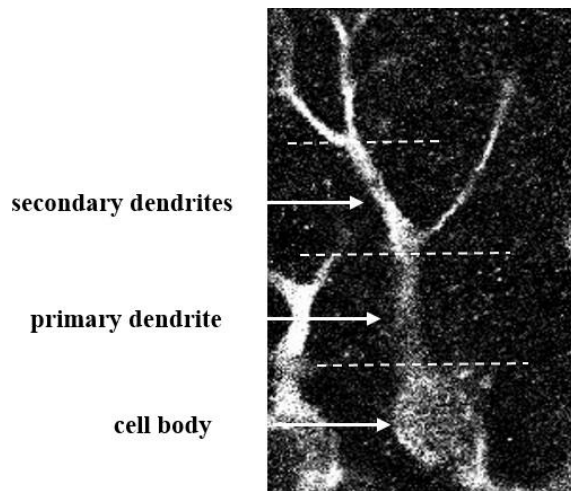


Figure 9: Representative example of a DCX-positive (DCX+) cell body and its dendritic arbor in the subgranular zone of the DG. (Figure modified from Frey et al., 2020).

5.5 Microdissection

5.5.1 Tissue preparation

This subsection has been previously published in Frey et al.,2020.

WT mice were euthanized, brains were quickly removed and stored at -80°C . Brains were dissected into 40 μm on-slide coronal slices using a cryotome (Product CM1850, Leica Microsystems, Germany). Brain slices were alternately distributed on two separate microscopic glass slide pairs (Superfrost, Carl Roth, Germany), every glass slide contained 5 brain slices and every second glass slide was taken for microdissection, according to systematic sampling (**Figure 10**). For division into a dorsal and a ventral part of the hippocampus, orientation according to Bregma -2.48mm was exploited

(**Figure 11**). Slides were stored at -80°C . For subsequent microdissection, Nissl staining was performed according to standard protocol from the Kiebler laboratory with additional advice from Jessica Olberz in the laboratory and manually microdissected as followed.

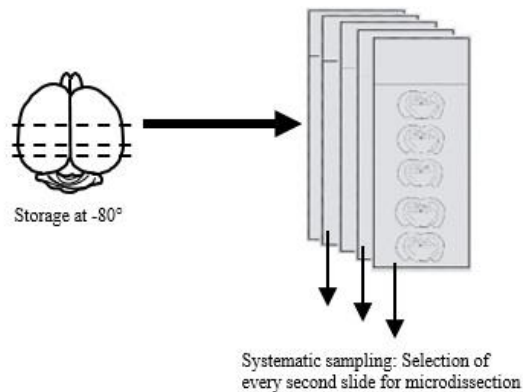


Figure 10: Tissue preparation of brain slices for microdissection. In total, five slices were mounted per microscope slide, every second one was processed for microdissection (indicated as systematic sampling in the figure; Figure modified from Frey et al., 2020).

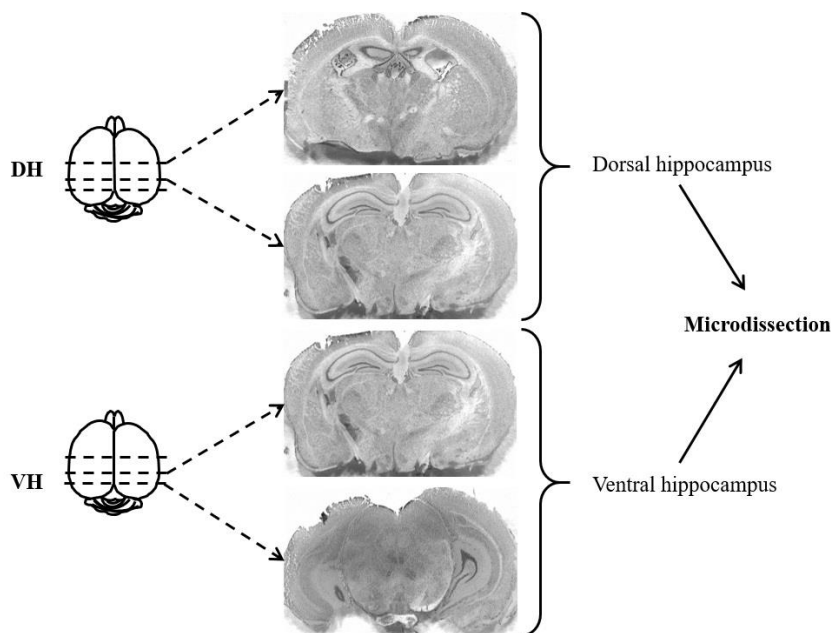


Figure 11: Manual selection of either dorsal (top) or ventral (bottom) hippocampal brain slices. All brain slices between these representative sections were collected and processed for microdissection of either the dorsal (top) or ventral hippocampus (bottom). Representative pictures of the brain slices taken with a Leica DM2500 bright-field microscope equipped with a DMC2900 CMOS camera (Bioimaging Facility BMC, Munich, Germany). Abbrev.: DH, dorsal hippocampus; VH, ventral hippocampus. (Figure modified from Frey et al., 2020).

5.5.2 Dissection using stereo microscopy

This subsection has been previously published in Frey et al.,2020.

The hippocampal neuropil and cell body layers were carefully microdissected by hand from each slice using a stereo microscope (Wild, Germany) under cooling conditions with

ice (Cajigas et al., 2012). The microdissection was separately done by using separate instruments and tubes to differentiate in between the sub regions DG, CA3 and CA1. For the DG, tissue was cut at the border of the stratum lacunosum-moleculare and the stratum moleculare of the DG. For the CA dissection, tissue was cut along the border of the stratum lacunosum-moleculare and the stratum oriens. Lateral cuts were made at the end of the DG axes, CA3-CA2, CA2-CA1 borders and near the end of region inferior in CA1 (**Figure 12**). The hippocampi from every brain of five animals per group were microdissected, giving 10 hippocampi and about 200 microdissected slices per group. Afterwards, the tissue was transmitted to frozen tubes filled with 80% ethanol and kept at -80°C before mass spectrometry. The division in ventral and dorsal hippocampus and additionally in the three sub regions led to 60 tubes for mass spectrometry.

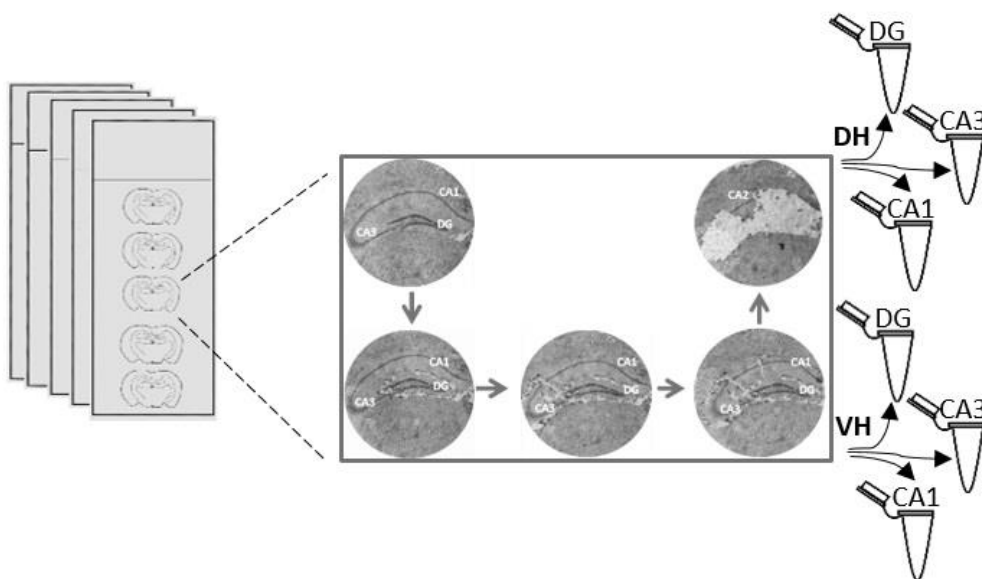


Figure 12: Microdissection and collection of hippocampal subregions (DG, CA3, CA1) from either the dorsal or the ventral hippocampus. Abbrev.: DH, dorsal hippocampus; VH, ventral hippocampus, DG, dentate gyrus; CA, cornu ammonis; (Figure modified from Frey et al., 2020).

5.6 LC Mass spectrometry

5.6.1 Tissue preparation and processing

This subsection has been previously published in Frey et al.,2020.

Proteins were extracted and trypsin digested with the Sample Preparation Kit by Preomics according to manufactures manual (see 5.1.4 Mass spectrometry preparation kit). Peptides were analyzed by LC-MS/MS by the core facility protein analytics (Prof. Axel Imhof, BMC Munich, Germany). In brief, the prepared peptide mixture was injected onto an Ultimate 3000 RSLC HPLC system (Thermo Fisher) set with an analytical column (12cm x 75µm) home-packed with C18RP Repositil-Pur AQ (2.4µm, 120 Å, Dr. Maisch, Germany) into an ESI-emitter tip (New Objective, USA). For peptide separation a linear gradient from 5-40% B (HPLC solvents A:0.1% FA, B:80% CAN, 0.1% FA) was applied

for 50 min. The HPLC was online coupled to an QExactive HF mass spectrometer (Thermo Fisher) and Data was examined by Maxquant1.5 using default parameters.

5.6.2 Data analysis

Peptide intensities were quantified using the iBAQ (intensity-based absolute quantification) values and protein intensities were compared between control and running wheel exposed animals by the core facility bioinformatics (Dr. Tobias Straub, BMC Munich, Germany).

Then, for quantitative analysis of the hippocampal proteome of both groups, with and without access to running wheels, only those proteins that were detected in all samples (57 samples) were included. The adjusted p-value < 0.20 was regarded as statistically significant (Frey et al., 2020). Since our samples showed a heterogeneous distribution of proteins in the different hippocampal regions, we additionally exploited a semi-quantitative approach to identify differentially expressed proteins. Therefore, we compared the number of replicates in which a protein was detected in a certain hippocampal subregion between control and test group. Thereby, proteins were considered as up- or downregulated when there was a difference of minimum three replicates when comparing control to test mice (**Figure 13**). An upregulated protein implies that the protein was not or less present in the biological replicates of the control group, but then detected in at least three mice of the test group. A downregulated, low abundant protein indicates that the protein was detected in the majority of control mice, but not or only less often detected in the test mice.

Regulated proteins were clustered for GO term analysis using the string database, excluding text mining (<https://string-db.org>) (Frey et al., 2020). Here, we looked into their appearance in cellular compartments, their molecular function, biological process, and KEGG pathways.

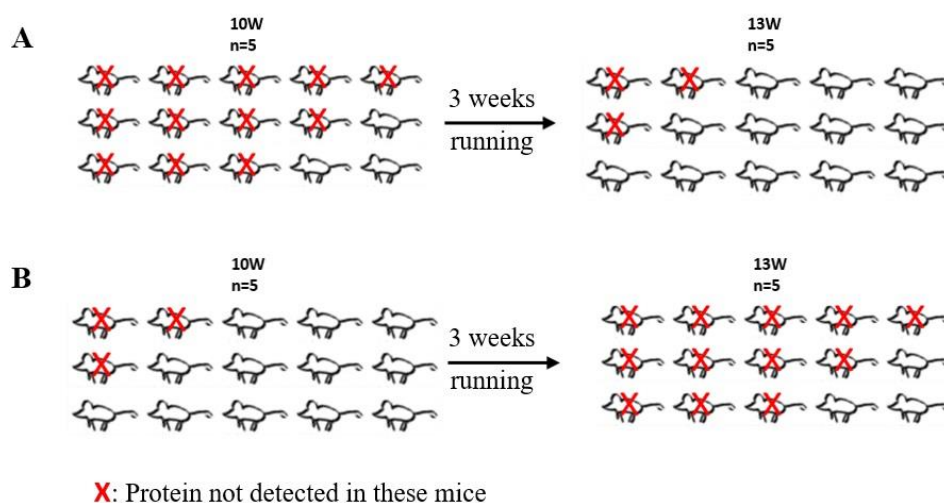


Figure 13: Experimental outline defining either the upregulation (**A**) or the downregulation (**B**) of low abundant proteins in test mice upon running compared to control mice (each group n=5). Abbrev.: W, weeks.

5.7 Statistical analysis

Data are presented as mean \pm SEM. Statistics were made with the software GraphPad Prism (Version 5; GraphPad, San Diego, USA). Data was tested for normal distribution. For two-group analysis, Mann-Whitney-U-test, for multi-group analysis Kruskal-Wallis-test was used to calculate P-values. Outliers were defined using Grubb's test (GraphPad). Statistics for proteome analysis after mass spectrometry were calculated using Student's t-test. P-value <0.05 was considered statistically significant if not stated otherwise.

6 Results

6.1 Cell proliferation and astrocytes in naive WT and *Stau2*^{GT} mice

First, we wanted to get a first overview on the cellular configuration of the dorsal and ventral hippocampus in naïve WT and naïve *Stau2*^{GT} mice. Thus, I performed Ki-67 immunostainings in both dorsal and ventral hippocampus, to quantify the number of proliferating cells in untrained WT and *Stau2*^{GT} animals.

Ki-67 is a marker for proliferation and is expressed in cell bodies. It is only present during late G1, S, M and G2 and negative in G0 phase, thus in mature neurons (Weigel et al., 2010). Ki67+ cells were present in the granular and subgranular zone of the DG, as well as rare occasionally in the pyramidal cell layer of the CA region. As expected, Ki-67+ cells were predominantly detected in the hilar region of the DG in both directions, where new neurons are generated (**Figure 14**).

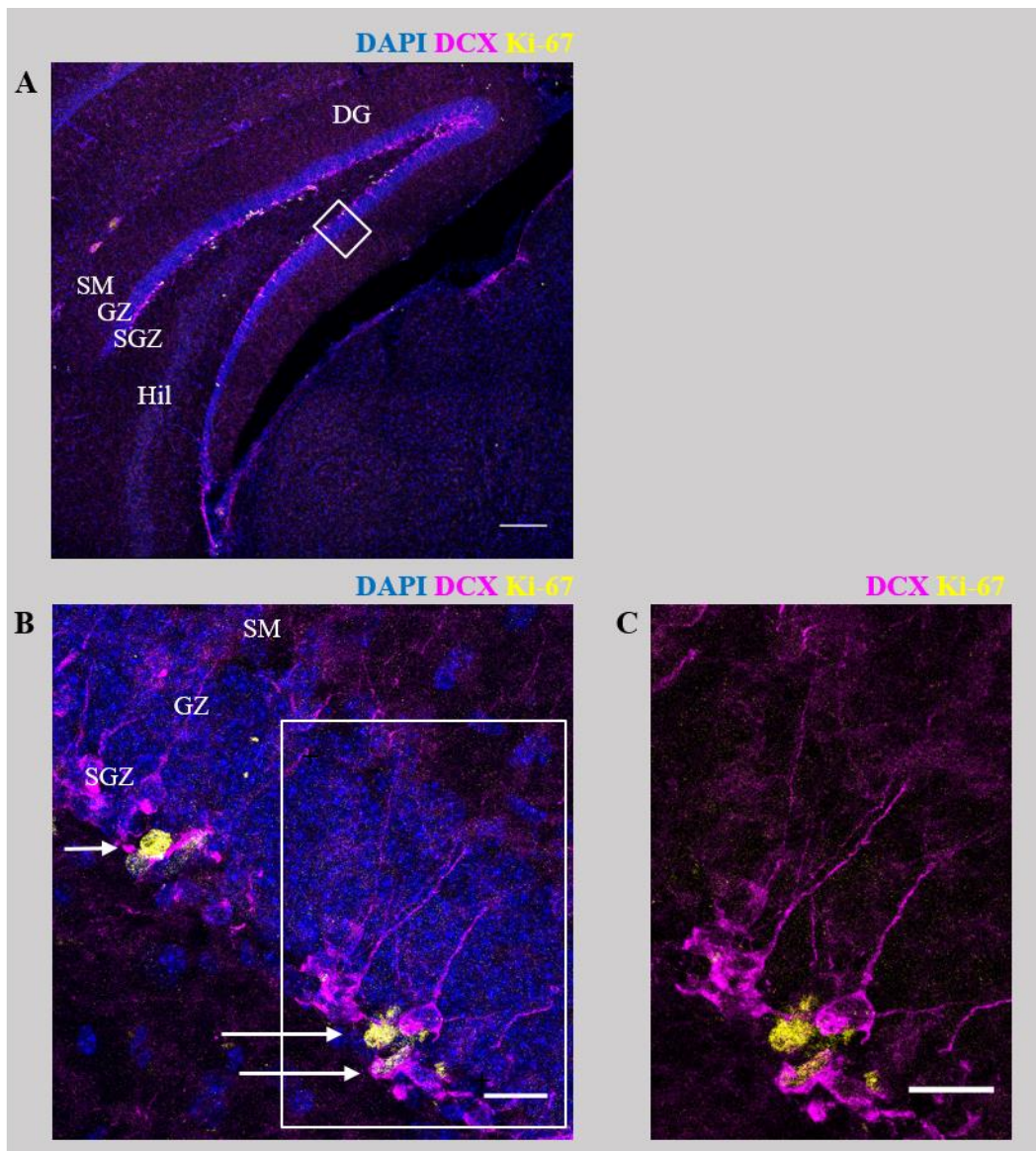


Figure 14: Immunostaining of the ventral DG of a WT control mouse using DAPI (nuclear marker), Ki-67 (proliferation marker) and DCX (marking immature neurons).

(A) Representative images of the ventral dentate gyrus showing the expression of DAPI, DCX, and Ki-67; Scale bar 150 μ m in (A).

(B) Magnified confocal image of the boxed area of the DG in A. Arrows pointing on Ki-67-positive cells (marked in yellow) in the subgranular zone.

(C) Magnified confocal image of the boxed area in B showing DCX+ and Ki-67+ cells.

Abbrev.: Hil, hilus; DG, dentate gyrus; SM, stratum moleculare; SGZ, subgranular zone; GZ, granular zone; Scale bar 15 μ m (B,C).

The absolute number of Ki67+ cells in the dorsal DG (n=3, 6 microscopic sections per entire dorsal DG) was 29.00 ± 7.292 in 10-week-old WT and 25.00 ± 4.583 in Stau2-deficient mice. In the ventral DG (n=3, 7 microscopic sections per entire ventral DG) there were 51.00 ± 20.07 Ki-67+ cells in WT mice, and 32.67 ± 5.897 ones in Stau2^{GT} mice (**Figure 15**). Thus, the initial situation in the control groups of both mice strains may differ and Stau2^{GT} mice show slightly decreased absolute numbers in proliferating cells. Yet, these results were not significant.

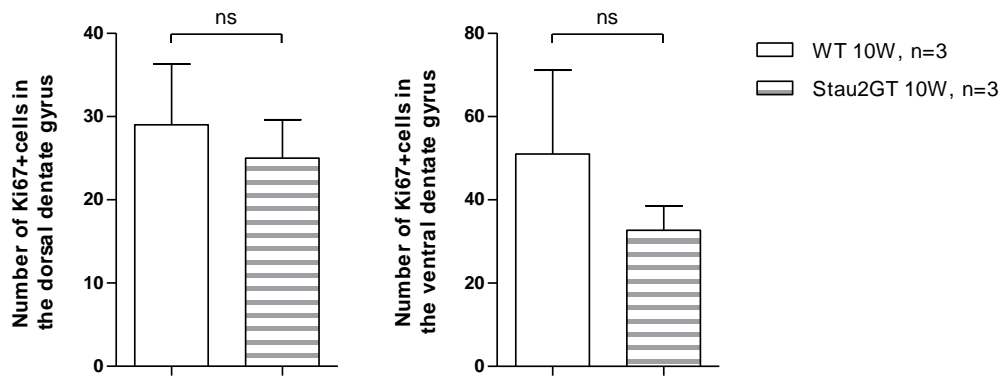


Figure 15: Absolute number of Ki-67+ cells in the dorsal (left panel) or ventral (right panel) dentate gyrus of either 10-week-old WT or Stau2^{GT} mice. Ki-67+ cell bodies located in the dentate gyrus subgranular and granular zone were counted; n=3 for both dorsal or ventral hippocampus, ns (not significant).

As mentioned above, astrocytes regulate the development, maturation and functional integration of adult-born neurons. To analyze the distribution of astrocytes slices were co-stained with GFAP. In the immunohistochemical experiments, the DCX+ neurons in the SGZ appeared to be located closely to GFAP+ astrocytes. In contrast to the SGZ, the granular zone contains a dense layer of NeuN+ mature neurons and fewer GFAP+ cells. This phenomenon has been previously observed (Song et al., 2002). There was no difference in the amount of GFAP stained cells in WT and Stau2-deficient mice, respectively.

After getting first insight into the different parts of the hippocampus, dorsal and ventral, in untrained WT and Stau2GT naïve mice, we wanted to investigate the effects of enhanced physical activity (EPA) on adult neurogenesis in the DG of dorsal and ventral hippocampus of trained WT, as well as Stau2^{GT} mice. Therefore, DCX-staining was performed to quantify the amount of newly-generated neurons and dendrites in the dentate gyrus. Then, I analyzed how EPA affects adult neurogenesis and differentiation in the dorsal and in the ventral hippocampus, and additionally whether there are differences between WT and Stau2^{GT} mice.

6.2 Enhanced physical activity selectively impacts neurogenesis in the hippocampus

The results in this subsection have been previously published in Frey et al.,2020. To investigate the impact of EPA on the generation of newborn neurons and the hippocampal proteome, I first tested whether EPA influences cellular alterations in WT mice. Therefore, I stained the hippocampus of naïve WT mice and WT mice with free access to running wheel against DCX, a marker for immature neurons as neurogenesis is known to increase in adult mice upon voluntary running (Couillard-Despres et al., 2005; Rao et al., 2004).

For EPA, mice had free access to the running wheel over a period of 3 weeks in their home cage, with voluntary use to any day-or nighttime. The revolutions were tracked, which revealed that mice constantly used their wheel provided in their cage and preferably exercised during nighttime (**Figure 16**).

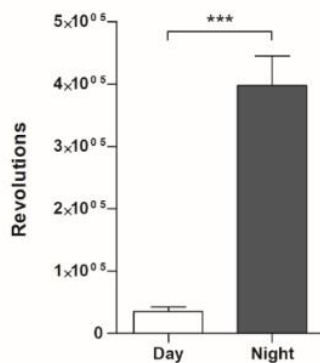


Figure 16: Number of revolutions of running wheel and day/night distribution of its use. In total, five WT mice used two wheels for a time period of three weeks. *** $P < 0.001$.

For the comparison of physical-activity-dependent adult neurogenesis, DCX staining was performed on both dorsal and ventral DG on naïve and test mice (see chapter 5.4.2 Selection of representative slices).

6.2.1 Activity-enhanced neurogenesis is limited in dorsal hippocampus

For the comparison of physical-activity-induced adult neurogenesis in WT mice, DCX staining was performed on the dorsal hippocampus (DH, see chapter 3.4.2 Selection of representative slices). For inter-individual comparison, as well as comparison in between the control and test groups identical Bregma-location of the DG was considered.

The overview image (taken with a 20x objective) presents DCX stained cells in the DG of one DH in control male WT mice (aged 10 weeks) and after EPA-induced adult neurogenesis (**Figure 17**).

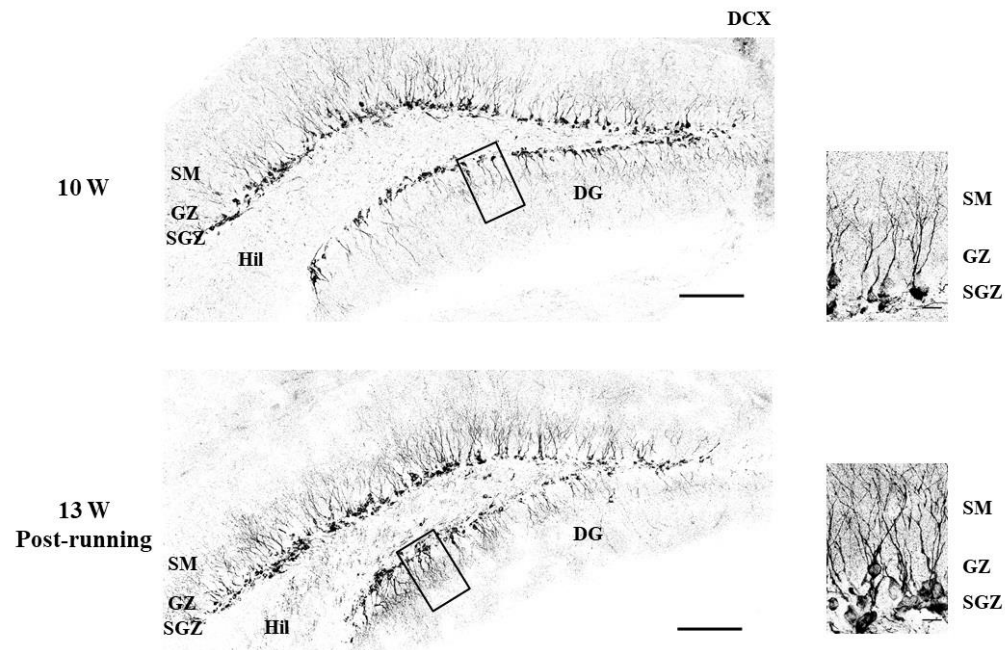


Figure 17: DCX staining of the dorsal dentate gyrus of WT mice with (13 weeks) or without running (10 weeks). Immunostaining shows intensive staining pattern of DCX+ cells and dendrites upon running (indicated as post-running). Magnified confocal images highlight DCX+ adult-born neurons in the SGZ. Black-white image conversion of the original data. Abbrev.: W, weeks; Hil, hilus; DG, dentate gyrus; SM, stratum moleculare; SGZ, subgranular zone; GZ, granular zone; Scale bar 150µm, 15µm (inset); (Figure modified from Frey et al., 2020).

Subsequently, the absolute number of DCX+ neurons and dendrites in the dorsal DG were quantified. Additionally, the length of these dendrites was measured (in µm). The manual quantification of the control mice (n=5) at the age of 10 weeks showed a broad variety in the number of DCX+ cell bodies (from 23 until up to 333 cells). This variety was not observed in the test mice post-running (n=5, mean= 206.8 ±10.18 cell bodies, **Figure A**). Due to this differential inter-individual distribution, the results on the absolute number of DCX+ cells and their number of primary and secondary dendrites were not significant, please note a possible trend towards an increase in cells and arborization.

Adult neurogenesis is not only about the generation of newborn neurons, but also about their maturation and functional synaptic integration into the neuronal network. To look into neuronal maturation, the extension of dendrites of DCX+ cells was investigated.

The quantification of dendrites revealed that activity-induced neurogenesis in mice resulted in an augmented number of primary dendrites (117.4 ± 7.167) than in controls (65.40 ± 22.34 , ns, **Figure B**). Similarly, the absolute number of secondary dendrites was increased upon running (control group: 67.20 ± 26.00 and test group: 129.6 ± 11.93 , ns, **Figure B**).

Next, the length of DCX+ primary and secondary dendrites was measured. The mean length of the primary dendrites in the controls was 14.39 ± 0.5097 µm (n=327) and of the secondary dendrites was 13.23 ± 0.4207 µm (n=336, **Figure C**). In the test group, the

measured length for both, primary and secondary dendrites, was found to be increased ($17.59 \pm 0.4509 \mu\text{m}$, $n=588$ and $15.35 \pm 0.3508 \mu\text{m}$, $n=648$, see **Fig. 18C**).

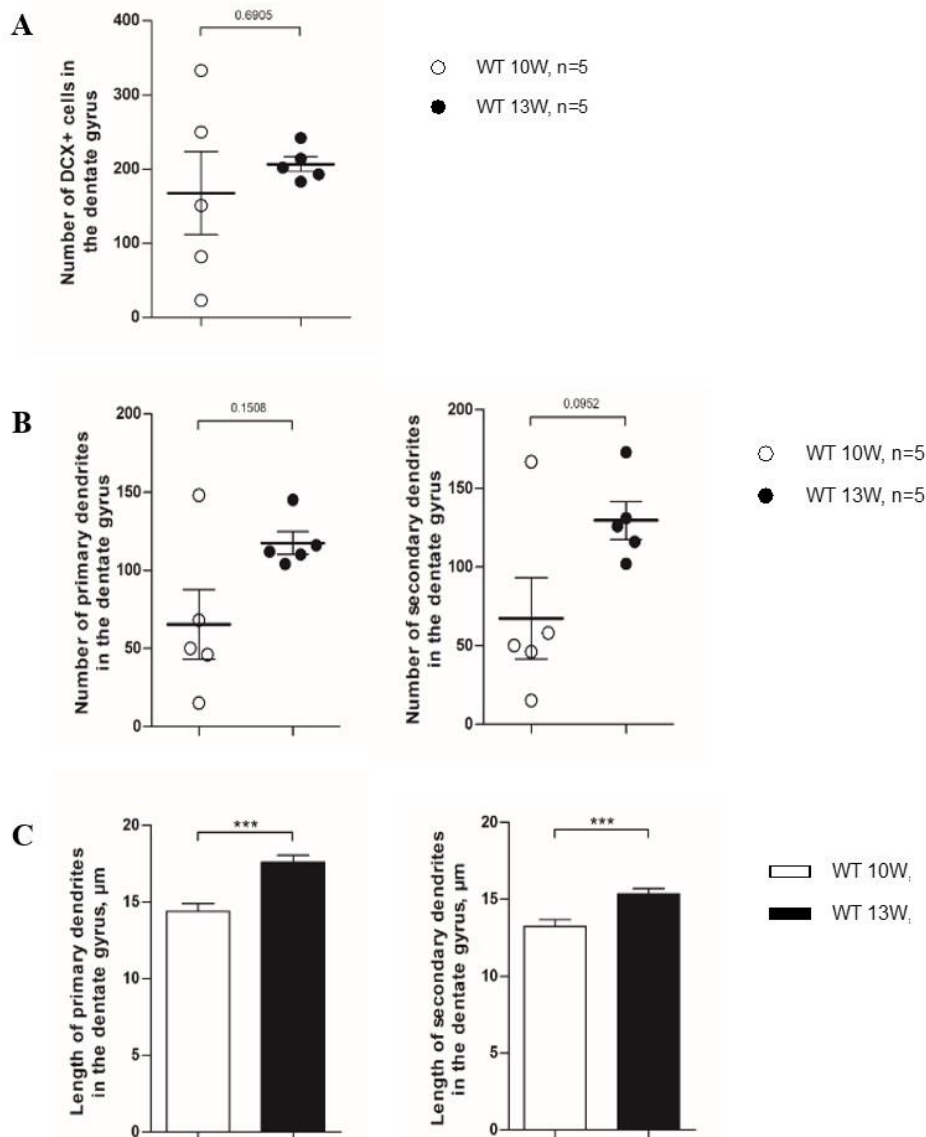


Figure 18: Quantification of DCX+ stained neurons and their dendrites in the dorsal dentate gyrus of WT aged 10 weeks (10W) and 13 weeks (13W) post-running (Figure modified from Frey et al., 2020).

(A) Absolute number of DCX+ cell bodies; $P=0.6905$;

(B) Absolute number of primary and secondary dendrites; $P=0.1508$; $P=0.0952$;

(C) Mean length of primary and secondary dendrites, respectively; primary dendrites $n=327$ (mice aged 10W) and $n=588$ (mice aged 13W post-running); secondary dendrites $n=336$ (mice aged 10W) and $n=648$ (mice aged 13W post-running); *** $P<0.001$.

To distinguish between activity-induced changes in the number of DCX+ cells and dendrites in test mice and controls, another control group containing untrained, naïve 13-week-old mice ($n=2$) was investigated. 10-week-old mice are considered as adult animals, but we wanted to assure that there are not any significant age-dependent effects.

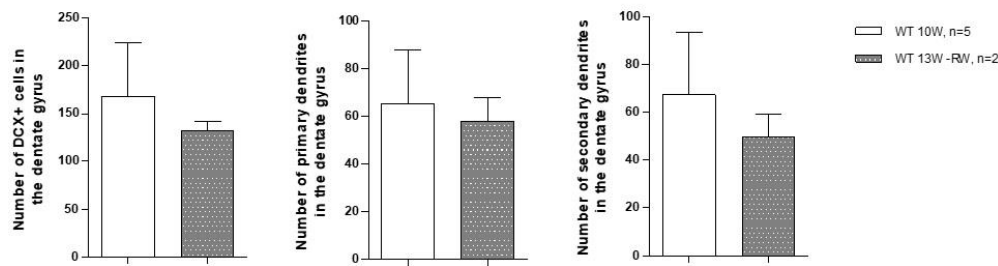


Figure 19: Comparison of absolute numbers of DCX+ cell bodies and dendrites from the dorsal dentate gyrus of either 10 week (10W, n=5) old or 13 week old mice that have not been exposed to the running wheel (13W-RW, n=2). Abbrev.: W, weeks; RW, running wheel. (Figure modified from Frey et al., 2020).

When comparing between two naïve groups, one aged 10 weeks, the other one 13 weeks, the older group showed neither an increase in the number of newly-generated neurons nor their primary and secondary dendrites (**Figure 19**). Here, all parameters were rather decreasing in the DH of aging mice and need to be investigated further with an increased number of age-even control mice. These findings are concordant with previous reports, that DCX, the marker for newly-generated neurons, is only transiently expressed and declines in aged animals (Brown et al., 2003; Couillard-Despres et al., 2005).

6.2.2 Activity-enhanced neurogenesis is increased in ventral hippocampus

The ventral parts of the hippocampus (VH) of adult WT mice were analyzed in the same manner as the dorsal hippocampus (DH, see chapter 5.4 Immunohistochemistry). After DCX staining, the absolute number of DCX+ cell bodies and their primary and secondary dendrites were counted and measured. This analysis was performed on the control group, naïve 10-week-old WT mice, and the test group, 13-week-old wild-type mice with access to running wheels for three weeks. Therefore, I investigated possible effects of EPA on adult neurogenesis in the ventral hippocampus as for the dorsal hippocampus to distinguish possible differences in the longitudinal axis of the hippocampus itself. For inter-individual comparison, as well as comparison in between the control and test group identical Bregma-location of the DG was considered.

The overview images (taken with a 20x objective) show DCX+ cell bodies in the DG of one ventral VH of the control group and one VH of the test group upon voluntary running. In the test group, the intensity of the DCX immunostaining was higher and showed a denser dendritic arborization (**Figure 20**).

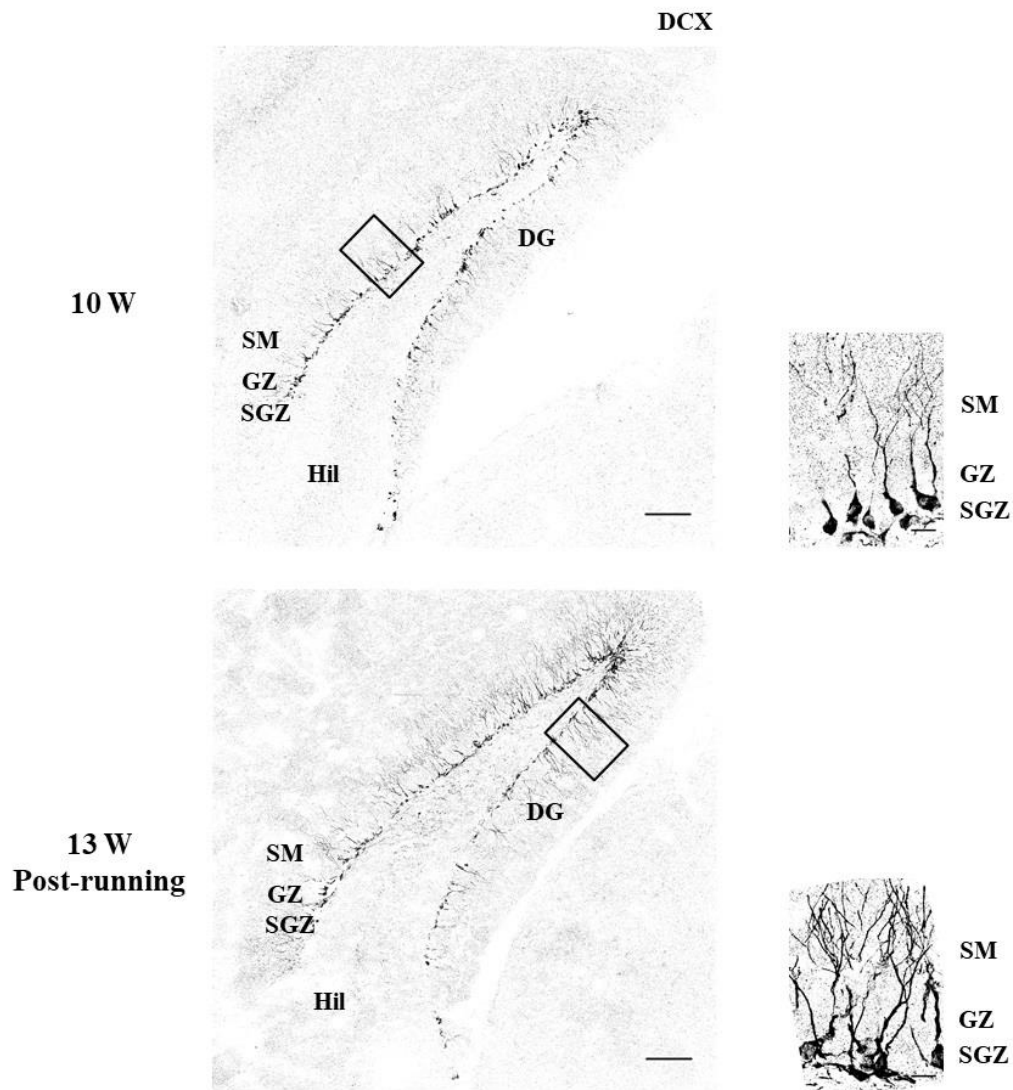


Figure 20: DCX staining of the ventral dentate gyrus of WT mice with (13 weeks) or without access to running wheels (10 weeks). Immunostaining shows an intensive staining pattern of DCX+ cells and dendrites upon running (indicated as post-running). Magnified confocal images highlight DCX+ adult-born neurons in the subgranular zone. Black-white image conversion. Abbrev.: W, weeks; Hil, hilus; DG, dentate gyrus; SM, stratum moleculare; SGZ, subgranular zone; GZ, granular zone; Scale bar 150 μ m, 15 μ m (inset); (Figure modified from Frey et al., 2020).

Consistent with the dorsal hippocampus, DCX-stained neurons of the ventral hippocampus of five biological replicates per group were quantified by counting their absolute number of DCX+ stained cells and their dendrites. On top of that, the length of these dendrites was measured (in μ m). The quantification of the control mice (n=5) at the age of 10 weeks revealed no inter-individual variety in the number of DCX+ cell bodies, as observed in the dorsal hippocampus. The absolute number of DCX+ neurons per dentate gyrus strongly increased from 130.8 ± 22.46 cells in controls to 214.0 ± 15.82 cells in test mice (**Figure 21A**).

The quantification of the absolute number of DCX+ dendrites revealed that running-induced neurogenesis in adult mice generates an absolute increase in primary dendrites (106.0 ± 10.01) compared to control mice (49.00 ± 8.385). Likewise, the total number of DCX stained secondary dendrites more than doubled (control group: 39.40 ± 11.11 , test group: 110.8 ± 16.35 dendrites, **Figure 21B**).

The mean length of primary dendrites in 10-week-old controls was $17.72 \pm 0.6665 \mu\text{m}$ ($n=245$) and of these secondary dendrites was $16.07 \pm 0.6921 \mu\text{m}$ ($n=197$). In the 13-week-old mice upon running the measured mean length for both, primary and secondary dendrites, was augmented ($19.72 \pm 0.4876 \mu\text{m}$, $n=530$ and $17.70 \pm 0.3987 \mu\text{m}$, $n=554$, **Figure 21C**).

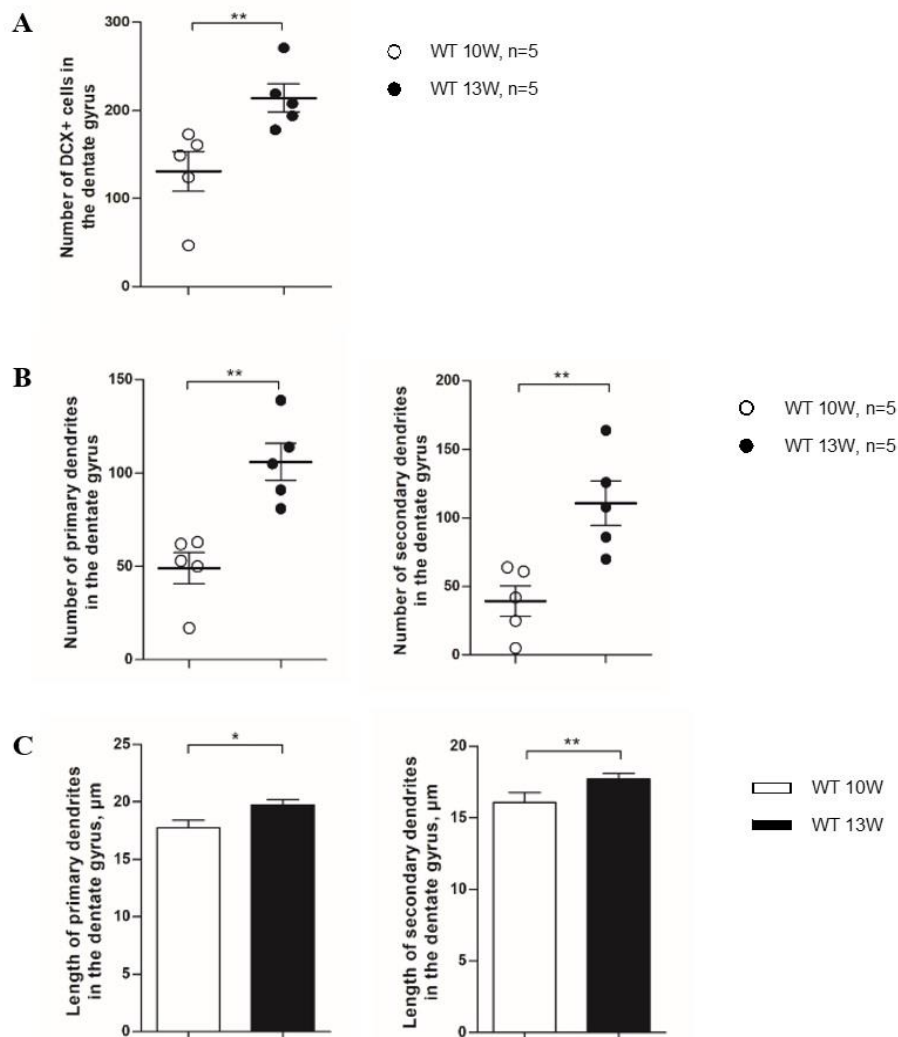


Figure 21: Quantification of DCX+ stained neurons and their dendrites in the ventral dentate gyrus of WT aged 10 weeks (10W) and 13 weeks (13W) post-running (Figure modified from Frey et al., 2020).

(A) Absolute number of DCX+ cell bodies; ** $P < 0.01$;

(B) Absolute number of primary and secondary dendrites; ** $P < 0.01$;

(C) Mean length of primary and secondary dendrites, respectively; primary dendrites $n=245$ (mice aged 10W) and $n=530$ (mice aged 13W post-running), * $P < 0.05$; secondary dendrites $n=197$ (mice aged 10W) and $n=554$ (mice aged 13W post-running), ** $P < 0.01$.

As for the DH, we investigated the VH of WT controls aged 13 weeks (n=2) that had no access to running wheels. Therefore, we could clarify that changes in the number of DCX+ cells and dendrites in test mice upon EPA are activity-induced and not due to age-dependent differences to control mice. When comparing between the two control groups both without access to running wheels, one aged 10 weeks, one aged 13 weeks, the 13-week-old mice did not show an increased absolute number of DCX+ newly generated neurons, nor an increase in primary or secondary dendrites in the VH (**Figure 22**). As mentioned above, this is consistent with the fact that 10-week-old mice are considered as adult and therefore fully mature.

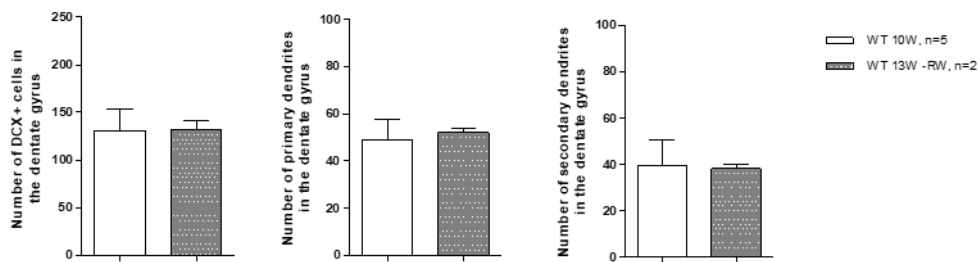


Figure 22: Comparison of absolute numbers of DCX+ cell bodies and dendrites from the ventral dentate gyrus of either 10 week (n=5) old or 13 week old mice (n=2) that have not been exposed to the running wheel. Abbrev.: W, weeks; RW, running wheel. (Figure modified from Frey et al., 2020).

Overall, quantification of DCX+ cells in the VH revealed a significant increase upon EPA (**Figure 21**). In contrast, I did not observe a significant effect on number of DCX+ cells post-EPA in the dorsal DG (**Figure**). Of note, control mice exhibited a higher variation in the number of DCX+ cells indicating great differences in neuronal maturation in the dorsal DG between individuals. These observations suggest that the number of newly born neurons differ between dorsal and ventral hippocampus upon EPA. Importantly, adult neurogenesis describes not only the generation of new neurons, but also the integration of these neurons into an existing neuronal circuit. Therefore, I also investigated the number of primary and secondary dendrites as well as their length as approximation for the ability of these DCX+ cells to integrate into an existing network. Interestingly, DCX+ cells in the ventral DG showed a higher number of primary and secondary dendrites (**Figure 21B**). The only parameter that was significantly altered in ventral and dorsal DG was the length of primary and secondary dendrites (**Figure 21C**). Importantly, the effects that I observed were specific for EPA since neither the number of DCX+ cells nor the number of primary or secondary dendrites changed between 13 and

10 weeks old control animals (**Figure 19, 22**). Thus, I concluded that EPA is sufficient to enhance neurogenesis in the hippocampus and yields distinct regional effects.

6.3 The role of Stau2 in activity-dependent adult neurogenesis

EPA activates numerous cellular processes such as neurogenesis, synaptogenesis and synaptic plasticity (Phillips et al., 2018). Even though very diverse, the processes have in common that RNA localization plays an important role. In this context, Stau2 has shown to be essential for RNA localization (Sharangdhar et al., 2017; Tang et al., 2001) and RNA transport in mature neurons (Bauer et al., 2019). To interpret a possible impact of Stau2 on EPA and the effects on adult neurogenesis, I first investigated Stau2 expression in neurons versus different glia cell types.

6.3.1 Expression of Stau2 in glial-labeled hippocampus

To see whether and in what intensity the RBP Stau2 is present in specific glia cell types, I co-stained the hippocampus of glial-labeled mouse brains with Stau2. The different brains were specifically labelled to differentiate between the different glial cell types: NG2-YFP for glial precursor cells, SOX10-GFP for oligodendrocytes and Aldh111-GFP for astrocytes. The intensity of Stau2 protein was significantly higher enriched in the dentate granule cells of the granular zone, as well as in the pyramidal cells of the CA regions. In labeled astrocytes, oligodendrocytes and NG2 glial cells, Stau2 was not specifically enriched and less expressed when compared to adjacent neurons (**Figure 23**).

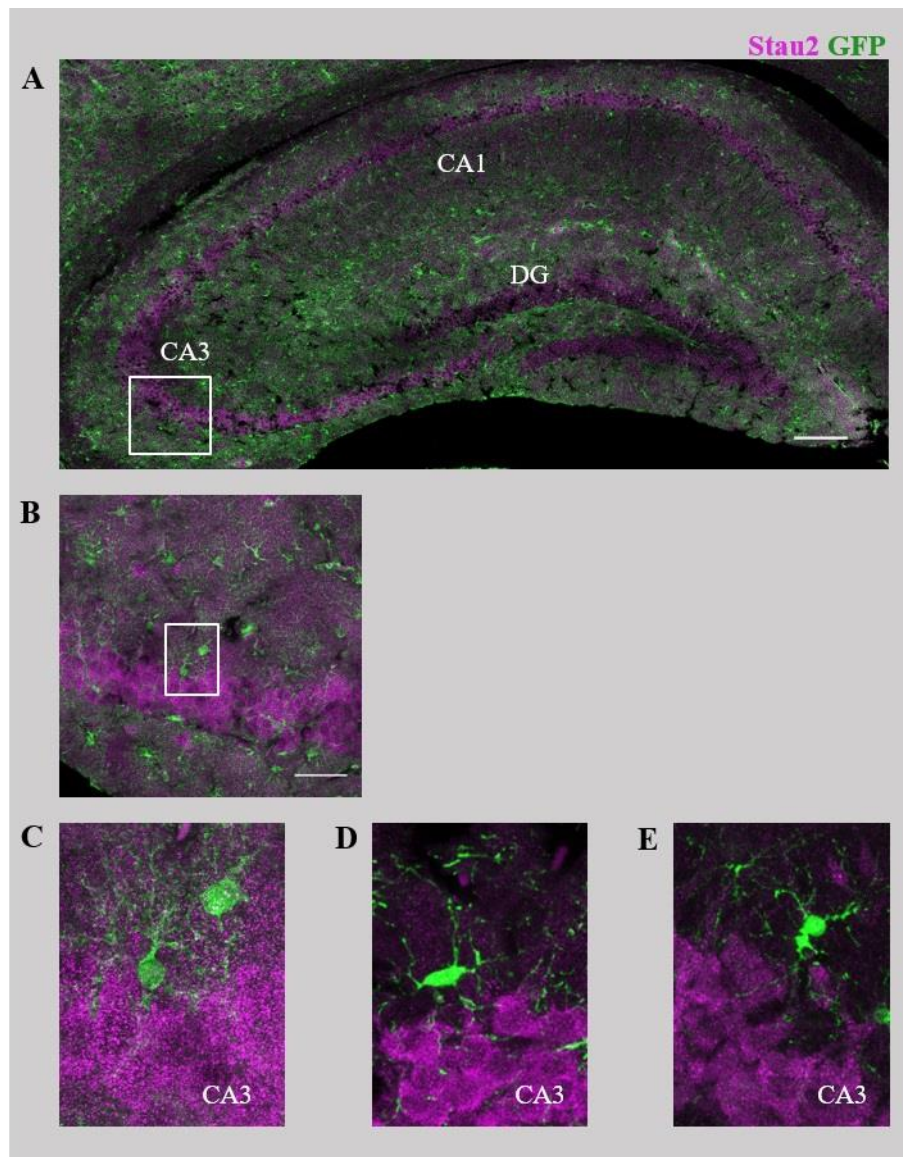


Figure 23: Immunostaining of a representative hippocampal section of glial-labeled mouse brains with GFP and Stau2.

(A) Overview of the hippocampus of *Aldh111*-targeted mice to label astrocytes. Scale bar 150 μ m.

(B) Magnified image of the boxed area in A: Stau2 positive cells and astrocytes in the CA3 region. Scale bar 15 μ m.

(C) Magnified image of the boxed area in B: GFP+ cells with typical astrocytic morphology showing low Stau2 staining when compared to the adjacent CA3 pyramidal cell layer.

(D) Magnified image of the hippocampus of *Sox10*-targeted mice to label oligodendrocytes (overview not shown): GFP+ cells with typical oligodendrocyte morphology showing low Stau2 co-staining when compared to the adjacent CA3 pyramidal cell layer.

(E) Magnified image of the hippocampus of *NG2*-targeted mice to label NG2 glia (overview not shown): GFP+ NG2 cells showing low Stau2 staining when compared to the adjacent CA3 pyramidal cell layer.

Thus, the RNA-binding protein Stau2 shows specific enrichment in neurons in the hippocampus (**Figure 23**).

Therefore, I decided to investigate the impact of Stau2 downregulation on EPA induced neurogenesis in the hippocampus. For this purpose, we used a previously published Stau2 knock-down mouse (Popper et al., 2018) and compared the number of newly-generated neurons and the extent of their dendrites by DCX-staining in naïve Stau2^{GT} controls and Stau2^{GT} mice with additional access to running wheels, and distinguished between the effects of EPA on the dorsal and ventral hippocampus, as previously applied for the WT model.

6.3.2 No effects on activity-enhanced neurogenesis in dorsal hippocampus of Stau2^{GT} mice

Here, we applied the same experimental setup aforementioned for WT mice on Stau2^{GT} mice resulting in (i) a naïve control group of Stau2^{GT} mice aged 10 weeks without running (n=3) and (ii) a test group aged 13 weeks (n=5) with free access to running wheels over a period of 3 weeks. The same Bregma-location of the dorsal part of the hippocampus as in the WT counterparts was analyzed. The overview image (taken with a 20x objective) presents DCX stained cells in the DG of one DH in Stau2^{GT} mice (aged 10 weeks) and after EPA-induced adult neurogenesis (**Figure 24**).

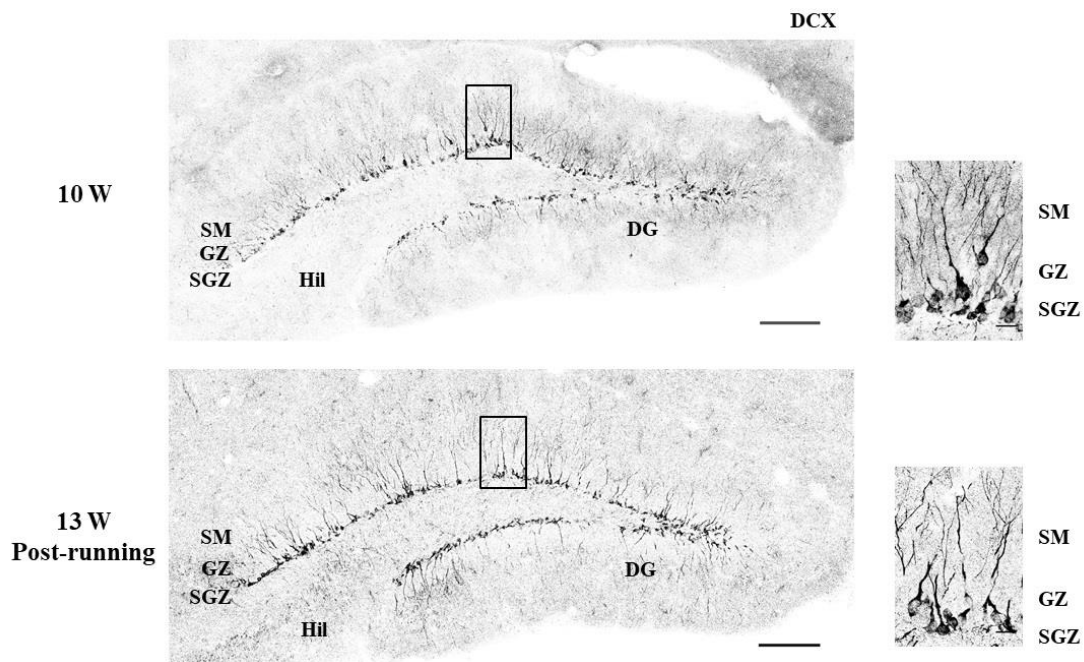


Figure 24: DCX staining of the dorsal DG of Stau2^{GT} mice with (13 weeks) or without access to running wheels (10 weeks). Immunostaining shows no increase in either DCX+ cells nor dendrites upon running. Magnified confocal images highlight DCX+ adult-born neurons in the SGZ. Black-white image conversion.

Abbrev.: W, weeks; Hil, hilus; DG, dentate gyrus; SM, stratum moleculare; SGZ, subgranular zone; GZ, granular zone; Scale bar 150µm, 15µm (inset).

The quantification of DCX revealed that there was no significant difference in neurogenesis or neuronal differentiation in *Stau2^{GT}* mice upon voluntary running, neither in newly generated neurons, nor in their primary and secondary dendrites (**Figure 25**).

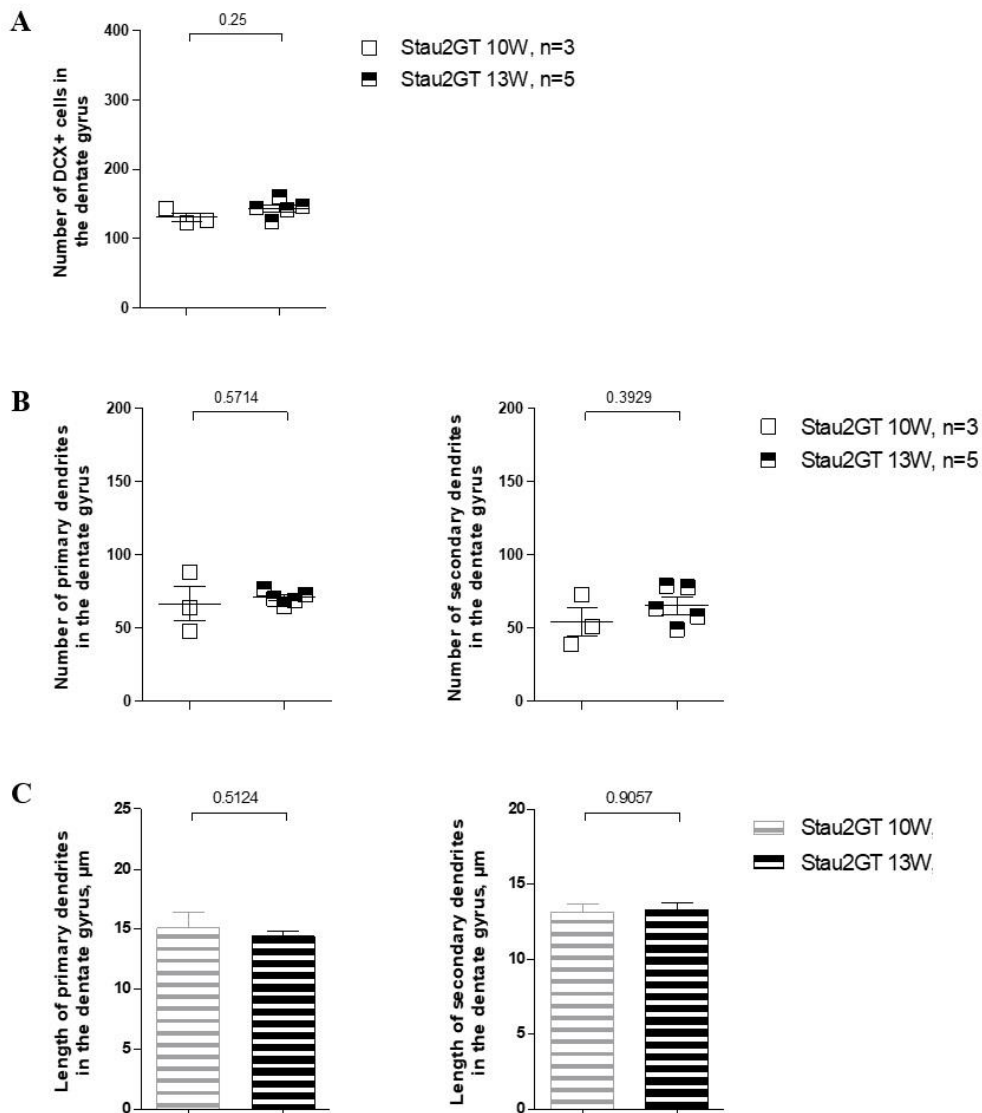


Figure 25: Quantification of DCX+ stained neurons and their dendrites in the dorsal dentate gyrus of *Stau2^{GT}* mice aged 10 weeks (10W) and 13 weeks (13W) upon running.

(A) Absolute number of DCX+ cell bodies; $P=0.25$;

(B) Absolute number of primary and secondary dendrites; $P=0.5714$; $P=0.3929$;

(C) Mean length of primary and secondary dendrites, respectively; primary dendrites $n=200$ (mice aged 10W) and $n=354$ (mice aged 13W post-running), $P=0.5124$; secondary dendrites $n=163$ (mice aged 10W) and $n=327$ (mice aged 13W post-running), $P=0.9057$.

The absolute number of DCX stained immature neurons between the groups is steady: 130.7 ± 6.227 vs. 143.4 ± 5.776 cell bodies (**Figure 25A**). The total number of primary dendrites per mice is at 66.67 ± 11.62 at 10 weeks and 70.80 ± 2.01 for mice at 13 weeks with free access to running wheels (**Figure 25B**). Consistently with these findings, the

absolute number of secondary dendrites is not increased in *Stau2^{GT}* mice upon running, 54.33±9.96 vs. 65.40±5.80, **Figure 25B**)

The mean length of primary as well as the one of secondary dendrites was not significantly changed. In 10-week-old mice, the mean length for a primary dendrite was 15.13±1.241 μm (n=200), the mean length for a secondary dendrite was 13.09±0.5990 μm long (n=163). In mice after voluntary running, the mean length for a primary dendrite was at 14.40±0.4777 μm (n=354), the secondary ones at 13.30±0.4593 μm (n=327, **Figure 25C**).

There are no effects of EPA on neurogenesis or neuronal differentiation in the dorsal dentate gyrus of adult *Stau2^{GT}* mice. Additionally, there are differences when comparing *Stau2* animals to their WT controls. In WT controls, the number of newly-generated neurons in the control group varied strongly. Upon voluntary running, the WT mice presented on average 206.8 ±10.18 and the *Stau2^{GT}* mice presented 143.4±5.776 DCX-positive cells. To investigate changes of adult neurogenesis in the entire hippocampus, this setup, for WT male mice and *Stau2^{GT}* male mice, was also explored on ventral parts of the hippocampus (see chapter 5.5.1 Tissue preparation).

6.3.3 Limited effects on activity-enhanced neurogenesis in ventral hippocampus of *Stau2^{GT}* mice

In the ventral DG, EPA shows only limited effects on the process of adult neurogenesis or differentiation. Consistent with the results in the dorsal dentate gyrus, there was no effect on the number of newborn neuron and their primary and secondary dendrites when *Stau2* is deficient. An increase in the mean length of primary and secondary dendrites could be observed. The overview images (taken with a 20x objective) show DCX+ cell bodies in the DG of one ventral VH of the *Stau2*-deficient controls and one VH of the *Stau2*-deficient test group upon voluntary running (**Figure 26**).

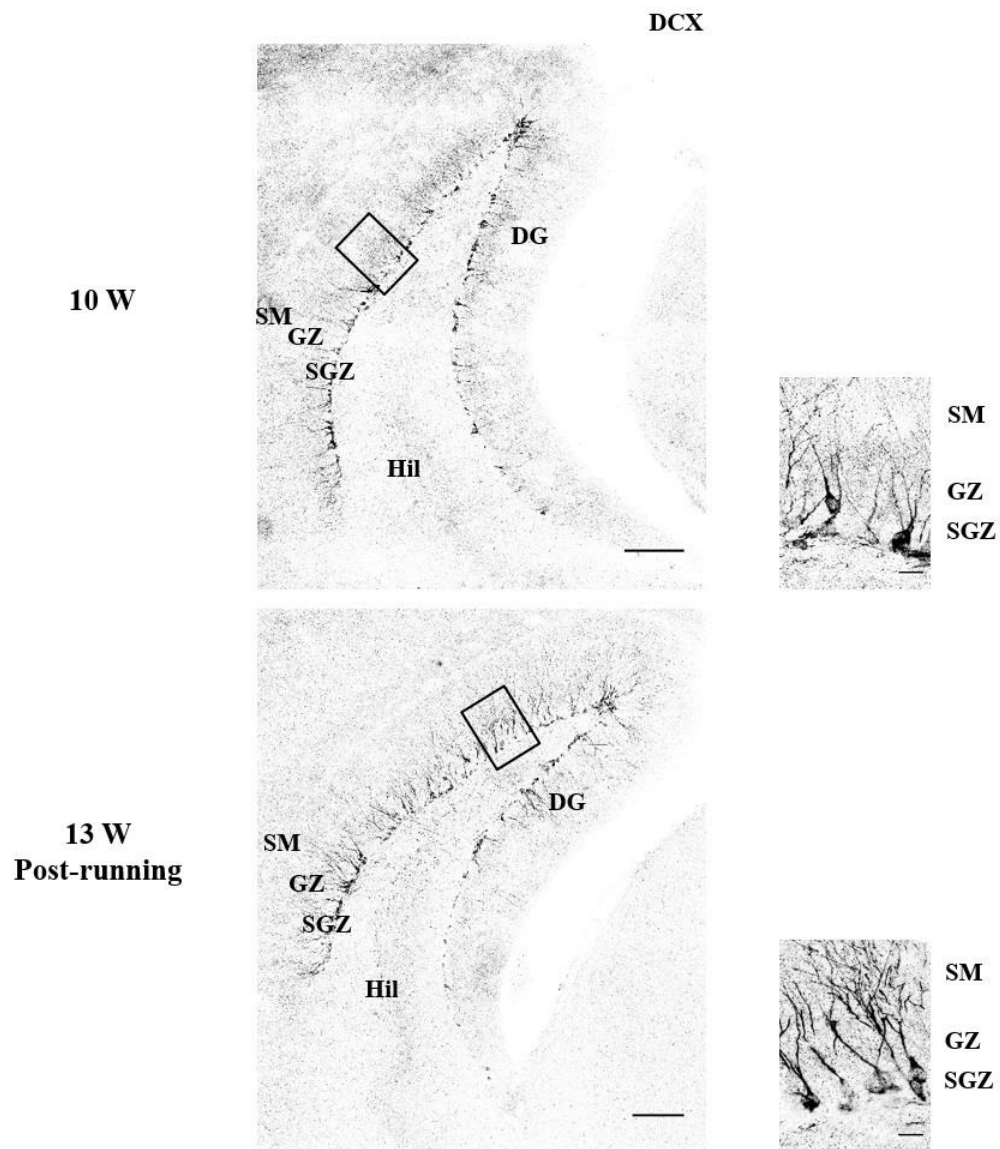


Figure 26: DCX staining of the ventral dentate gyrus of *Stau2^{GT}* mice with (13 weeks) or without running (10 weeks). Immunostaining shows no difference in the amount of DCX+ cells upon running, with a slight increase in dendritic branching. Magnified confocal images highlight DCX+ adult-born neurons in the SGZ. Black-white image conversion.

Abbrev.: W, weeks; Hil, hilus; DG, dentate gyrus; SM, stratum moleculare; SGZ, subgranular zone; GZ, granular zone; Scale bar 150 μ m, 15 μ m (inset).

There was no significant difference in the total number of DCX+ cell bodies when comparing *Stau2*-deficient controls to the *Stau2*-deficient test group after voluntary running (156.3 \pm 14.45 vs. 186.0 \pm 26.29 cells in test group, **Figure 27A**).

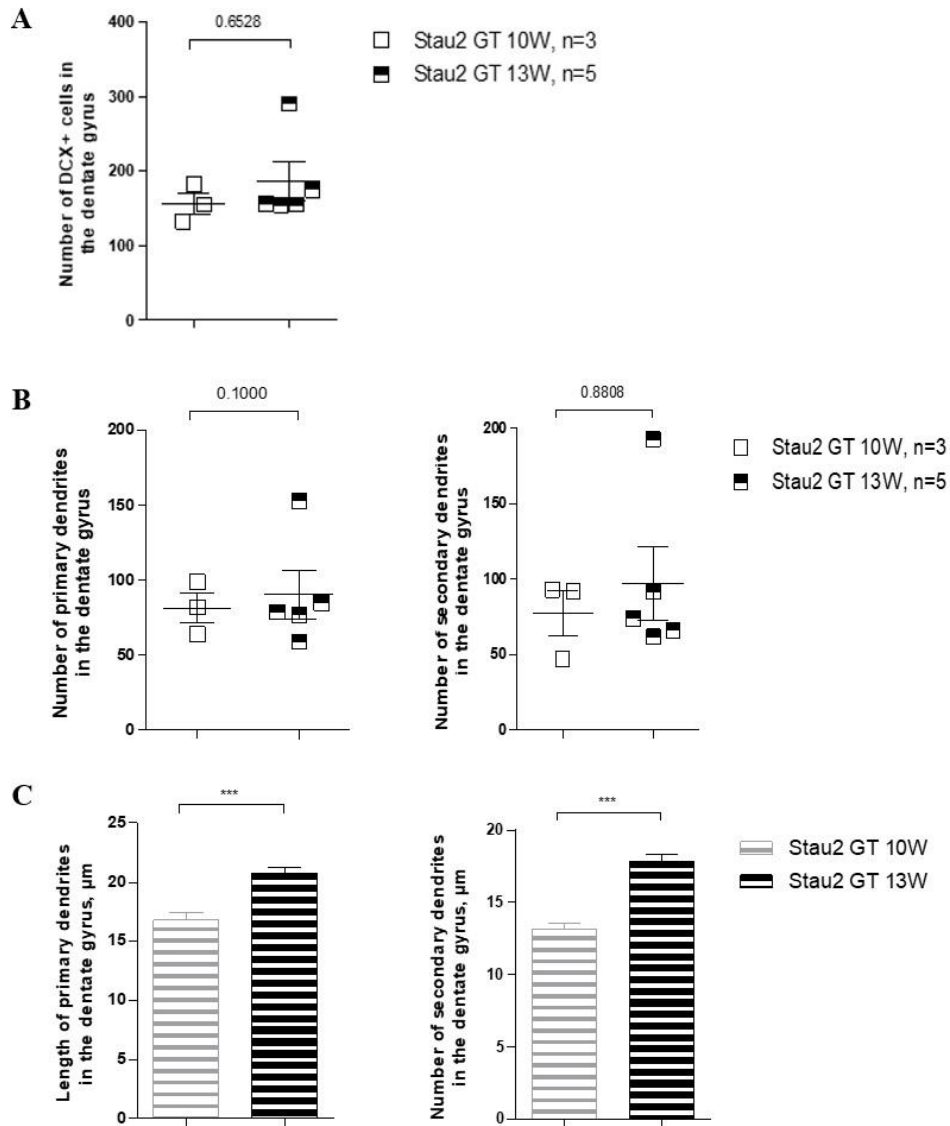


Figure 27: Quantification of DCX immunostaining in the ventral DG of Stau2^{GT} mice aged 10W and 13W post-running;

(A) Absolute number of DCX+ cell bodies; P=0.6528;

(B) Absolute number of primary and secondary dendrites; P=0.1; P=0.8808;

(C) Mean length of primary and secondary dendrites, respectively; primary dendrites n=245 (mice aged 10W) and n=453 (mice aged 13W post-running); secondary dendrites n=232 (mice aged 10W) and n=487 (mice aged 13W post-running), ***P<0.001.

Moreover, after three weeks of exercise, the absolute number of dendrites of newborn neurons did not change either. The number of primary dendrites was 81.67 ± 10.11 in controls and 90.60 ± 16.19 in test mice, and the absolute number of secondary dendrites was 77.33 ± 15.17 in controls and 97.40 ± 24.45 in test mice (**Figure 27B**). However, the mean length was significantly higher after inducing adult neurogenesis: the mean primary dendrite measures $16.78 \pm 0.6565 \mu\text{m}$ (n=245) in controls and $20.73 \pm 0.53 \mu\text{m}$ (n=453) in test mice; the mean length of secondary dendrite increased from $13.14 \pm 0.4579 \mu\text{m}$ (n=232) towards $17.86 \pm 0.4122 \mu\text{m}$ (n=487) post-running (**Figure 27C**).

Overall, there seems to be a different effect of EPA on both the longitudinal axis of the hippocampus itself and between different strains, WT versus *Stau2*^{GT} rodents. In WT mice, physical activity in the ventral hippocampus may induce adult neurogenesis. There was a significant increase in newly-generated, immature neurons, their number of dendrites as well as their observable length. In the dorsal hippocampus in WT mice, the number of DCX+ cells and dendrites did not significantly change, and the parameters of the control group strongly vary within the group. However, in the absence of *Stau2*, EPA showed no effect. There was no significant generation of new neurons, nor of their number of primary and secondary dendrites in either dorsal or ventral hippocampus, despite an increase in the mean length of dendrites in the ventral hippocampus.

Regarding the differences in the immunohistochemical experiments, mainly focusing on the generation of newly born neurons upon EPA, DCX+ cells and dendrites respectively, we decided to go a step further and look into the proteome of naïve untrained WT mice and WT mice upon physical activity.

Is the hippocampal proteome after three weeks voluntary running different towards the control groups without running? Are *Stau2* and other RBPs upregulated upon EPA? And within the hippocampus itself, do hippocampal subregions have differential proteins changing under adult neurogenesis?

6.4 Enhanced physical activity conveys proteomic alterations in the hippocampus

Naïve, untrained WT mice (n=5) and trained WT mice (n=5) with free access to running wheels for 3 weeks were compared. The subdivision in dorsal and ventral hippocampus and into the three different subregions led to 60 distinct samples for label-free mass spectrometry. After mass spectrometry analysis, we received an extensive data set showing proteomic changes upon EPA. The following results are comparing the proteome of untrained WT controls with the proteome of WT mice with additional three weeks' access to running wheels. The results in this chapter have been previously published in Frey et al., 2020.

6.4.1 Hippocampal proteome analysis

To get first insight into proteomic changes upon EPA, I first focused on the entire hippocampus. Therefore, all ventral and dorsal parts were merged and analyzed. This analysis only included proteins that were detected in all dissected samples (see chapter 5.5.2 Dissection using stereo microscopy). From all 60 samples, three replicates could not be validated by mass spectrometry, leading to a total of 57 samples. This resulted in 1627 proteins that were detected in all samples. Interestingly, 70 proteins were significantly changed upon EPA (adjusted p-value <0.2). A detailed analysis of these

proteins revealed that 20 proteins are known to have a role in growth or apoptotic processes, in locomotory behavior or in the process of neurogenesis (**Figure 28**).

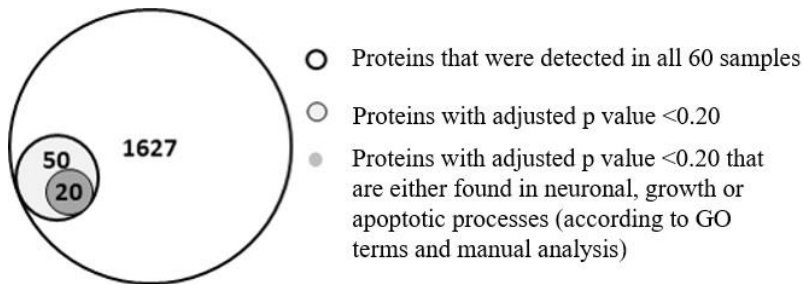


Figure 28: Venn diagram representation of the proteins identified in the DG, CA3 and CA1 region, respectively, of either the dorsal or ventral hippocampus of control and test mice. This diagram only includes proteins that were detected in all 57 samples (3 subregions per hippocampus, one dorsal and one ventral hippocampus per mice, 2 experimental groups including each 5 mice leading to 60 samples in total, excluding 3 samples that could not be detected by mass spectrometry). The number of proteins with an adjusted p value lower than 0.20 were considered to be significantly changed after EPA. (Figure modified from Frey et al., 2020).

This strict analysis identified proteins that are changed in all 57 samples upon voluntary running (n=1697 proteins). When looking into this further, proteins can either be significantly up- or downregulated in the comparison between the naïve controls and the test group after EPA regarding their fold change (significant for n=70 proteins). In the volcano plot, one can see that there were far more proteins that are significantly upregulated (n=62) than downregulated (n=8, **Figure 29**) upon EPA.

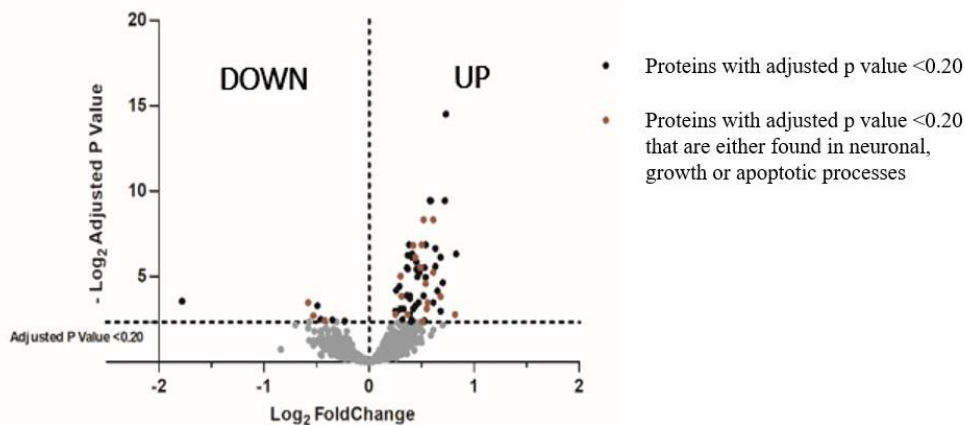


Figure 29: Volcano plot to visualize the proteomic change upon EPA. Mostly, proteins were found to be upregulated upon voluntary running. The plot shows $-\log_2$ p values versus the \log_2 fold change. Proteins in black indicate those with an adjusted p value < 0.20 (n=70); individually selected proteins are shown in red (n=20, see text for details); (Figure modified from Frey et al., 2020).

6.4.1.1 Upregulated proteins

To further nail down their possible molecular function, I clustered these proteins using Gene Ontology Terms and KEGG pathways. Interestingly, 17 upregulated proteins are located to myelin sheaths, and 26 proteins are located in mitochondrion (**Table 3**).

Table 3: Cellular component analysis of significantly upregulated proteins (n=62) in test mice upon EPA. Abbrev.: FDR, false discovery rate.

cellular component	gene count	FDR
myelin sheath	17	2.02E-18
mitochondrion	26	4.52E-12
cytoplasm	52	5.13E-11
cytoplasmic part	44	5.13E-11
membrane-bounded vesicle	32	1.18E-10

The significantly changed proteins contribute to distinct biological processes: 18 proteins generate precursor metabolites and energy; 18 overlapping proteins are involved in the nucleotide metabolic process and 16 contribute directly to energy production via the ATP metabolic pathway. The KEGG analysis revealed interesting pathways coming up. These pathways are mainly linked to molecular energy metabolism such as citrate cycle, glycolysis and gluconeogenesis, oxidative phosphorylation, as well as the synthesis of amino acids as the basic component of proteins. All these pathways contribute to molecular growth processes of cells and provide energy substrates to augment neuronal function and therefore also takes an essential part in brain plasticity.

Importantly, 9 proteins are involved in pathways that are associated with neurodegenerative disorders: Alzheimer's, Parkinson's and Huntington's disease (**Figure 30**). These proteins are preferentially located to mitochondria, namely mitochondrial ATP synthase-coupling factor 6 (ATP5J), mitochondrial ATP synthase subunit O (ATPO), mitochondrial cytochrome c oxidase subunit 7A2 (CX7A2), NADH dehydrogenase [ubiquinone] 1 alpha subcomplex subunit 12 (NDUAC), mitochondrial NADH dehydrogenase [ubiquinone] 1 alpha subcomplex subunit 2 (NDUA2), mitochondrial acyl carrier protein (ACPM), mitochondrial NADH dehydrogenase [ubiquinone] flavoprotein 1 (NDUV1), mitochondrial cytochrome b-c1 complex subunit 1 (QCR1), mitochondrial cytochrome b-c1 complex subunit 2 (QCR2), and additionally the superoxide dismutase [Cu-Zn] (SODC) for Huntington's disease.

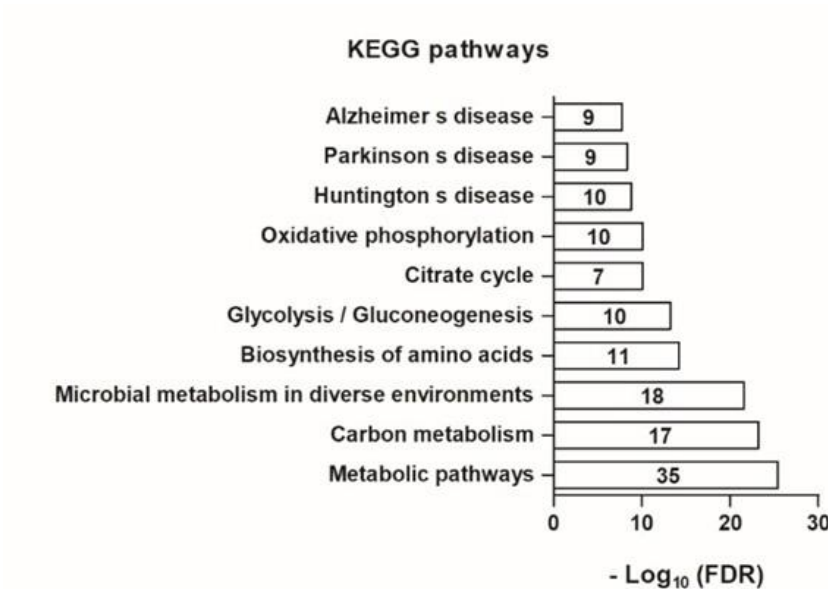


Figure 30: KEGG pathways that are significantly enriched in the upregulated proteome (n=62) of mice upon running. Abbrev.: FDR, false discovery rate; (Figure modified from Frey et al., 2020).

6.4.1.2 Downregulated proteins

From those proteins that were significantly changed upon EPA, only a small amount was significantly downregulated (n=8, **Table 4**). This group of proteins did not show any significant pathway enrichment.

Table 4: Significantly downregulated proteins in test mice upon running. Fold change <1 implies downregulation. Abbrev.: FC, fold change; Adj.P, adjusted p value.

Protein name	Gene	Adj. P	FC
Trypsin	Trypsin	0.09	0.29
Calcium-binding mitochondrial carrier protein SCaMC-3	Slc25a23	0.09	0.67
Tumor protein D52	Tpd52	0.15	0.69
Sorting nexin-12	Snx12	0.10	0.71
V-type proton ATPase subunit S1	Atp6ap1	0.18	0.73
Neuronal pentraxin-1	Nptx1	0.19	0.75
Glutathione S-transferase Mu 5	Gstm5	0.18	0.79
26S proteasome non-ATPase regulatory subunit 3	Psm3	0.19	0.85

6.4.1.3 Upregulated proteins with role in either neuronal, apoptotic or proliferative processes or locomotory behavior

In a detailed analysis of the significantly changed proteome upon EPA, I researched for proteins that are known to be involved in either neuronal, proliferative or apoptotic processes or linked to locomotory behavior in mammals (n=20), as neurogenesis and neuronal plasticity depend on a balance of positive and negative regulatory factors.

Of this selected group of 20 proteins, 17 proteins were upregulated and 3 proteins were downregulated, respectively. For each of the detected proteins, I summarized a list of published functional implications in the following, to reflect their particular function and biological processes, in which they are known to be involved in (**Table 5**).

Table 5: Manual selection of upregulated proteins with implication in neuronal, growth or apoptotic processes (n=17). Specific functional implication was individually researched; Fold change >1 indicates an upregulation.

Abbrev.: FC, fold change; Adj. P, adjusted p value; mit, mitochondrial.

Protein	Function/ Biological process	Adj. P	FC
Thioredoxin	Redox homeostasis (Berndt et al., 2006), embryonal differentiation and morphogenesis (Matsui et al., 1996), neuroprotective (Takagi et al., 1999; Zhou et al., 2013)	0.15	1.77
Prolyl endopeptidase	DNA & protein metabolic process (Nihon et al., 1998)	0.07	1.60
Elongation factor 1-alpha 2	Regulation of apoptotic process, translational elongation (Ruest et al., 2002)	0.003	1.53
Bifunctional purine biosynthesis protein PURH	Cerebral cortex development (Micheli et al., 2011)	0.03	1.53
Superoxide dismutase	Axonal transport (Shi et al., 2010), neuronal transmission (Flood et al., 1999), response to axonal injury (Reaume et al., 1996)	0.09	1.47
Mit. calcium uniporter protein	Mitochondrial calcium transport and uptake (Baughman et al., 2011), synaptic vesicle endocytosis in the CNS (Marland et al., 2016)	0.12	1.46
Sepiapterin reductase	Cell morphogenesis in neuron differentiation, dopamine & serotonin & norepinephrin metabolic process (Yang et al., 2006)	0.04	1.45
Mit. aspartat Aminotransferase	Glutamate catabolic process, neuronal mitochondrial energy metabolism (Arun et al., 2013)	0.003	1.43

Profilin-2	Actin cytoskeleton organization, regulation of synaptic vesicle exocytosis, novelty-seeking behavior (Pilo Boyl et al., 2007)	0.19	1.42
Aspartat Aminotransferase	Glutamate catabolic process, synaptic plasticity (Zhang et al., 2017)	0.01	1.41
Transforming protein RhoA	Cerebral cortex cell migration, negative regulation of neuron apoptotic process, neuron projection development, regulation of neural precursor cell proliferation & differentiation (see text for sources)	0.02	1.40
Hypoxanthine-guanine phosphoribosyltransferase	Central role in generation of purine nucleotides, neuron differentiation, positive regulation of dopamine metabolic process (Boer et al., 2001), locomotory behavior (Jinnah et al., 1992)	0.01	1.36
Glucose-6-p-isomerase	Learning and memory (Yang et al., 2012), embryonic development (Merkle et al., 1992), regulation of neuron apoptotic process (Knight et al., 2014)	0.01	1.34
Rho-related GTP-binding protein RhoB	Regulation of apoptosis (Liu et al., 2001)	0.15	1.29
Mit. succinate-semialdehyde dehydrogenase	Post-embryonic development, GABA & Glutamate metabolic process (Chowdhury et al., 2007; Gupta et al., 2004)	0.07	1.24
Mit. 2-oxoglutarate dehydrogenase	Hippocampus development (Sadakata et al., 2006)	0.03	1.23
Alanine-tRNA ligase	Negative regulation of neuron apoptotic process (J. W. Lee et al., 2006)	0.15	1.19

The analysis of pathways of these particularly selected proteins revealed implications in small molecule, carboxylic acid, amino acid and ribonucleotide metabolic processes. Six proteins, namely the hypoxanthine-guanine phosphoribosyltransferase (HPRT), mitochondrial 2-oxoglutarate dihydrogenase (ODO1), Alanine-tRNA ligase (SYAC) mitochondrial succinate-semialdehyde dehydrogenase (SSDH), bifunctional purine biosynthesis protein PURH (PUR9) as well as the transforming protein RhoA (RHOA), are implemented in the pathway for central nervous system development. While the RNA-binding protein Stau2 itself was not detected in the mass spectrometry analysis, RhoA as an upregulated protein, is a known RNA target of Stau2 (see Discussion 7.3 Actin cytoskeleton as a crucial process during EPA).

There was no significant pathway enrichment in the investigated GO Terms of the selected downregulated proteins, most likely due to its small number.

6.4.2 Hippocampal subregion proteome analysis

To systematically compare the different hippocampal subregions DG, CA3 and CA1 along the dorso-ventral axis, I exploited a semi-quantitative approach (see chapter 5.6.2 Data analysis). Thus, I compared the hippocampal dorsal parts to the ventral parts, as well as the hippocampal subregions to each other. Adult neurogenesis occurs in the DG of the hippocampus, by generating new immature neurons, but also the regions CA3 and CA1 display crucial parts in understanding this complex process and in investigating the effects of EPA, as these regions contribute to the functional circuitry of the hippocampus (Vazdarjanova et al., 2004; Vivar et al., 2012).

6.4.2.1 Changes in the dorsal hippocampus

Here, I first merged the proteomic changes upon EPA of the three subregions of the dorsal hippocampus. In the dorsal hippocampus, proteins were preferably up- rather than downregulated upon inducing adult neurogenesis: 146 proteins were increased; 51 proteins were decreased in WT mice upon running compared to their WT controls.

The GO Term analysis of the increased proteome of the dorsal hippocampus (regarding their highest significance) revealed that they amongst others mainly contribute to cellular processes (n=89), intracellular transports (n=20) and also metabolic processes (n=70), (**Table 6**).

Table 6: Biological processes of significantly upregulated proteins (n=146) in the dorsal hippocampus upon EPA. Abbrev.: FDR, false discovery rate.

Biological process	gene count	FDR
cellular process	89	0.00294
intracellular transport	20	0.00294
regulation of biological quality	34	0.00294
single-organism intracellular transport	18	0.00301
metabolic process	70	0.0102

KEGG pathway analysis demonstrated that some enriched proteins are implemented in purine metabolism (n=7) and mRNA surveillance pathway (n=5). Additionally, four proteins are involved in the regulation of mammalian target of rapamycin (mTOR) signaling (**Table 7**).

Table 7: KEGG pathways of significantly upregulated proteins (n=146) in the dorsal hippocampus of test mice upon EPA. Abbrev.: FDR, false discovery rate.

KEGG pathway	gene count	FDR
Purine metabolism	7	0.0223
mRNA surveillance pathway	5	0.0275
mTOR signaling pathway	4	0.0457

The GO Term analysis of the downregulated proteome (n=51) in the dorsal hippocampus displayed that regarding biological processes, a small number of proteins can be mapped to organelle disassembly: the mitochondrial Ribosome-recycling factor, and the three following Ubiquitin-like protein ATG12, and GABA-receptor-associated protein and protein-like 1, that over and above are involved in KEGG pathways for the regulation of autophagy. Additionally, four proteins are involved in RNA transport, that namely are the Eukaryotic translation initiation factors 1A and 1AX (IF1A and IF1AX), the protein Sec13 homolog (SEC13) and the fragile X mental retardation protein (FMRP). Interestingly, FMRP is a RNA-binding protein that acts as a negative regulator of translation and has been associated with Stau2, as they both co-localize in dendrites of mature neurons (Heraud-Farlow et al., 2014).

6.4.2.2 Subregion-specific proteome in the dorsal hippocampus

As the subregions were separately microdissected and processed for mass spectrometry, the altered proteome upon EPA can further be differentiated. The DG presented 33 proteins that were up- and 16 proteins that were downregulated. In the CA3 region, 44 proteins were enriched and 19 decreased. Importantly, the CA1 region had the highest amount of altered proteins upon activity-induced neurogenesis: 69 proteins were up- and 16 downregulated (**Figure 31**).

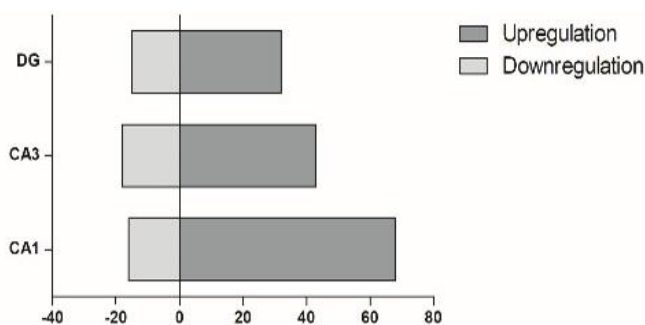


Figure 31: Differential distribution of low abundant proteins in either the DG, CA3 or CA1 of the dorsal hippocampus: light-grey bars mark the number of downregulated proteins (left part), dark-grey bars reflect the number of upregulated proteins (right part). Abbrev.: DG, dentate gyrus; CA, cornu ammonis.

Surprisingly, when comparing the proteome of the different subregions of the dorsal hippocampus with each other, the upregulated proteins in the different regions rarely

overlapped (see **Figure 32**). These few overlapping proteins could not be addressed to specific pathways.

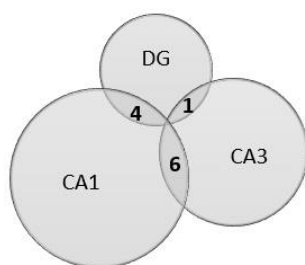


Figure 32: Venn diagram showing the subregion-specific distribution of upregulated proteins with minimal overlap in the dorsal hippocampus. Abbrev.: DG, dentate gyrus; CA, cornu ammonis.

As for the other proteome analysis, I individually selected those proteins that were upregulated upon EPA and additionally of further interest regarding an implication in proliferative, apoptotic, or neuronal processes and locomotory behavior. In a subsequent analysis, I researched proteins individually for all three subregions (**Table 8** for DG, **Table 9** for CA3, **Table 10** for CA1).

Table 8: Manual selection of upregulated proteins in the DG of the dorsal hippocampus with implications in growth, apoptotic or neuronal processes or locomotory behavior (n=11).

Protein	Function/ Biological process
Potassium/sodium hyperpolarization-activated cyclic nucleotide-gated channel 2&4	Neuronal pacemaker activity (Chen et al., 2015), glial scar formation after ischemic brain injury (Honsa et al., 2014)
Tyrosine-protein kinase JAK1	Cytokine-mediated signaling pathway, Parkinson's disease (Qin et al., 2016)
Adenylate cyclase type 8	Hippocampus dependent long-term memory (Wong et al., 1999)
Rho family-interacting cell polarization regulator 1	RhoA effector protein (Mardakheh et al., 2016)
Pumilio homolog 1	RBP and posttranscriptional regulation, locomotory behavior (Gennarino et al., 2015b)
G-protein coupled receptor family C group 5 member B	Positive regulation of neuron differentiation (Cool et al., 2010), locomotory behavior (Sano et al., 2011)
Rab5 GDP/GTP exchange factor	Neurite morphogenesis in hippocampal neurons (Mori et al., 2013)
Junctophilin-3	Regulation of neuronal synaptic plasticity, memory and exploration behavior in hippocampal neurons (Moriguchi et al., 2006), locomotory behavior (Nishi et al., 2002)

Prolactin regulatory element-binding protein	Transcription factor activity (Taylor Clelland et al., 2000)
ADP-ribosyl cyclase/cyclic ADP-ribose hydrolase 1	Dendritic organization in hippocampus (Nelissen et al., 2018)

Table 9: Manual selection of upregulated proteins in the CA3 region of the dorsal hippocampus with implications in growth, apoptotic or neuronal processes or locomotory behavior (n=18).

Protein	Function/ Biological process
Transcription elongation factor SPT5	Chromatin binding and mRNA processing (Hartzog et al., 2013)
Nuclear factor 1 B-type	Glial cell differentiation, commissural neuron axon guidance (Piper et al., 2009)
Laminin subunit alpha-4	Neuromuscular junction regulation (K. M. Lee et al., 2017)
Sister chromatid cohesion protein PDS5 homolog B	Brain atrophy, cognitive impairment (E. Lee et al., 2017)
T-lymphoma invasion and metastasis-inducing protein 1	Positive regulation of axonogenesis (Miyamoto et al., 2006; Tanaka et al., 2003)
Glutamate receptor ionotropic, delta-1	Social behavior, anxiety, neuropsychiatric diseases (Yadav et al., 2012)
Cytosolic carboxypeptidase 1	Cerebellum development, adult walking behavior (Fernandez-Gonzalez et al., 2002)
Ras-related GTP-binding protein A & B	Cell death through involvement in Ras pathway (Shibutani et al., 2017)
SLIT and NTRK-like protein 5	Social behavior, anxiety, dendrite morphogenesis (Shmelkov et al., 2010), axonogenesis (Aruga et al., 2003)
5'-AMP-activated protein kinase catalytic subunit alpha-2	Negative regulation of apoptotic process, response to stress and muscle activity (Bungard et al., 2010)
Fructose-2,6-bisphosphatase TIGAR	Neuroprotective after ischemic brain injury (Zhou et al., 2016)
Phosphatidylinositide phosphatase SAC2	Negative regulation of axon regeneration (Zou et al., 2015)
Protein farnesyltransferase subunit beta	Regulation of cell proliferation (Mijimolle et al., 2005)
Nuclear receptor-binding factor 2	Autophagy in neurons, neurodegeneration (Zhong et al., 2014)

Casein kinase I isoform delta	Dopaminergic neuron differentiation, amphetamine-induced locomotory behavior, neurite outgrowth (Li et al., 2012; Penas et al., 2015)
Rab5 GDP/GTP exchange factor	Neurite morphogenesis in hippocampal neurons (Mori et al., 2013)
Melanoma-associated antigen D1	Neuronal differentiation and survival (Mouri et al., 2013)

Table 10: Manual selection of upregulated proteins in the CA1 region of the dorsal hippocampus with implications in growth, apoptotic or neuronal processes or locomotory behavior (n=18).

Protein	Function/ Biological process
Dystonin	Axonal transport (Seehusen et al., 2016)
Ninjurin-1	Cell adhesion in brain, neuroinflammation after ischemic brain injury (H. K. Lee et al., 2017)
Tyrosine-protein kinase JAK1	Cytokine-mediated signaling pathway, Parkinson's disease (Qin et al., 2016)
Bis(5'-nucleosyl)-tetra-phosphatase [asymmetrical]	Neuroprotective after ischemic brain injury or in Parkinson's disease model (Wang et al., 2003)
GRB2-associated and regulator of MAPK protein	Growth factor receptor signaling, MAPK regulator (Taniguchi et al., 2013)
E3 ubiquitin-protein ligase UBR3	Regulation of sensory pathways, embryonic development (Tasaki et al., 2007)
Glutamate receptor ionotropic, delta-1	Social behavior, anxiety, neuropsychiatric diseases (Yadav et al., 2012)
Phosphatidylinositide phosphatase SAC2	Negative regulation of axon regeneration (Zou et al., 2015)
Huntingtin-interacting protein 1	Apoptotic process, Huntington's disease (Gervais et al., 2002)
Short transient receptor potential channel 4	Dendritic GABA release (Munsch et al., 2003), involvement in epileptiform discharges (Wang et al., 2007)
Protein quaking	RBP, myelination, oligodendrocyte differentiation, axon ensheathment (Darbelli et al., 2017)
Mitochondrial evolutionarily conserved signaling intermediate in Toll pathway	Embryonic development, role in BMP signaling pathway (Xiao et al., 2003)
Annexin A2	Cerebral angiogenesis, social behavior, anxiety

	(Weiss et al., 2016)
PRKCA-binding protein	Synaptodepressive effects in Alzheimer's disease (Alfonso et al., 2014)
Protein farnesyltransferase subunit beta	Regulation of cell proliferation (Mijimolle et al., 2005)
Fucose mutarotase	Neuron differentiation, sexual behavior (Park et al., 2010)
NIF3-like protein 1	Neuron differentiation (Akiyama et al., 2003)
Zinc finger and BTB domain-containing protein 18	Hippocampus, cerebellum, cerebral cortex development, neuron development (Okado et al., 2009)

6.4.2.3 Changes in the ventral hippocampus

Likewise, as in the dorsal hippocampus, proteins in the ventral hippocampus were preferably upregulated rather than downregulated after EPA. 87 proteins were enriched and 57 proteins were decreased in test mice after running compared to their controls.

The GO Term analysis of the increased proteome of the ventral hippocampus regarding their highest significance in biological processes, revealed participation in single-organism, and likewise as in the dorsal hippocampus, in cellular and metabolic processes (**Table 11**).

Table 11: Biological processes of significantly upregulated proteins (n=87) in the ventral hippocampus upon EPA. Abbrev.: FDR, false discovery rate.

Biological process	gene count	FDR
single-organism biosynthetic process	15	0.00741
organophosphate metabolic process	12	0.0126
cellular metabolic process	43	0.0164
metabolic process	47	0.0235
single-organism cellular process	49	0.0359
response to stimulus	36	0.0359

KEGG analysis confirmed that some enriched proteins are implemented in different pathways (**Table 12**). Cell proliferative processes were upregulated as in purine metabolism (n=5). Additionally, proteins are involved in mTOR signaling (n=3): 5'-AMP-activated protein kinase catalytic subunit alpha-2 (Prkaa2), GTP-binding protein Rheb and Hamartin. On top of that, others are implemented in Rap signaling paths: Adenylate cyclase types 3, 5, and 8, Ras-related C3 botulinum toxin substrate 3 (Rac3) and Ras-related protein Rap-1b (Rap1b) itself. Interestingly those proteins from these two specific pathways play a further role in hormone signaling related to Oxytocin (n=5) and Insulin (n=4). Moreover, they have specific implications in neuronal processes (separately described in the following tables).

Table 12: KEGG pathways of significantly upregulated proteins (n=87) in the ventral hippocampus of test mice upon running. Abbrev.: FDR, false discovery rate.

KEGG pathways	gene count	FDR
Purine metabolism	5	0.037
Oxytocin signaling pathway	5	0.037
Pancreatic secretion	4	0.037
Dilated cardiomyopathy	4	0.037
Rap1 signaling pathway	5	0.0498
mTOR signaling pathway	3	0.0498
Platelet activation	4	0.0498
Insulin signaling pathway	4	0.0498

The downregulated proteome of the ventral hippocampus could not be subdivided into specific pathways, only the cellular component, indicating that the downregulated proteome is mainly located intracellular and in the cytoplasmic component of cells.

6.4.2.4 Subregion-specific proteome in the ventral hippocampus

In parallel to the analysis of the dorsal hippocampus, the ventral hippocampal subregions, DG, CA3 and CA1 region were separately analyzed.

The DG encloses 20 proteins that were up- and 17 that were downregulated, in the CA3 region 30 proteins were enriched and 20 decreased, and the CA1 region presents the highest amount of altered proteins after activity-induced neurogenesis: 37 proteins were up- and 20 downregulated (**Figure 33**).

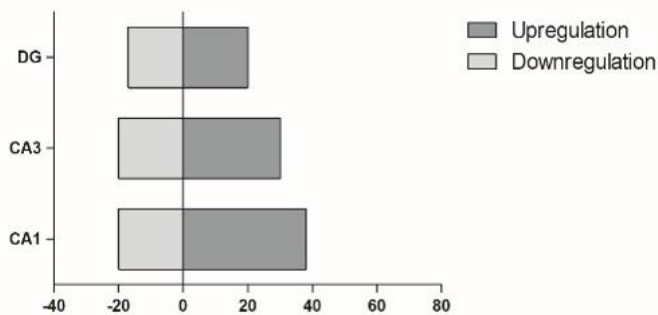


Figure 33: Differential distribution of proteins in either the DG, CA3 or CA1 of the ventral hippocampus: light-grey bars mark the number of downregulated proteins (left part, negative absolute numbers), dark-grey bars reflect the number of upregulated proteins (right part, positive absolute numbers). Abbrev.: DG, dentate gyrus; CA, cornu ammonis.

As observed in the dorsal hippocampus, the proteome data sets of the three different subregions DG, CA3 and CA1 in the ventral hippocampus showed little overlap. Only two proteins were enriched in CA3 as well as CA1 (**Figure 34**): Cad protein (PYR1) and the protein farnesyltransferase subunit beta (FNTB), that are both implicated in proliferative processes (Mijimolle et al., 2005; Sato et al., 2015). Interestingly, FNTB was also upregulated in CA3 and CA1 region of the dorsal hippocampus (**Tables 9 and 10**).

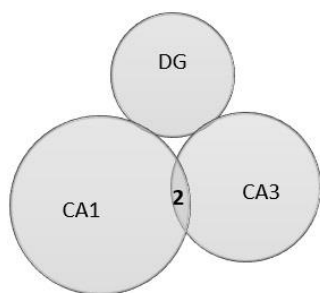


Figure 34: Venn diagram showing the subregion-specific distribution of upregulated proteins with minimal overlap in the ventral hippocampus.

Abbrev.: DG, dentate gyrus; CA, cornu ammonis.

Subsequently, I individually selected proteins independently for all three subregions that are of further interest regarding an implication in proliferative, apoptotic, and especially neuronal processes and locomotory behavior (**Table 13** for the DG, **Table 14** for CA3 and **Table 15** for CA1).

Table 13: Manual selection of upregulated proteins in the DG of the ventral hippocampus with implications in growth, apoptotic or neuronal processes or locomotory behavior (n=9).

Protein	Function/ Biological process
Adenine phosphoribosyltransferase	Purine ribonucleoside salvage pathway (C. L. Wu et al., 1993)
Potassium voltage-gated channel subfamily A member 2	Regulation of dopamine secretion (Fulton et al., 2011), neuron excitability (Douglas et al., 2007)
O-acetyl-ADP-ribose deacetylase MACROD2	Brain development (Maas et al., 2007)
Fructose-2,6-bisphosphatase TIGAR	Neuroprotective after ischemic brain injury (Zhou et al., 2016)
Ras-related protein Rap-1b	Synaptic plasticity and vesicle exocytosis, fear learning, cortico-amygdala plasticity (Subramanian et al., 2013)
Hamartin	Hippocampus and cerebral cortex development, myelination (Meikle et al., 2007)
Tumor necrosis factor receptor superfamily member 21	Neuron apoptotic process (Nikolaev et al., 2009), myelination, oligodendrocyte differentiation and apoptotic process (Mi et al., 2011)
Ubiquitin conjugation factor E4 B	Neuron projection development (Kaneko-Oshikawa et al., 2005)
Amyloid-like protein 1	forebrain development (Herms et al., 2004)

Table 14: Manual selection of upregulated proteins in the CA3 region of the ventral hippocampus with implications in growth, apoptotic or neuronal processes or locomotory behavior (n=13).

Protein	Function/ Biological process
CAD protein	Pyrimidine synthesis, downstream effector of Rheb (Sato et al., 2015)
Neurogranin	Synaptic loss, associated with Alzheimer's disease (Esteve et al., 2017)
Cytosolic carboxypeptidase 1	Cerebellum development, adult walking behavior (Fernandez-Gonzalez et al., 2002)
Voltage-dependent calcium channel subunit α -2/d-2	Synaptic transmission, cerebellar pacemaking (Walter et al., 2006)
Guanine nucleotide-binding protein G(olf) subunit alpha	Dopamine and adenosine signaling, response to amphetamine, locomotory behavior (Herve et al., 2001)
Adenylate cyclase type 3	Olfactory learning, cAMP synthesis (Wong et al., 2000)
SLIT-ROBO Rho GTPase-activating protein 1	Neuronal migration, Rho protein signal transduction (Wong et al., 2001)
GTP-binding protein Rheb	Cell growth through pyrimidine synthesis (Sato et al., 2015), positive regulation of oligodendrocyte differentiation (Zou et al., 2014)
GRB2-associated and regulator of MAPK protein	Growth factor receptor signaling, MAPK regulator (Taniguchi et al., 2013)
Protein argonaute-2	Post-embryonic development (Cheloufi et al., 2010)
Protein farnesyltransferase subunit beta	Regulation of cell proliferation (Mijimolle et al., 2005)
Myotubularin-related protein 2	Neuron development, myelin assembly (Vaccari et al., 2011)
Transforming acidic coiled-coil-containing protein 1	Neurogenesis, cerebral cortex development (Xie et al., 2007)

Table 15: Manual selection of upregulated proteins in the CA1 region of the ventral hippocampus with implications in growth, apoptotic or neuronal processes or locomotory behavior (n=13).

Protein	Function/ Biological process
CAD protein	Pyrimidine synthesis, downstream effector of Rheb (Sato et al., 2015)
ADP-ribosylation factor-like protein 6	brain development (Zhang et al., 2011)
Adenylate cyclase type 8	Hippocampus dependent long-term memory (S. T. Wong et al., 1999)
Neuropathy target esterase	Embryonic development, axonal integrity (Moser et al., 2004)
Cytochrome P450 7B1	Neurosteroid metabolism (Yau et al., 2003)
Glutamate receptor ionotropic, delta-1	Social behavior, anxiety, neuropsychiatric diseases (Yadav et al., 2012)
5'-AMP-activated protein kinase catalytic subunit alpha-2	Negative regulation of apoptotic process, response to stress and muscle activity (Bungard et al., 2010)
Netrin receptor UNC5A	Axon guidance in thalamus (Powell et al., 2008)
Protein farnesyltransferase subunit beta	Regulation of cell proliferation (Mijimolle et al., 2005)
Neuroigin-1	Neuron system development and differentiation (Scheiffele et al., 2000), synaptogenesis, dendritic spine development (Kwon et al., 2012)
Ubiquitin-like-conjugating enzyme ATG3	Apoptotic process, mitochondrial homeostasis, pluripotency maintenance of embryonic stem cells (Liu et al., 2016)
Adenylate cyclase type 5	Adenylate cyclase-activating dopamine receptor signaling pathway, neuroleptic effects of antipsychotics (K.-W. Lee et al., 2002), locomotory behavior (Iwamoto et al., 2003)
Ras-related C3 botulinum toxin substrate 3	Rho family of GTPases member, cerebral cortex and hippocampal GABAergic interneuron development, neuron maturation and synaptic transmission (Vaghi et al., 2014), locomotory behavior (Corbetta et al., 2005)

The complete mass spectrometry protein dataset is available in electronic form upon request from Prof. Kiebler, BMC Munich.

7 Discussion

7.1 Differential effects of enhanced physical activity on dorsal and ventral hippocampus

The mammalian hippocampus can be divided in its different subregions, the DG, the CA regions and the subiculum (Du et al., 2016; Vivar et al., 2012). The DG presents its major input region and sends its efferent structures mainly to the pyramidal cells of the CA3 region, but also to mossy cells and interneurons located in the DG itself. Additionally, the hippocampus of rodents presents a dorso-ventral axis with differences in input and output connectivity (Fanselow et al., 2010; Kheirbek et al., 2013). Furthermore, some connected brain regions show topographical connectivity to the hippocampus too (Dolorfo & Amaral, 1998; Kishi et al., 2006; Li et al., 1994).

Although the dorso-ventral axis within the hippocampus might be a fluent transition, differences in input and output and distinct functional implications have been identified, suggesting a role in memory and spatial learning for the dorsal part and in emotion-related behavior for the ventral part (see Introduction; Bast et al., 2001; Henke, 1990; Kheirbek et al., 2013; Kjelstrup et al., 2002; E. I. Moser et al., 1993; Pothuizen et al., 2004; Shah et al., 2016). Interestingly, cognitive flexibility of acquired and emotionally charged memories relies on the ability of the hippocampus to produce new neurons, a process that is termed (adult) neurogenesis (Anacker et al., 2017).

In this context, it is interesting to note that immunohistochemical analysis and subsequent quantification of DCX+ neurons and their arborization revealed distinct responses on physical-activity dependent neurogenesis in the dorsal versus ventral part of the hippocampus. Interestingly, in the ventral hippocampus we quantified a significant enrichment in the number of DCX+ neurons, whereas the effect in the dorsal hippocampus did not reach statistical significance (**Figure 18A** and **Figure 21A**). The increase in number of adult-born neurons is consistent with studies that observed similar changes under voluntary physical activity, but without looking into regional differences (Van Praag et al., 1999). Additionally, the same trend could be observed for the number of dendrites. In the dorsal hippocampus there was no significant effect, whereas in the ventral hippocampus the absolute number of primary and secondary dendrites was significantly increased (**Figure 18B** and **Figure 21B**). Importantly, in the DH of control mice, the number of DCX+ neurons, as well as primary and secondary dendrites varied highly (**Figure 18A**). Surprisingly, in test mice upon voluntary physical activity, this variance in DH between the different animals was lower. The only experimental parameters that were significantly increased upon voluntary running in both dorsal and ventral hippocampus of WT mice were the mean length of primary and secondary dendrites (**Figure 18C** and **Figure 21C**) (Frey et al., 2020).

These results strengthen the idea that EPA not only affects the genesis of new neurons, but also affects neuronal differentiation by dendritic extension and branching. However, in an earlier study by Zhao *et al.* (2006), no changes in dendritic length and branching were observed when comparing naive mice with mice upon four weeks of exercise. A potential explanation for this could be that Zhao *et al.* used different staining for immature neurons (namely GFP+ stainings), or that the mice used were different in sex (female), age (7-10 weeks), and exposure to the running wheel when compared to our experimental setup.

Importantly, to exclude age-dependent effects on the amount of immature neurons, 13-week-old naïve WT mice without access to running wheel did not show any significant increase in either numbers of newly-generated neurons nor in dendrites compared to 10-week-old controls. Therefore, I conclude that the observed effects are related to activity-enhanced neurogenesis and not due to age-dependent effects (**Figure 19** and **Figure 22**). Overall, these findings suggest a selective contribution of the ventral versus the dorsal part of the hippocampus to physical activity induced neurogenesis and differentiation in adult mice (Frey *et al.*, 2020).

In this study, differences in the dorsal or ventral part of the hippocampus and additionally in the different subregions, DG, CA3 and CA1, were investigated. The differential expression of mRNA has already been described for the hippocampal subregions (Farris *et al.*, 2019; Habib *et al.*, 2016). However, there are several limitations that restrict conclusions drawn from transcriptome data. First, there is a poor correlation between mRNA and protein levels (Schwanhäusser *et al.*, 2011). Second, protein steady-state levels do not correlate with the ribosome occupancy on mRNAs (van Heesch *et al.*, 2019). And third, for some mRNAs a phenomenon so called “translational buffering” occurs (Liu *et al.*, 2018). Therefore, as proteins are the main effectors in cells, it is of utmost interest to reveal proteomic changes and pathway-specific alterations upon enhanced physical activity. Therefore, I have decided to pursue this avenue and went for selective microdissection of dorsal and ventral hippocampus and their different subregions, followed by mass spectrometry and subsequent protein analysis in order to get insight into proteomic differences upon EPA.

When comparing this semi-quantitative analysis of the different subregions DG, CA3 and CA1 of the dorsal to the ventral hippocampus, the two parts surprisingly showed little or even no overlap (**Figure 35**).

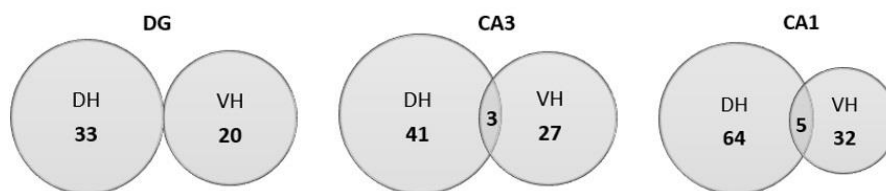


Figure 35: Venn diagrams showing differentially expressed upregulated proteins of either the dorsal (DH) or ventral hippocampus (VH) in the different subregions: DG, CA3 and CA1. First, the regions vary regarding the number of upregulated proteins. Second, an overlap can only be found in the CA regions, however, this effect is small (n=3 and n=5).

Abbrev.: DG, dentate gyrus; CA, cornu ammonis.

Additionally, the dorsal hippocampus revealed a higher amount of differentially expressed proteins (n=197) than the ventral one (n=144). However, there were more downregulated, low abundant proteins in the ventral hippocampus (n=57) than in its dorsal counterpart (n=51). Thus, the amount of altered proteins but also their relation to increased or decreased proteins upon exercise differs in the two hippocampal regions.

Interestingly, when comparing the proteome data sets of the subregions with each other within the dorsal hippocampus and within the ventral hippocampus respectively, the proteins in the different regions hardly overlapped (**Figure 32** and **34**).

Hence it is tempting to speculate that dorsal and ventral hippocampus exploit different molecular pathways in response to EPA. Indeed, in the dorsal hippocampus proteins involved in purine metabolism (n=7), mRNA surveillance (n=5) and mTOR signaling (n=4) were upregulated (**Table 7**). In the ventral hippocampus, upregulated proteins showed an enrichment for purine metabolism (n=5) and mTOR signaling (n=3) and in addition for Rap1, oxytocin, and insulin signaling pathways (**Table 12**).

KEGG analysis revealed that both dorsal and ventral hippocampus are related to purine metabolism and mTOR signaling pathways. The enzyme mTOR is a serine/threonine kinase that has its central role in the regulation of protein translation and particularly in the brain, where it is important during embryonal neurogenesis as well as synaptic plasticity in the adult brain (Lafourcade et al., 2013). Additionally, the ventral hippocampus appears to be involved in hormone related pathways, e.g. oxytocin and steroidogenesis and insulin signaling. Both, oxytocin and glucocorticoids have shown to be involved in social behavior in mammals: Oxytocin is a neuropeptide and promotes adult neurogenesis in DG of mice and ventral DG of rats. (Leuner et al., 2012; Lin et al., 2017). Glucocorticoids are hormones that are crucial for stress response and their dysregulation contributes to neuropsychiatric disorders like depression. Studies have directly linked glucocorticoid secretion to adult neurogenesis in voluntary exercise and enriched environment experiments (Droste et al., 2007; Lehmann et al., 2013; Snyder et al., 2011). Thus, these findings support the notion that the ventral hippocampus regulates social behavior, emotion and stress response with its connectivity to the amygdala, the nucleus accumbens and HPA axis (Henke, 1990; Shah et al., 2016; Strange et al., 2014).

Interestingly, the proteomic changes upon EPA revealed that in both dorsal and ventral hippocampus, proteins involved in social behavior, especially anxiety processes were enriched (**Tables 9,10 and 15**). Thus, both hippocampal subregions might contribute to these specific processes.

When comparing the proteomic subset between dorsal and ventral hippocampus, and the different subregions, DG, CA3 and CA1 there was no significant overlap (for subregional comparison **Figure 32 and 34**; for dorsal and ventral comparison **Figure 35**). Thus, the proteomic analysis revealed that the ventral and dorsal hippocampus share some pathway involvements. However they are implicated in different pathways too and possess a distinct proteomic set which supports hypothesis that they are separate regions with distinct major functions (Fanselow et al., 2010).

Taken together, these findings on the proteomic level together with the quantification of DCX+, newly-born neurons and number of dendrites, lead me to assume that EPA has a selective effect on adult neurogenesis in the dorsal and ventral part of the hippocampus. In conclusion my data supports hypothesis that dorsal and ventral hippocampus are two anatomically distinct regions (Fanselow et al., 2010).

7.2 Metabolic enzymes as main drivers of activity-enhanced alterations in the hippocampal proteome

To elucidate crucial pathways that are important for EPA induced proteomic alterations, I first performed Gene Ontology analysis for the entire hippocampus to identify pathways that are enriched.

Interestingly, upregulated proteins were preferentially located to myelin sheath and mitochondrion (depicting the ones with highest significance and lowest FDR, **Table 3**). The myelin sheath, which is generated by oligodendrocytes is crucial for fast axonal conduction in the brain. Several studies aim to understand how physical activity, neurogenesis and oligodendrogenesis are linked to each other. In a study using AD mice, running exercise had protective effects on demyelination (Chao et al., 2018) and *in vivo* experiments in mice revealed that activation of premotor cortex neurons led to proliferation of oligodendrocytes and thickening of myelin sheaths in the stimulated regions (Gibson et al., 2014). Therefore, it is plausible that EPA promotes myelination to allow proper connectivity formation.

The link to mitochondria indicates higher energy demands after EPA, perhaps due to axonal or dendritic outgrowth and protein remodeling upon neuronal plasticity. Mitochondria continually provide energy, mainly through oxidative phosphorylation, and are involved in synaptic functions through calcium signaling pathways. Under aging, stress or in neurodegenerative diseases, oxidative stress increases and disturbs the precisely regulated balance between energy supply and oxidative stress, that can lead to decreased energy production and oxidative damage and subsequently to synaptic

dysfunction. In particular, oxidative stress is decreased in rodents after running exercise (Mattson & Liu, 2002; Vaynman et al., 2006). In my proteome data, thioredoxin is upregulated upon exercise. It is a known protein in cell redox homeostasis and possess neuroprotective effects after brain damage (Berndt et al., 2006; F. Zhou et al., 2013), which further reinforces the link between exercise-induced neurogenesis and reduced oxidative stress.

Concomitant with that, it has been shown in human neuronal progenitor cells that during neuronal differentiation from NPCs to neurons, a metabolic shift from aerobic glycolysis towards oxidative phosphorylation takes place (Zheng et al., 2016). Interestingly, we also found proteins implicated in oxidative phosphorylation such as ATP-synthase-coupling factor 6 (Atp5j) or Cytochrome b-c1 complex subunit 1 (Uqcrc1) upregulated upon physical exercise (Frey et al., 2020). Moreover, EM studies observed an increase in mitochondrial mass reflected by the amount of mtDNA during neuronal growth, or by comparing the mitochondrial volume in NPCs, IPCs and newborn neurons (Beckervordersandforth et al., 2017; Zheng et al., 2016). These observations with an enriched localization in mitochondria and upregulated proteins involved in oxidative phosphorylation upon voluntary running might reflect higher energetic costs, and possibly induced neurogenesis and neuronal differentiation. On top of that, KEGG pathway analysis showed that some upregulated proteins upon EPA were involved in learning and memory and neuronal differentiation, e.g. the glycolytic enzyme glucose-6-P-isomerase (**Table 5**) (Knight et al., 2014; Moon et al., 2019).

To understand the significantly changed proteome upon voluntary physical exercise, I identified 20 out of 70 proteins that are known to be involved in either neuronal, proliferative or apoptotic processes or linked to locomotor behavior in rodents and humans (detailed analysis in **Table 5**). When comparing the proteome of test mice to their naïve littermates, one can also see a small number of proteins being downregulated upon voluntary running (**Table 4**). Within the group of proteins decreased after EPA, we revealed some targets with remarkable functions, namely Neuronal pentraxin-1, and the Calcium-binding mitochondrial carrier protein SCaMC-3 (Frey et al., 2020). SCaMC-3 is a mitochondrial ATP-Mg/P_i-carrier and important for mitochondrial calcium uptake and transport. Additionally, it has been shown to have neuroprotective effects against excitotoxicity by glutamate (Rueda et al., 2015). Neuronal pentraxin-1 (NP1) is considered as pro-apoptotic and activated by low neuronal activity. In cortical neurons after knockdown of NP1, the number of synapses and neuronal excitability is enriched and *in vivo* experiments demonstrate that NP1 knockdown in mice show increased LTP (Figueiro-Silva et al., 2015).

In conclusion, EPA strongly modulates the proteome in WT mice and reveals alterations towards cellular components, metabolic processes and pathways that are involved in neurogenesis, development or differentiation, respectively. In general, the shift is mainly represented by an upregulation of proteins upon EPA. Taking these results in various

pathways together, they present reasonable dynamic changes in growth, apoptotic, and neuronal processes that are required for neurogenesis and neuronal differentiation.

Importantly, neurons need active metabolism as well as mitochondria function to control (localized) translation (Rangaraju et al., 2019). Protein synthesis critically contributes to synaptic plasticity, neurogenesis and neuronal differentiation, thereby demanding high energetic costs in neurons (Baser et al., 2019; Rangaraju et al., 2019). Mitochondria supply energy for local translation at synapses in neurons and are required during synaptic plasticity (Rangaraju et al., 2019). Therefore, it is tempting to speculate that EPA promotes metabolism as well as mitochondrial function to cope with higher energy costs during the process of neurogenesis and neuronal differentiation. Based on published data, enhanced metabolism might preferentially increase translation. Further studies are clearly needed to unravel the role of EPA in metabolic and translational activity.

7.3 Actin cytoskeleton as a crucial process during EPA

The dorsal and ventral hippocampus both contain upregulated proteins upon EPA that are part of Rap1 signaling, namely the adenylate cyclase types 3, 5, and 8, Rac3 and Rap-1b, as well as Ras signaling, like Ras-related GTP-binding protein A & B, Rheb, Cad protein and Rac3 (**Tables 14** and **15**). Both subregions show increase in proteins involved in Rap1 and Ras signaling, however, the individual subset of proteins do not overlap and occur in both dorsal and ventral hippocampus. Ras and Rap are small GTPases, guanine-nucleotide binding proteins that operate in an active (GTP-bound) and inactive (GDP-bound) state. Both Ras and Rap proteins are related, but contribute to different signaling pathways, as Rap1 preferentially mediates cell adhesion and junction formation and Ras regulates cytoskeleton organization and by that cell growth (reviewed in Raaijmakers & Bos, 2010). Regarding neurons, both pathways seem to influence synaptic plasticity, presumably independently, and are therefore important for the integration of newly born neurons into an existing circuit (Stornetta et al., 2011).

Support for the notion that actin cytoskeleton is reorganized upon EPA are the findings that the protein Ras homolog family member A (RhoA) and Profilin-2 were upregulated upon EPA (**Figure 36**) (Frey et al., 2020). RhoA belongs to the three major proteins of the Ras superfamily of small GTP-binding proteins, along with Rac and Cdc42 (Cachero et al., 1998). These small GTPases are known regulators of the cytoskeleton, that undergo constant remodeling.

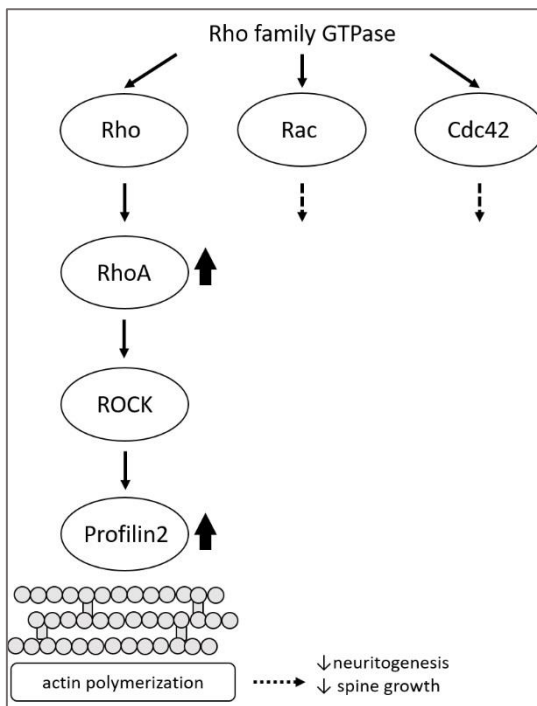


Figure 36: Simplified scheme showing the candidate protein RhoA during cytoskeleton remodeling. Interestingly, RhoA and its downstream effector Profilin-2, of the indicated signaling proteins were detected by mass spectrometry, indicated by bold arrows.

Abbrev.: ROCK, RhoA kinase.

RhoA interacts through its Rho kinase (ROCK) thereby directly effecting Profilin-2a (Pfn2a). Profilin-2 is brain-specific and involved in negative regulation of neuritogenesis (Da Silva et al., 2003; Pilo Boyl et al., 2007). Thus, upregulation of RhoA and its downstream effector Pfn2 during EPA-dependent adult hippocampal neurogenesis suggests that actin cytoskeleton is remodeled in response to EPA. Interestingly, actin cytoskeleton remodeling in neurons is known to be crucial for dendritic spine formation during brain plasticity (Briz et al., 2015; Penzes et al., 2012). Moreover, both proteins regulate dendrite morphogenesis by increasing actin stability and subsequently inhibit neurite sprouting (Sala & Segal, 2014). Therefore, it is plausible that EPA changes the actin cytoskeleton network to enhance synaptic plasticity and to enable the integration of newly generated neurons.

7.4 Stau2 is necessary for activity-enhanced adult neurogenesis

Actin cytoskeleton is regulated by RNA-binding proteins such as Musashi, FMRP via Cofilin and Stau2 (Goetze et al., 2006; Hadziselimovic et al., 2014; Luo et al., 2010). Importantly, RhoA upregulated upon EPA, is a known target of the RBP Stau2. It co-localizes with *RhoA* mRNA at the growth cone (K. Y. Wu et al., 2005). After knockdown of Stau2 in cortical neurons, RNA levels of RhoA were greatly elevated (PhD thesis by Lucia Schoderböck, Kiebler laboratory). However, another recent study on Stau2-deficient cortical neurons described reduced *RhoA* mRNA levels when comparing to

controls (Berger et al., 2017). Overall, Stau2 seems to have an effect on *RhoA* mRNA. Interestingly, Stau2 could not be detected by mass spectrometry, whereas RhoA was significantly upregulated in mice upon EPA. Another RNA-binding protein, FMRP, is also changed upon EPA in dorsal hippocampus. It acts as negative regulator of translation (Darnell et al., 2011) and has been associated with Staufen2, as they both co-localize in dendrites in the adult rat brain (Heraud-Farlow et al., 2014). Thus, it is tempting to speculate that FMRP and Stau2 are necessary for EPA dependent neurogenesis. Supportive for this hypothesis is the finding that FMRP regulates stem cell maintenance (Luo et al., 2010) and mitochondrial mRNA expression in mouse adult neural stem cells (B. Liu et al., 2018). For Stau2, it was shown that its deficiency lead to a shift in embryonic neurogenesis, from the radial glial stem cell state towards neuronal differentiation (Kusek et al., 2012; Vessey et al., 2012). Interestingly in my research project, Stau2 deficient mice show less proliferation of progenitor cells in the DG. Concomitant with that, the amount of newly-generated neurons was lower in both dorsal and ventral DG of Stau2^{GT} mice upon EPA when compared to their trained WT counterparts (**Figure 18A, 21A, 25A, 27A**). These results further strengthen the hypothesis that in the adult hippocampus, there may be less capacity for generating new neurons when Stau2 is deficient. Subsequently, I tested for whether adult Stau2-deficient mice react similarly to physical exercise as their WT counterparts and found very small effects of activity-dependent adult neurogenesis and neuronal differentiation. In detail, Stau2 is necessary for both EPA enhanced neurogenesis and dendritic branching of newly born neurons. These findings are of particular interest to understand learning and memory formation as they are both linked to adult neurogenesis (Anacker et al., 2017). Interestingly, spatial learning and response to novelty, both hippocampus-dependent tasks, are significantly impaired in Stau2 deficient rats (Berger et al., 2017; Broadbent et al., 2004; Popper et al., 2018).

Taken together, these results suggest that first RBPs are essential for crucial processes during EPA like actin cytoskeleton remodelling and that Stau2 is not only crucial in embryonic neurogenesis, but also seems to alter the normal process of physical-activity dependent adult neurogenesis, especially in regard of the DG of ventral hippocampus.

7.5 Activity-enhanced adult neurogenesis and neurodegenerative diseases – an outlook

Numerous studies observed a reduced amount of newly-generated neurons in the process of adult neurogenesis in neurodegenerative diseases, concluding that the dysfunction of this process might potentially initiate these diseases, contributes to symptoms or accelerate the disease state (see 3.3 Involvement of adult neurogenesis in neuropsychiatric disorders). Interestingly, in my research project, several of the proteins that are upregulated upon EPA can directly be linked to functional pathways of

Huntington's, Parkinson's or Alzheimer's diseases (AD) (**Figure 30, Tables 10 and 14**) (Frey et al., 2020).

Many of the aforementioned proteins that are significantly changed upon EPA are additionally implemented in the pathomechanism of AD. In the proteomic analysis of the entire hippocampus, the upregulated proteins are located to mitochondria. Mitochondrial alterations have been already linked to AD, but a recent study goes as far as claiming that when mitochondrial function is augmented, impaired adult neurogenesis in an AD mouse model could be rescued and restored (Richetin et al., 2017). On top of that, the glucose-6-P-isomerase was changed upon EPA and is involved in learning and memory (G6PI, **Table 5**), but also linked to AD disease as it has shown to be significantly reduced in the hippocampus of AD mouse models (Yang et al., 2012). Another protein of particular interest is an upregulated protein in the CA1 region of the ventral hippocampus, the Cytochrome P450 7B1, an enzyme involved in steroid metabolism (Yau et al., 2003). Furthermore, the authors observed a significant decline of CYP7B1 in DG and CA1 region in human post-mortem tissue of AD patients, concluding a link between the cognitive decline in AD and neurosteroid expression. Recent studies have shown that neurosteroids influence LTP and long-term depression, two types of synaptic plasticity in the brain (reviewed in Hojo & Kawato, 2018). In the downregulated proteome upon EPA, there are some proteins, e.g. Neuronal pentraxin 1 and Sorting nexin-12 (Snx-12) that are also known to be associated with AD. Np1 has been identified as part of the neurodegenerative cascade induced by β -amyloid. In AD brains, Np1 seems to accumulate in dystrophic neurites (Abad et al., 2006). Snx-12 from the SNX family, a group of trafficking proteins, is involved in AD, too. It is interacting with BACE 1, the beta-site APP-cleaving enzyme 1 that is elevated and activated in AD brains. Additionally, the protein level of Snx-12 was strongly decreased in AD brains, concluding that an alteration may contribute to the disease (Y. Zhao et al., 2012). Especially AD, the most common neurodegenerative illness, is currently undergoing much academic debate. Recent studies directly link impaired adult hippocampal neurogenesis to AD disease in human brains (Moreno-Jiménez et al., 2019; Tobin et al., 2019). On top of that, the impairment in adult neurogenesis can already be measured in early stage of AD, where pathological products such as fibrillary tangles and senile plaques are yet not present (Moreno-Jiménez et al., 2019; Tobin et al., 2019).

Thus, the proteome analysis reinforces the relation between proteomic changes under physical activity dependent adult neurogenesis and their association with neurodegenerative disorders. These findings may eventually contribute to future approaches for early diagnosis and treatment of neurodegenerative diseases.

References

- Abad, M. A., Enguita, M., DeGregorio-Rocasolano, N., Ferrer, I., & Trullas, R. (2006). Neuronal pentraxin 1 contributes to the neuronal damage evoked by amyloid- β and is overexpressed in dystrophic neurites in Alzheimer's brain. *Journal of Neuroscience*, 26(49), 12735–12747. <https://doi.org/10.1523/JNEUROSCI.0575-06.2006>
- Akiyama, H., Fujisawa, N., Tashiro, Y., Takanabe, N., Sugiyama, A., & Tashiro, F. (2003). The role of transcriptional corepressor Nif311 in early stage of neural differentiation via cooperation with Trip15/CSN2. *Journal of Biological Chemistry*, 278(12), 10752–10762. <https://doi.org/10.1074/jbc.M209856200>
- Alfonso, S., Kessels, H. W., Banos, C. C., Chan, T. R., Lin, E. T., Kumaravel, G., Scannevin, R. H., Rhodes, K. J., Haganir, R., Guckian, K. M., Dunah, A. W., & Malinow, R. (2014). Synapto-depressive effects of amyloid beta require PICK1. *European Journal of Neuroscience*, 39(7), 1225–1233. <https://doi.org/10.1111/ejn.12499>
- Altman, J. (1962). Are new neurons formed in the brains of adult mammals? *Science*, 135(3509), 1127–1128. <http://science.sciencemag.org.emedien.ub.uni-muenchen.de/content/sci/135/3509/1127.full.pdf>
- Altman, J., & Das, G. D. (1965). Autoradiographic and histological evidence of postnatal hippocampal neurogenesis in rats. *The Journal of Comparative Neurology*, 124(3), 319–335.
- Anacker, C., & Hen, R. (2017). Adult hippocampal neurogenesis and cognitive flexibility-linking memory and mood. In *Nature Reviews Neuroscience* (Vol. 18, Issue 6, pp. 335–346). <https://doi.org/10.1038/nrn.2017.45>
- Aruga, J., & Mikoshiba, K. (2003). Identification and characterization of Slitrk, a novel neuronal transmembrane protein family controlling neurite outgrowth. *Molecular and Cellular Neuroscience*, 24(1), 117–129. [https://doi.org/10.1016/S1044-7431\(03\)00129-5](https://doi.org/10.1016/S1044-7431(03)00129-5)
- Arun, P., Abu-Taleb, R., Oguntayo, S., Wang, Y., Valiyaveetil, M., Long, J. B., & Nambiar, M. P. (2013). Acute mitochondrial dysfunction after blast exposure: potential role of mitochondrial glutamate oxaloacetate transaminase. *Journal of Neurotrauma*, 30(19), 1645–1651. <https://doi.org/10.1089/neu.2012.2834>
- Baser, A., Skabkin, M., Kleber, S., Dang, Y., Gülcüler Balta, G. S., Kalamakis, G., Göpferich, M., Ibañez, D. C., Schefzik, R., Lopez, A. S., Bobadilla, E. L., Schultz, C., Fischer, B., & Martin-Villalba, A. (2019). Onset of differentiation is post-transcriptionally controlled in adult neural stem cells. *Nature*, 566(7742), 100–104. <https://doi.org/10.1038/s41586-019-0888-x>
- Bast, T., Zhang, W. N., & Feldon, J. (2001). The ventral hippocampus and fear conditioning in rats: Different anterograde amnesias of fear after tetrodotoxin inactivation and infusion of the GABAA agonist muscimol. *Experimental Brain Research*, 139(1), 39–52. <https://doi.org/10.1007/s002210100746>
- Bauer, K. E., Segura, I., Gaspar, I., Scheuss, V., Illig, C., Ammer, G., Hutten, S., Basyuk, E., Fernández-Moya, S. M., Ehses, J., Bertrand, E., & Kiebler, M. A. (2019). Live cell imaging reveals 3'-UTR dependent mRNA sorting to synapses. *Nature Communications*, 10(1). <https://doi.org/10.1038/s41467-019-11123-x>
- Baughman, J. M., Perocchi, F., Girgis, H. S., Plovovich, M., Belcher-Timme, C. A., Sancak, Y., Bao, X. R., Strittmatter, L., Goldberger, O., Bogorad, R. L., Kotliansky, V., & Mootha, V. K. (2011). Integrative genomics identifies MCU as an essential component of the mitochondrial calcium uniporter. *Nature*, 476(7360), 341–345. <https://doi.org/10.1038/nature10234>

- Beckervordersandforth, R., Ebert, B., Schäffner, I., Moss, J., Fiebig, C., Shin, J., Moore, D. L., Ghosh, L., Trinchero, M. F., Stockburger, C., Friedland, K., Steib, K., von Wittgenstein, J., Keiner, S., Redecker, C., Hölter, S. M., Xiang, W., Wurst, W., Jagasia, R., ... Lie, D. C. (2017). Role of Mitochondrial Metabolism in the Control of Early Lineage Progression and Aging Phenotypes in Adult Hippocampal Neurogenesis. *Neuron*, 93(3), 560-573.e6. <https://doi.org/10.1016/j.neuron.2016.12.017>
- Berger, S. M., Fernández-Lamo, I., Schöning, K., Fernández Moya, S. M., Ehses, J., Schieweck, R., Clementi, S., Enkel, T., Grothe, S., von Bohlen und Halbach, O., Segura, I., Delgado-García, J. M., Gruart, A., Kiebler, M. A., & Bartsch, D. (2017). Forebrain-specific, conditional silencing of *Staufen2* alters synaptic plasticity, learning, and memory in rats. *Genome Biology*, 18(1), 222. <https://doi.org/10.1186/s13059-017-1350-8>
- Berndt, C., Lillig, C. H., & Holmgren, A. (2006). Thiol-based mechanisms of the thioredoxin and glutaredoxin systems: implications for diseases in the cardiovascular system. *AJP: Heart and Circulatory Physiology*, 292(3), H1227–H1236. <https://doi.org/10.1152/ajpheart.01162.2006>
- Boer, P., Brosh, S., Wasserman, L., Hammel, I., Zoref-Shani, E., & Sperling, O. (2001). Decelerated rate of dendrite outgrowth from dopaminergic neurons in primary cultures from brains of hypoxanthine phosphoribosyltransferase-deficient knockout mice. *Neuroscience Letters*, 303(1), 45–48. [https://doi.org/10.1016/S0304-3940\(01\)01716-5](https://doi.org/10.1016/S0304-3940(01)01716-5)
- Boldrini, M., Fulmore, C. A., Tartt, A. N., Dwork, A. J., Hen, R., & Mann, J. J. (2018). Human hippocampal neurogenesis persists throughout aging. *Cell Stem Cell*, 22(4), 589–599. <https://doi.org/10.1016/j.stem.2018.03.015>
- Boldrini, M., Santiago, A. N., Hen, R., Dwork, A. J., Rosoklija, G. B., Tamir, H., Arango, V., & John Mann, J. (2013). Hippocampal granule neuron number and dentate gyrus volume in antidepressant-treated and untreated major depression. *Neuropsychopharmacology*, 38(6), 1068–1077. <https://doi.org/10.1038/npp.2013.5>
- Boldrini, M., Underwood, M. D., Hen, R., Rosoklija, G. B., Dwork, A. J., John Mann, J., & Arango, V. (2009). Antidepressants increase neural progenitor cells in the human hippocampus. *Neuropsychopharmacology*, 34(11), 2376–2389. <https://doi.org/10.1038/npp.2009.75>
- Briz, V., Zhu, G., Wang, Y., Liu, Y., Avetisyan, M., Bi, X., & Baudry, M. (2015). Activity-Dependent Rapid Local RhoA Synthesis Is Required for Hippocampal Synaptic Plasticity. *Journal of Neuroscience*, 35(5), 2269–2282. <https://doi.org/10.1523/JNEUROSCI.2302-14.2015>
- Broadbent, N. J., Squire, L. R., & Clark, R. E. (2004). Spatial memory, recognition memory, and the hippocampus. *Proceedings of the National Academy of Sciences of the United States of America*, 101(40), 14515–14520. <https://doi.org/10.1073/pnas.0406344101>
- Brown, J. P., Couillard-Després, S., Cooper-Kuhn, C. M., Winkler, J., Aigner, L., & Kuhn, H. G. (2003). Transient Expression of Doublecortin during Adult Neurogenesis. *Journal of Comparative Neurology*, 467(1), 1–10. <https://doi.org/10.1002/cne.10874>
- Bungard, D., Fuerth, B. J., Zeng, P. Y., Faubert, B., Maas, N. L., Viollet, B., Carling, D., Thompson, C. B., Jones, R. G., & Berger, S. L. (2010). Signaling kinase AMPK activates stress-promoted transcription via histone H2B phosphorylation. *Science*, 329(5996), 1201–1205. <https://doi.org/10.1126/science.1191241>
- Cachero, T. G., Morielli, a D., & Peralta, E. G. (1998). The small GTP-binding protein RhoA regulates a delayed rectifier potassium channel. *Cell*, 93(6), 1077–1085. [https://doi.org/10.1016/S0092-8674\(00\)81212-X](https://doi.org/10.1016/S0092-8674(00)81212-X)

- Cahoy, J., Emery, B., Kaushal, A., Foo, L., Zamanian, J., Christopherson, K., Xing, Y., Lubischer, J., Krieg, P., Krupenko, S., Thompson, W., & Barres, B. (2008). A Transcriptome Database for Astrocytes, Neurons, and Oligodendrocytes: A New Resource for Understanding Brain Development and Function. *Journal of Neuroscience*, 28(1), 264–278. <https://doi.org/10.1523/JNEUROSCI.4178-07.2008>
- Cajigas, I. J., Tushev, G., Will, T. J., Tom Dieck, S., Fuerst, N., & Schuman, E. M. (2012). The Local Transcriptome in the Synaptic Neuropil Revealed by Deep Sequencing and High-Resolution Imaging. *Neuron*, 74(3), 453–466. <https://doi.org/10.1016/j.neuron.2012.02.036>
- Cameron, H. A., Woolley, C. S., McEwen, B. S., & Gould, E. (1993). Differentiation of newly born neurons and glia in the dentate gyrus of the adult rat. *Neuroscience*, 56(2), 337–344. [https://doi.org/10.1016/0306-4522\(93\)90335-D](https://doi.org/10.1016/0306-4522(93)90335-D)
- Chao, F. lei, Zhang, L., Zhang, Y., Zhou, C. ni, Jiang, L., Xiao, Q., Luo, Y. min, Lv, F. lin, He, Q., & Tang, Y. (2018). Running exercise protects against myelin breakdown in the absence of neurogenesis in the hippocampus of AD mice. *Brain Research*, 1684, 50–59. <https://doi.org/10.1016/j.brainres.2018.01.007>
- Cheloufi, S., Dos Santos, C. O., Chong, M. M. W., & Hannon, G. J. (2010). A dicer-independent miRNA biogenesis pathway that requires Ago catalysis. *Nature*, 465(7298), 584–589. <https://doi.org/10.1038/nature09092>
- Chen, L., Xu, R., Sun, F. J., Xue, Y., Hao, X. M., Liu, H. X., Wang, H., Chen, X. Y., Liu, Z. R., Deng, W. S., Han, X. H., Xie, J. X., & Yung, W. H. (2015). Hyperpolarization-activated cyclic nucleotide-gated (HCN) channels regulate firing of globus pallidus neurons in vivo. *Molecular and Cellular Neuroscience*, 68, 46–55. <https://doi.org/10.1016/j.mcn.2015.04.001>
- Chowdhury, G. M. I., Gupta, M., Gibson, K. M., Patel, A. B., & Behar, K. L. (2007). Altered cerebral glucose and acetate metabolism in succinic semialdehyde dehydrogenase-deficient mice: Evidence for glial dysfunction and reduced glutamate/glutamine cycling. *Journal of Neurochemistry*, 103(5), 2077–2091. <https://doi.org/10.1111/j.1471-4159.2007.04887.x>
- Clark, P. J., Kohman, R. A., Miller, D. S., Bhattacharya, T. K., Brzezinska, W. J., & Rhodes, J. S. (2011). Genetic influences on exercise-induced adult hippocampal neurogenesis across 12 divergent mouse strains. *Genes, Brain and Behavior*, 10(3), 345–353. <https://doi.org/10.1111/j.1601-183X.2010.00674.x>
- Clelland, C. D., Choi, M., Romberg, C., Clemenson, G. D., Fragniere, A., Tyers, P., Jessberger, S., Saksida, L. M., Barker, R. A., Gage, F. H., & Bussey, T. J. (2009). A functional role for adult hippocampal neurogenesis in spatial pattern separation. *Science*, 325(5937), 210–213. <https://doi.org/10.1126/science.1173215>
- Cool, B. H., Chan, G. C.-K., Lee, L., Oshima, J., Martin, G. M., & Hu, Q. (2010). A flanking gene problem leads to the discovery of a Gprc5b splice variant predominantly expressed in C57BL/6J mouse brain and in maturing neurons. *PLoS ONE*, 5(4), e10351. <https://doi.org/10.1371/journal.pone.0010351>
- Corbetta, S., Gualdoni, S., Albertinazzi, C., Paris, S., Croci, L., Consalez, G. G., & de Curtis, I. (2005). Generation and characterization of Rac3 knockout mice. *Molecular and Cellular Biology*, 25(13), 5763–5776. <https://doi.org/10.1128/MCB.25.13.5763-5776.2005>
- Couillard-Despres, S., Winner, B., Schauback, S., Aigner, R., Vroemen, M., Weidner, N., Bogdahn, U., Winkler, J., Kuhn, H. G., & Aigner, L. (2005). Doublecortin expression levels in adult brain reflect neurogenesis. *European Journal of Neuroscience*, 21(1), 1–14. <https://doi.org/10.1111/j.1460-9568.2004.03813.x>
- Da Silva, J. S., Medina, M., Zuliani, C., Di Nardo, A., Witke, W., & Dotti, C. G. (2003). RhoA/ROCK regulation of neuritogenesis via profilin IIa-mediated control of actin stability. *Journal of Cell Biology*, 162(7), 1267–1279.

- <https://doi.org/10.1083/jcb.200304021>
- Danielson, N. B. B., Kaifosh, P., Zaremba, J. D. D., Lovett-Barron, M., Tsai, J., Denny, C. A. A., Balough, E. M. M., Goldberg, A. R. R., Drew, L. J. J., Hen, R., Losonczy, A., & Kheirbek, M. A. A. (2016). Distinct Contribution of Adult-Born Hippocampal Granule Cells to Context Encoding. *Neuron*, *90*(1), 101–112. <https://doi.org/10.1016/j.neuron.2016.02.019>
- Darbelli, L., Choquet, K., Richard, S., & Kleinman, C. L. (2017). Transcriptome profiling of mouse brains with qkI-deficient oligodendrocytes reveals major alternative splicing defects including self-splicing. *Scientific Reports*, *7*(1), 1–13. <https://doi.org/10.1038/s41598-017-06211-1>
- Darnell, J. C., Van Driesche, S. J., Zhang, C., Ying, K., Hung, S., Mele, A., Fraser, C. E., Stone, E. F., Chen, C., Fak, J. J., Chi, S. W., Licatalosi, D. D., Richter, J. D., & Darnell, R. B. (2011). *FMRP stalls ribosomal translocation on mRNAs linked to synaptic function and autism*.
- Dolorfo, C. L., & Amaral, D. G. (1998). Entorhinal cortex of the rat: Topographic organization of the cells of origin of the perforant path projection to the dentate gyrus. *Journal of Comparative Neurology*, *398*(1), 25–48. [https://doi.org/10.1002/\(SICI\)1096-9861\(19980817\)398:1<25::AID-CNE3>3.0.CO;2-B](https://doi.org/10.1002/(SICI)1096-9861(19980817)398:1<25::AID-CNE3>3.0.CO;2-B)
- Donovan, M. H., Yazdani, U., Norris, R. D., Games, D., German, D. C., & Eisch, A. J. (2006). Decreased adult hippocampal neurogenesis in the PDAPP mouse model of Alzheimer's disease. *Journal of Comparative Neurology*, *495*(1), 70–83. <https://doi.org/10.1002/cne.20840>
- Douglas, C. L., Vyazovskiy, V., Southard, T., Chiu, S. Y., Messing, A., Tononi, G., & Cirelli, C. (2007). Sleep in *Kcna2* knockout mice. *BMC Biology*, *5*(1), 42. <https://doi.org/10.1186/1741-7007-5-42>
- Droste, S. K., Chandramohan, Y., Hill, L. E., Linthorst, A. C. E., & Reul, J. M. H. M. (2007). Voluntary exercise impacts on the rat hypothalamic-pituitary-adrenocortical axis mainly at the adrenal level. *Neuroendocrinology*, *86*(1), 26–37. <https://doi.org/10.1159/000104770>
- Du, H., Deng, W., Aimone, J. B., Ge, M., Parylak, S., Walch, K., Zhang, W., Cook, J., Song, H., Wang, L., Gage, F. H., & Mu, Y. (2016). Dopaminergic inputs in the dentate gyrus direct the choice of memory encoding. *Proceedings of the National Academy of Sciences*, *113*(37), E5501–E5510. <https://doi.org/10.1073/pnas.1606951113>
- Dubnau, J., Chiang, A. S., Grady, L., Barditch, J., Gossweiler, S., McNeil, J., Smith, P., Buldoc, F., Scott, R., Certa, U., Broger, C., & Tully, T. (2003). The *staufen/pumilio* pathway is involved in *Drosophila* long-term memory. *Current Biology*, *13*(4), 286–296. [https://doi.org/10.1016/S0960-9822\(03\)00064-2](https://doi.org/10.1016/S0960-9822(03)00064-2)
- Duchaîne, T. F., Hemraj, I., Furic, L., Deitinghoff, A., Kiebler, M. a, & DesGroseillers, L. (2002). *Staufen2* isoforms localize to the somatodendritic domain of neurons and interact with different organelles. *Journal of Cell Science*, *115*, 3285–3295.
- Eriksson, P. S., Perfilieva, E., Bjork-Eriksson, T., Alborn, A. M., Nordborg, C., Peterson, D. A., & Gage, F. H. (1998). Neurogenesis in the adult human hippocampus. *Nat Med*, *4*(11), 1313–1317. <https://doi.org/10.1038/3305>
- Esteve, C., Jones, E. A., Kell, D. B., Boutin, H., & McDonnell, L. A. (2017). Mass spectrometry imaging shows major derangements in neurogranin and in purine metabolism in the triple-knockout 3×Tg Alzheimer mouse model. *Biochimica et Biophysica Acta - Proteins and Proteomics*, *1865*(7), 747–754. <https://doi.org/10.1016/j.bbapap.2017.04.002>
- Fanselow, M., & Dong, H.-W. (2010). Are the Dorsal and Ventral Hippocampus functionally distinct structures. *Neuron*, *65*(1), 1–25.

- <https://doi.org/10.1016/j.neuron.2009.11.031>.Are
- Farris, S., Ward, J. M., Carstens, K. E., Samadi, M., Wang, Y., & Dudek, S. M. (2019). Hippocampal Subregions Express Distinct Dendritic Transcriptomes that Reveal Differences in Mitochondrial Function in CA2. *Cell Reports*, 29(2), 522-539.e6. <https://doi.org/10.1016/j.celrep.2019.08.093>
- Fernandez-Gonzalez, A., La Spada, A. R., Treadaway, J., Higdon, J. C., Harris, B. S., Sidman, R. L., Morgan, J. I., & Zuo, J. (2002). Purkinje cell degeneration (pcd) phenotypes caused by mutations in the axotomy-induced gene, Nnal. *Science*, 295(5561), 1904–1906. <https://doi.org/10.1126/science.1068912>
- Figueiro-Silva, J., Gruart, A., Clayton, K. B., Podlesniy, P., Abad, M. A., Gasull, X., Delgado-García, J. M., & Trullas, R. (2015). Neuronal pentraxin 1 negatively regulates excitatory synapse density and synaptic plasticity. *Journal of Neuroscience*, 35(14), 5504–5521. <https://doi.org/10.1523/JNEUROSCI.2548-14.2015>
- Fiore, R., Khudayberdiev, S., Christensen, M., Siegel, G., Flavell, S. W., Kim, T. K., Greenberg, M. E., & Schratt, G. (2009). Mef2-mediated transcription of the miR379-410 cluster regulates activity-dependent dendritogenesis by fine-tuning Pumilio2 protein levels. *EMBO Journal*, 28(6), 697–710. <https://doi.org/10.1038/emboj.2009.10>
- Flood, D. G., Reaume, A. G., Gruner, J. A., Hoffman, E. K., Hirsch, J. D., Lin, Y. G., Dorfman, K. S., & Scott, R. W. (1999). Hindlimb motor neurons require Cu/Zn superoxide dismutase for maintenance of neuromuscular junctions. *American Journal of Pathology*, 155(2), 663–672. [https://doi.org/10.1016/S0002-9440\(10\)65162-0](https://doi.org/10.1016/S0002-9440(10)65162-0)
- Follwaczny, P., Schieweck, R., Riedemann, T., Demleitner, A., Straub, T., Klemm, A. H., Bilban, M., Sutor, B., Popper, B., & Kiebler, M. A. (2017). Pumilio2-deficient mice show a predisposition for epilepsy. *Disease Models & Mechanisms*, 10(11), 1333–1342. <https://doi.org/10.1242/dmm.029678>
- Frey, S., Schieweck, R., Forné, I., Imhof, A., Straub, T., Popper, B., & Kiebler, M. A. (2020). Physical activity dynamically regulates the hippocampal proteome along the dorso-ventral axis. *International Journal of Molecular Sciences*, 21(10), 1–15. <https://doi.org/10.3390/ijms21103501>
- Fulton, S., Thibault, D., Mendez, J. A., Lahaie, N., Tirota, E., Borrelli, E., Bouvier, M., Tempel, B. L., & Trudeau, L. E. (2011). Contribution of Kv1.2 voltage-gated potassium channel to D2 autoreceptor regulation of axonal dopamine overflow. *Journal of Biological Chemistry*, 286(11), 9360–9372. <https://doi.org/10.1074/jbc.M110.153262>
- Gage, F. H. (2000). Mammalian Neural Stem Cells. *Science*, 287(5457), 1433–1438. <https://doi.org/10.1126/science.287.5457.1433>
- Ge, S., Yang, C.-H., Hsu, K.-S., Ming, G.-L., & Song, H. (2007). A critical period for enhanced synaptic plasticity in newly generated neurons of the adult brain. *Neuron*, 54(4), 559–566. <https://doi.org/10.1016/j.neuron.2007.05.002>
- Gennarino, V. A., Singh, R. K., White, J. J., De Maio, A., Han, K., Kim, J. Y., Jafar-Nejad, P., Di Ronza, A., Kang, H., Sayegh, L. S., Cooper, T. A., Orr, H. T., Sillitoe, R. V., & Zoghbi, H. Y. (2015a). Pumilio1 haploinsufficiency leads to SCA1-like neurodegeneration by increasing wild-type Ataxin1 levels. *Cell*, 160(6), 1087–1098. <https://doi.org/10.1016/j.cell.2015.02.012>
- Gennarino, V. A., Singh, R. K., White, J. J., De Maio, A., Han, K., Kim, J. Y., Jafar-Nejad, P., Di Ronza, A., Kang, H., Sayegh, L. S., Cooper, T. A., Orr, H. T., Sillitoe, R. V., & Zoghbi, H. Y. (2015b). Pumilio1 haploinsufficiency leads to SCA1-like neurodegeneration by increasing wild-type Ataxin1 levels. *Cell*, 160(6), 1087–1098. <https://doi.org/10.1016/j.cell.2015.02.012>

- Gervais, F. G., Singaraja, R., Xanthoudakis, S., Gutekunst, C. A., Leavitt, B. R., Metzler, M., Hackam, A. S., Tam, J., Vaillancourt, J. P., Houtzager, V., Rasper, D. M., Roy, S., Hayden, M. R., & Nicholson, D. W. (2002). Recruitment and activation of caspase-8 by the Huntingtin-interacting protein Hip-1 and a novel partner Hipp1. *Nature Cell Biology*, *4*(2), 95–105. <https://doi.org/10.1038/ncb735>
- Gibson, E. M., Purger, D., Mount, C. W., Goldstein, A. K., Lin, G. L., Wood, L. S., Inema, I., Miller, S. E., Bieri, G., Zuchero, B., Barres, B. A., Woo, P. J., Vogel, H., & Monje, M. (2014). Neuronal Activity Promotes Oligodendrogenesis and Adaptive Myelination in the Mammalian Brain. *Science*, *344*(6183), 480–481. <https://doi.org/10.1126/science.1254446>
- Gleeson, J. G., Lin, P. T., Flanagan, L. A., & Walsh, C. A. (1999). Doublecortin Is a Microtubule-Associated Protein and Is Expressed Widely by Migrating Neurons. *Neuron*, *23*, 257–271. [https://doi.org/10.1016/S0896-6273\(00\)80778-3](https://doi.org/10.1016/S0896-6273(00)80778-3)
- Goetze, B., Tuebing, F., Xie, Y., Dorostkar, M. M., Thomas, S., Pehl, U., Boehm, S., Macchi, P., & Kiebler, M. A. (2006). The brain-specific double-stranded RNA-binding protein Stauf2 is required for dendritic spine morphogenesis. *Journal of Cell Biology*, *172*(2), 221–231. <https://doi.org/10.1083/jcb.200509035>
- Goncalves, J. T., Schafer, S. T., & Gage, F. H. (2016). Adult Neurogenesis in the Hippocampus: From Stem Cells to Behavior. In *Cell* (Vol. 167, Issue 4, pp. 897–914). <https://doi.org/10.1016/j.cell.2016.10.021>
- Gupta, M., Polinsky, M., Senephansiri, H., Snead, O. C., Jansen, E. E. W., Jakobs, C., & Gibson, K. M. (2004). Seizure evolution and amino acid imbalances in murine succinate semialdehyde dehydrogenase (SSADH) deficiency. *Neurobiology of Disease*, *16*(3), 556–562. <https://doi.org/10.1016/j.nbd.2004.04.008>
- Habib, N., Li, Y., Heidenreich, M., Swiech, L., Avraham-Davidi, I., Trombetta, J. J., Hession, C., Zhang, F., & Regev, A. (2016). Div-Seq: Single-nucleus RNA-Seq reveals dynamics of rare adult newborn neurons. *Science*, *353*(6302), 925–928. <https://doi.org/10.1126/science.aad7038>
- Hadziselimovic, N., Vukojevic, V., Peter, F., Milnik, A., Fastenrath, M., Fenyves, B. G., Hieber, P., Demougin, P., Vogler, C., De Quervain, D. J. F., Papassotiropoulos, A., & Stetak, A. (2014). Forgetting is regulated via musashi-mediated translational control of the Arp2/3 complex. *Cell*, *156*(6), 1153–1166. <https://doi.org/10.1016/j.cell.2014.01.054>
- Hartzog, G. A., & Fu, J. (2013). The Spt4-Spt5 complex: A multi-faceted regulator of transcription elongation. In *Biochimica et Biophysica Acta - Gene Regulatory Mechanisms* (Vol. 1829, Issue 1, pp. 105–115). Elsevier. <https://doi.org/10.1016/j.bbagr.2012.08.007>
- Henke, P. G. (1990). Hippocampal pathway to the amygdala and stress ulcer development. *Brain Research Bulletin*, *25*(5), 691–695. [https://doi.org/10.1016/0361-9230\(90\)90044-Z](https://doi.org/10.1016/0361-9230(90)90044-Z)
- Heraud-Farlow, J. E., & Kiebler, M. A. (2014). The multifunctional Stauf proteins: Conserved roles from neurogenesis to synaptic plasticity. *Trends in Neurosciences*, *37*(9), 470–479. <https://doi.org/10.1016/j.tins.2014.05.009>
- Herms, J., Anliker, B., Heber, S., Ring, S., Fuhrmann, M., Kretzschmar, H., Sisodia, S., & Müller, U. (2004). Cortical dysplasia resembling human type 2 lissencephaly in mice lacking all three APP family members. *EMBO Journal*, *23*(20), 4106–4115. <https://doi.org/10.1038/sj.emboj.7600390>
- Herve, D., Le Moine, C., Corvol, J. C., Belluscio, L., Ledent, C., Fienberg, A. A., Jaber, M., Studler, J. M., & Girault, J. A. (2001). Galph_o levels are regulated by receptor usage and control dopamine and adenosine action in the striatum. *Journal of Neuroscience*, *21*(12), 4390–4399. <https://doi.org/10.1523/JNEUROSCI.2112-01.2001> [pii]
- Ho, N., Hooker, J., Sahay, A., Holt, D., & Roffman, J. (2013). In vivo imaging of adult

- human hippocampal neurogenesis: progress, pitfalls and promise. *Molecular Psychiatry*, 18(4), 404–416. <https://doi.org/10.1038/mp.2013.8>
- Höglinger, G. U., Rizk, P., Muriel, M. P., Duyckaerts, C., Oertel, W. H., Caille, I., & Hirsch, E. C. (2004). Dopamine depletion impairs precursor cell proliferation in Parkinson disease. *Nature Neuroscience*, 7(7), 726–735. <https://doi.org/10.1038/nn1265>
- Hojo, Y., & Kawato, S. (2018). Neurosteroids in Adult Hippocampus of Male and Female Rodents: Biosynthesis and Actions of Sex Steroids. *Frontiers in Endocrinology*, 9(April), 183. <https://doi.org/10.3389/fendo.2018.00183>
- Holt, C. E., & Bullock, S. L. (2009). Actin, a central player in cell shape and movement. In *Science* (Vol. 326, Issue 5957, pp. 1212–1215). <https://doi.org/10.1126/science.1175862>
- Honsa, P., Pivonkova, H., Harantova, L., Butenko, O., Kriska, J., Dzamba, D., Rusnakova, V., Valihrach, L., Kubista, M., & Anderova, M. (2014). Increased expression of hyperpolarization-activated cyclic nucleotide-gated (HCN) channels in reactive astrocytes following ischemia. *GLIA*, 62(12), 2004–2021. <https://doi.org/10.1002/glia.22721>
- Iwamoto, T., Okumura, S., Iwatsubo, K., Kawabe, J. I., Ohtsu, K., Sakai, I., Hashimoto, Y., Izumitani, A., Sango, K., Ajiki, K., Toya, Y., Umemura, S., Goshima, Y., Arai, N., Vatner, S. F., & Ishikawa, Y. (2003). Motor dysfunction in type 5 adenylyl cyclase-null mice. *Journal of Biological Chemistry*, 278(19), 16936–16940. <https://doi.org/10.1074/jbc.C300075200>
- Jinnah, H. A., Langlais, P. J., & Friedmann, T. (1992). Functional analysis of brain dopamine systems in a genetic mouse model of Lesch-Nyhan syndrome. *Journal of Pharmacology and Experimental Therapeutics*, 263(2), 596–607. <http://jpet.aspetjournals.org/emedien.ub.uni-muenchen.de/content/jpet/263/2/596.full.pdf>
- Jung, H., Gkogkas, C. G., Sonenberg, N., & Holt, C. E. (2014). Remote control of gene function by local translation. In *Cell* (Vol. 157, Issue 1, pp. 26–40). Cell Press. <https://doi.org/10.1016/j.cell.2014.03.005>
- Kaneko-Oshikawa, C., Nakagawa, T., Yoshikawa, H., Matsumoto, M., Hatakeyama, S., Nakayama, K., Nakayama, K. I., & Yamada, M. (2005). Mammalian E4 Is Required for Cardiac Development and Maintenance of the Nervous System Mammalian E4 Is Required for Cardiac Development and Maintenance of the Nervous System. *Molecular and Cellular Biology*, 25(24), 10953–10964. <https://doi.org/10.1128/MCB.25.24.10953>
- Kempermann, G., Gast, D., Kronenberg, G., Yamaguchi, M., & Gage, F. H. (2003). Early determination and long-term persistence of adult-generated new neurons in the hippocampus of mice. *Development*, 130, 391–399. <https://doi.org/10.1242/dev.00203>
- Kheirbek, M. A., Drew, L. J., Burghardt, N. S., Costantini, D. O., Tannenholz, L., Ahmari, S. E., Zeng, H., Fenton, A. A., & Henl, R. (2013). Differential control of learning and anxiety along the dorsoventral axis of the dentate gyrus. *Neuron*, 77(5), 955–968. <https://doi.org/10.1016/j.neuron.2012.12.038>
- Kheirbek, M. A., Tannenholz, L., & Hen, R. (2012). NR2B-Dependent Plasticity of Adult-Born Granule Cells is Necessary for Context Discrimination. *Journal of Neuroscience*, 32(25), 8696–8702. <https://doi.org/10.1523/JNEUROSCI.1692-12.2012>
- Kiebler, M. A., & Bassell, G. J. (2006). Neuronal RNA Granules: Movers and Makers. In *Neuron* (Vol. 51, Issue 6, pp. 685–690). Elsevier Inc. <https://doi.org/10.1016/j.neuron.2006.08.021>
- Kiebler, M. A., Hemraj, I., Verkade, P., Köhrmann, M., Fortes, P., Marión, R. M., Ortín,

- J., & Dotti, C. G. (1999). The mammalian staufer protein localizes to the somatodendritic domain of cultured hippocampal neurons: implications for its involvement in mRNA transport. *The Journal of Neuroscience*, *19*(1), 288–297. <http://www.jneurosci.org.emedien.uni-muenchen.de/content/jneuro/19/1/288.full.pdf>
- Kishi, T., Tsumori, T., Yokota, S., & Yasui, Y. (2006). Topographical projection from the hippocampal formation to the amygdala: A combined anterograde and retrograde tracing study in the rat. *Journal of Comparative Neurology*, *496*(3), 349–368. <https://doi.org/10.1002/cne.20919>
- Kjelstrup, K. G., Tuvnes, F. A., Steffenach, H.-A., Murison, R., Moser, E. I., & Moser, M.-B. (2002). Reduced fear expression after lesions of the ventral hippocampus. *Proceedings of the National Academy of Sciences*, *99*(16), 10825–10830. <https://doi.org/10.1073/pnas.152112399>
- Knight, A. L., Yan, X., Hamamichi, S., Ajjuri, R. R., Mazzulli, J. R., Zhang, M. W., Daigle, J. G., Zhang, S., Borom, A. R., Roberts, L. R., Lee, S. K., DeLeon, S. M., Viollet-Djelassi, C., Krainc, D., O'Donnell, J. M., Caldwell, K. A., & Caldwell, G. A. (2014). The glycolytic enzyme, GPI, is a functionally conserved modifier of dopaminergic neurodegeneration in Parkinson's models. *Cell Metabolism*, *20*(1), 145–157. <https://doi.org/10.1016/j.cmet.2014.04.017>
- Kusek, G., Campbell, M., Doyle, F., Tenenbaum, S. A., Kiebler, M., & Temple, S. (2012). Asymmetric segregation of the double-stranded RNA binding protein Staufer2 during mammalian neural stem cell divisions promotes lineage progression. *Cell Stem Cell*, *11*(4), 505–516. <https://doi.org/10.1016/j.stem.2012.06.006>
- Kwon, H. B., Kozorovitskiy, Y., Oh, W. J., Peixoto, R. T., Akhtar, N., Saulnier, J. L., Gu, C., & Sabatini, B. L. (2012). Neuroligin-1-dependent competition regulates cortical synaptogenesis and synapse number. *Nature Neuroscience*, *15*(12), 1667–1674. <https://doi.org/10.1038/nn.3256>
- Lafourcade, C. A., Lin, T. V., Feliciano, D. M., Zhang, L., Hsieh, L. S., & Bordey, A. (2013). Rheb Activation in Subventricular Zone Progenitors Leads to Heterotopia, Ectopic Neuronal Differentiation, and Rapamycin-Sensitive Olfactory Micronodules and Dendrite Hypertrophy of Newborn Neurons. *Journal of Neuroscience*, *33*(6), 2419–2431. <https://doi.org/10.1523/JNEUROSCI.1840-12.2013>
- Lazic, S. E., Grote, H., Armstrong, R. J., Blakemore, C., Hannan, A. J., van Dellen, A., & Barker, R. A. (2004). Decreased hippocampal cell proliferation in R6/1 Huntington's mice. *Neuroreport*, *15*(5), 811–813. <https://doi.org/10.1097/01.wnr.0000122486.43641.90>
- Lazic, S. E., Grote, H. E., Blakemore, C., Hannan, A. J., Van Dellen, A., Phillips, W., & Barker, R. A. (2006). Neurogenesis in the R6/1 transgenic mouse model of Huntington's disease: Effects of environmental enrichment. *European Journal of Neuroscience*, *23*(7), 1829–1838. <https://doi.org/10.1111/j.1460-9568.2006.04715.x>
- Lebeau, G., Miller, L. C., Tartas, M., McAdam, R., Laplante, I., Badeaux, F., DesGroseillers, L., Sossin, W. S., & Lacaille, J.-C. (2011). Staufer 2 regulates mGluR long-term depression and Map1b mRNA distribution in hippocampal neurons. *Learning & Memory*, *18*(5), 314–326. <https://doi.org/10.1101/lm.2100611>
- Lee, E., Giovanello, K. S., Saykin, A. J., Xie, F., Kong, D., Wang, Y., Yang, L., Ibrahim, J. G., Doraiswamy, P. M., & Zhu, H. (2017). Single-nucleotide polymorphisms are associated with cognitive decline at Alzheimer's disease conversion within mild cognitive impairment patients. *Alzheimer's and Dementia: Diagnosis, Assessment and Disease Monitoring*, *8*, 86–95. <https://doi.org/10.1016/j.dadm.2017.04.004>
- Lee, H. K., Kim, I. D., Lee, H., Luo, L., Kim, S. W., & Lee, J. K. (2017, November 14).

- Neuroprotective and Anti-inflammatory Effects of a Dodecamer Peptide Harboring Ninjurin 1 Cell Adhesion Motif in the Postischemic Brain. *Molecular Neurobiology*, 1–18. <https://doi.org/10.1007/s12035-017-0810-1>
- Lee, J. W., Beebe, K., Nangle, L. A., Jang, J., Longo-Guess, C. M., Cook, S. A., Davisson, M. T., Sundberg, J. P., Schimmel, P., & Ackerman, S. L. (2006). Editing-defective tRNA synthetase causes protein misfolding and neurodegeneration. *Nature*, 443(7107), 50–55. <https://doi.org/10.1038/nature05096>
- Lee, K.-W., Hong, J.-H., Choi, I. Y., Che, Y., Lee, J.-K., Yang, S.-D., Song, C.-W., Kang, H. S., Lee, J.-H., Noh, J. S., Shin, H.-S., & Han, P.-L. (2002). Impaired D2 dopamine receptor function in mice lacking type 5 adenylyl cyclase. *The Journal of Neuroscience: The Official Journal of the Society for Neuroscience*, 22(18), 7931–7940. <https://doi.org/22/18/7931> [pii]
- Lee, K. M., Chand, K. K., Hammond, L. A., Lavidis, N. A., & Noakes, P. G. (2017). Functional decline at the aging neuromuscular junction is associated with altered laminin- α 4 expression. *Aging*, 9(3), 880–899. <https://doi.org/10.18632/aging.101198>
- Lehmann, M. L., Brachman, R. A., Martinowich, K., Schloesser, R. J., & Herkenham, M. (2013). Glucocorticoids orchestrate divergent effects on mood through adult neurogenesis. *Journal of Neuroscience*, 33(7), 2961–2972. <https://doi.org/10.1523/JNEUROSCI.3878-12.2013>
- Leuner, B., Caponiti, J. M., & Gould, E. (2012). Oxytocin stimulates adult neurogenesis even under conditions of stress and elevated glucocorticoids. *Hippocampus*, 22(4), 861–868. <https://doi.org/10.1002/hipo.20947>
- Li, D., Herrera, S., Bubula, N., Nikitina, E., Palmer, a a, Hanck, D. a, Loweth, J. a, & Vezina, P. (2012). Casein kinase 1 enables nucleus accumbens amphetamine induced locomotion by regulating AMPA receptor phosphorylation. *J Neurochem*, 118(2), 237–247. <https://doi.org/10.1111/j.1471-4159.2011.07308.x>.Casein
- Li, X. -G, Somogyi, P., Ylinen, A., & Buzsáki, G. (1994). The hippocampal CA3 network: An in vivo intracellular labeling study. *Journal of Comparative Neurology*, 339(2), 181–208. <https://doi.org/10.1002/cne.903390204>
- Lim, D. A., & Alvarez-Buylla, A. (2014). Adult neural stem cells stake their ground. In *Trends in Neurosciences* (Vol. 37, Issue 10, pp. 563–571). <https://doi.org/10.1016/j.tins.2014.08.006>
- Lin, A. C., & Holt, C. E. (2007). Local translation and directional steering in axons. In *EMBO Journal* (Vol. 26, Issue 16, pp. 3729–3736). <https://doi.org/10.1038/sj.emboj.7601808>
- Lin, Y. T., Chen, C. C., Huang, C. C., Nishimori, K., & Hsu, K. Sen. (2017). Oxytocin stimulates hippocampal neurogenesis via oxytocin receptor expressed in CA3 pyramidal neurons. *Nature Communications*, 8(1). <https://doi.org/10.1038/s41467-017-00675-5>
- Liu Ax, Cerniglia, G. J., Bernhard, E. J., & Prendergast, G. C. (2001). RhoB is required to mediate apoptosis in neoplastically transformed cells after DNA damage. *Proceedings of the National Academy of Sciences of the United States of America*, 98(11), 6192–6197. <https://doi.org/10.1073/pnas.111137198>
- Liu, B., Li, Y., Stackpole, E. E., Novak, A., Gao, Y., Zhao, Y., Zhao, X., & Richter, J. D. (2018). Regulatory discrimination of mRNAs by FMRP controls mouse adult neural stem cell differentiation. *Proceedings of the National Academy of Sciences of the United States of America*, 115(48), E11397–E11405. <https://doi.org/10.1073/pnas.1809588115>
- Liu, K., Zhao, Q., Liu, P., Cao, J., Gong, J., Wang, C., Wang, W., Li, X., Sun, H., Zhang, C., Li, Y., Jiang, M., Zhu, S., Sun, Q., Jiao, J., Hu, B., Zhao, X., Li, W., Chen, Q., ... Zhao, T. (2016). ATG3-dependent autophagy mediates mitochondrial

- homeostasis in pluripotency acquirement and maintenance. *Autophagy*, *12*(11), 2000–2008. <https://doi.org/10.1080/15548627.2016.1212786>
- Lucassen, P. J., Stumpel, M. W., Wang, Q., & Aronica, E. (2010). Decreased numbers of progenitor cells but no response to antidepressant drugs in the hippocampus of elderly depressed patients. *Neuropharmacology*, *58*(6), 940–949. <https://doi.org/10.1016/j.neuropharm.2010.01.012>
- Luo, Y., Shan, G., Guo, W., Smrt, R. D., Johnson, E. B., Li, X., Pfeiffer, R. L., Szulwach, K. E., Duan, R., Barkho, B. Z., Li, W., Liu, C., Jin, P., & Zhao, X. (2010). Fragile X mental retardation protein regulates proliferation and differentiation of adult neural stem/progenitor cells. *PLoS Genetics*, *6*(4). <https://doi.org/10.1371/journal.pgen.1000898>
- Maas, N. M. C., Van De Putte, T., Melotte, C., Francis, A., Schrandt-Stumpel, C. T. R. M., Sanlaville, D., Genevieve, D., Lyonnet, S., Dimitrov, B., Devriendt, K., Fryns, J. P., & Vermeesch, J. R. (2007). The C20orf133 gene is disrupted in a patient with Kabuki syndrome. *Journal of Medical Genetics*, *44*(9), 562–569. <https://doi.org/10.1136/jmg.2007.049510>
- Malberg, J. E., Eisch, A. J., Nestler, E. J., & Duman, R. S. (2000). Chronic antidepressant treatment increases neurogenesis in adult rat hippocampus. *The Journal of Neuroscience*, *20*(24), 9104–9110. <https://doi.org/10.1523/JNEUROSCI.2024-9104.2000> [pii]
- Manganas, L. N., Zhang, X., Li, Y., Hazel, R., Smith, D., Wagshul, M., Henn, F., Benveniste, H., Djuric, P., Enikolopov, G., & Maletic-Savatic, M. (2007). Magnetic Resonance Spectroscopy identifies neural progenitor cells in the live human brain. *Science*, *318*(5852), 980–985. <https://doi.org/10.1126/science.1147379>
- Mardakheh, F. K., Self, A., & Marshall, C. J. (2016). RHO binding to FAM65A regulates Golgi reorientation during cell migration. *Journal of Cell Science*, *129*(24), jcs.198614. <https://doi.org/10.1242/jcs.198614>
- Marín-Burgin, A., Mongiat, L. A., Pardi, M. B., & Schinder, A. F. (2012). Unique processing during a period of high excitation/inhibition balance in adult-born neurons. *Science*, *335*(6073), 1238–1242. <https://doi.org/10.1126/science.1214956>
- Marland, J. R. K., Hasel, P., Bonnycastle, K., & Cousin, M. A. (2016). Mitochondrial Calcium Uptake Modulates Synaptic Vesicle Endocytosis in Central Nerve Terminals. *The Journal of Biological Chemistry*, *291*(5), 2080–2086. <https://doi.org/10.1074/jbc.M115.686956>
- Martin, K. C., & Ephrussi, A. (2009). mRNA Localization: Gene Expression in the Spatial Dimension. In *Cell* (Vol. 136, Issue 4, pp. 719–730). <https://doi.org/10.1016/j.cell.2009.01.044>
- Martin, K. C., & Zukin, R. S. (2006). RNA Trafficking and Local Protein Synthesis in Dendrites: An Overview. *Journal of Neuroscience*, *26*(27), 7131–7134. <https://doi.org/10.1523/JNEUROSCI.1801-06.2006>
- Matsui, M., Oshima, M., Oshima, H., Takaku, K., Maruyama, T., Yodoi, J., & Taketo, M. M. (1996). Early embryonic lethality caused by targeted disruption of the mouse thioredoxin gene. *Developmental Biology*, *178*(1), 179–185. <https://doi.org/10.1006/dbio.1996.0208>
- Mattson, M. P., & Liu, D. (2002). Energetics and oxidative stress in synaptic plasticity and neurodegenerative disorders. In *NeuroMolecular Medicine* (Vol. 2, Issue 2, pp. 215–231). Humana Press. <https://doi.org/10.1385/NMM:2:2:215>
- McCall, M. a, Gregg, R. G., Behringer, R. R., Brenner, M., Delaney, C. L., Galbreath, E. J., Zhang, C. L., Pearce, R. A., Chiu, S. Y., & Messing, A. (1996). Targeted deletion in astrocyte intermediate filament (Gfap) alters neuronal physiology. *Proceedings of the National Academy of Sciences of the United States of America*, *93*(June 1996), 6361–6366. <https://doi.org/10.1073/pnas.93.13.6361>
- Meikle, L., Talos, D. M., Onda, H., Pollizzi, K., Rotenberg, A., Sahin, M., Jensen, F. E.,

- & Kwiatkowski, D. J. (2007). A Mouse Model of Tuberous Sclerosis: Neuronal Loss of Tsc1 Causes Dysplastic and Ectopic Neurons, Reduced Myelination, Seizure Activity, and Limited Survival. *Journal of Neuroscience*, 27(21), 5546–5558. <https://doi.org/10.1523/JNEUROSCI.5540-06.2007>
- Merkle, S., & Pretsch, W. (1992). A glucosephosphate isomerase (GPI) null mutation in *Mus musculus*: evidence that anaerobic glycolysis is the predominant energy delivering pathway in early post-implantation embryos. *Comparative Biochemistry and Physiology -- Part B: Biochemistry And*, 101(3), 309–314. [https://doi.org/10.1016/0305-0491\(92\)90004-B](https://doi.org/10.1016/0305-0491(92)90004-B)
- Mi, S., Lee, X., Hu, Y., Ji, B., Shao, Z., Yang, W., Huang, G., Walus, L., Rhodes, K., Gong, B. J., Miller, R. H., & Pepinsky, R. B. (2011). Death receptor 6 negatively regulates oligodendrocyte survival, maturation and myelination. *Nature Medicine*, 17(7), 816–821. <https://doi.org/10.1038/nm.2373>
- Micheli, V., Camici, M., Tozzi, M. G., Ipata, P. L., Sestini, S., Bertelli, M., & Pompucci, G. (2011). Neurological disorders of purine and pyrimidine metabolism.pdf. *Current Topics in Medicinal Chemistry*, 1(8), 923–947. <https://doi.org/10.2174/156802611795347645>
- Mijimolle, N., Velasco, J., Dubus, P., Guerra, C., Weinbaum, C. A., Casey, P. J., Campuzano, V., & Barbacid, M. (2005). Protein farnesyltransferase in embryogenesis, adult homeostasis, and tumor development. *Cancer Cell*, 7(4), 313–324. <https://doi.org/10.1016/j.ccr.2005.03.004>
- Ming, G. li, & Song, H. (2011). Adult Neurogenesis in the Mammalian Brain: Significant Answers and Significant Questions. *Neuron*, 70(4), 687–702. <https://doi.org/10.1016/j.neuron.2011.05.001>
- Miyamoto, Y., Yamauchi, J., Tanoue, A., Wu, C., & Mobley, W. C. (2006). TrkB binds and tyrosine-phosphorylates Tiam1, leading to activation of Rac1 and induction of changes in cellular morphology. *Proceedings of the National Academy of Sciences of the United States of America*, 103(27), 10444–10449. <https://doi.org/10.1073/pnas.0603914103>
- Mongiat, L. A., Espósito, M. S., Lombardi, G., & Schinder, A. F. (2009). Reliable activation of immature neurons in the adult hippocampus. *PLoS ONE*, 4(4). <https://doi.org/10.1371/journal.pone.0005320>
- Moon, H. Y., Javadi, S., Stremlau, M., Yoon, K. J., Becker, B., Kang, S. U., Zhao, X., & van Praag, H. (2019). Conditioned media from AICAR-treated skeletal muscle cells increases neuronal differentiation of adult neural progenitor cells. *Neuropharmacology*, 145(October 2018), 123–130. <https://doi.org/10.1016/j.neuropharm.2018.10.041>
- Moreno-Jiménez, E. P., Flor-García, M., Terreros-Roncal, J., Rábano, A., Cafini, F., Pallas-Bazarra, N., Ávila, J., & Llorens-Martín, M. (2019). Adult hippocampal neurogenesis is abundant in neurologically healthy subjects and drops sharply in patients with Alzheimer’s disease. In *Nature Medicine* (Vol. 25, Issue 4, pp. 554–560). Springer US. <https://doi.org/10.1038/s41591-019-0375-9>
- Mori, Y., Matsui, T., & Fukuda, M. (2013). Rabex-5 protein regulates dendritic localization of small GTPase Rab17 and neurite morphogenesis in hippocampal neurons. *Journal of Biological Chemistry*, 288(14), 9835–9847. <https://doi.org/10.1074/jbc.M112.427591>
- Moriguchi, S., Nishi, M., Komazaki, S., Sakagami, H., Miyazaki, T., Masumiya, H., Saito, S.-Y., Watanabe, M., Kondo, H., Yawo, H., Fukunaga, K., & Takeshima, H. (2006). Functional uncoupling between Ca²⁺ release and afterhyperpolarization in mutant hippocampal neurons lacking junctophilins. *Proceedings of the National Academy of Sciences of the United States of America*, 103(28), 10811–10816. <https://doi.org/10.1073/pnas.0509863103>

- Moser, E. I., Moser, M., & Andersen, P. (1993). Spatial learning impairment parallels the magnitude of dorsal hippocampal lesions, but is hardly present following ventral lesions. *The Journal of Neuroscience*, *13*(9), 3916–3925. [https://doi.org/10.1016/S0378-8733\(97\)00003-8](https://doi.org/10.1016/S0378-8733(97)00003-8)
- Moser, M., Li, Y., Vaupel, K., Kretschmar, D., Kluge, R., Glynn, P., & Buettner, R. (2004). Placental failure and impaired vasculogenesis result in embryonic lethality for neuropathy target esterase-deficient mice. *Molecular and Cellular Biology*, *24*(4), 1667–1679. <https://doi.org/10.1128/MCB.24.4.1667-1679.2004>
- Mouri, A., Noda, Y., Watanabe, K., & Nabeshima, T. (2013). The roles of MAGE-D1 in the neuronal functions and pathology of the central nervous system. *Reviews in the Neurosciences*, *24*(1), 61–70. <https://doi.org/10.1515/revneuro-2012-0069>
- Mullen, R. J., Buck, C. R., & Smith, A. M. (1992). NeuN, a neuronal specific nuclear protein in vertebrates. *Development*, *116*, 201–211. <https://doi.org/VL-116>
- Munsch, T., Freichel, M., Flockerzi, V., & Pape, H.-C. (2003). Contribution of transient receptor potential channels to the control of GABA release from dendrites. *Proceedings of the National Academy of Sciences of the United States of America*, *100*(26), 16065–16070. <https://doi.org/10.1073/pnas.2535311100>
- Nakashiba, T., Cushman, J. D., Pelkey, K. A., Renaudineau, S., Buhl, D. L., McHugh, T. J., Barrera, V. R., Chittajallu, R., Iwamoto, K. S., McBain, C. J., Fanselow, M. S., & Tonegawa, S. (2012). Young dentate granule cells mediate pattern separation, whereas old granule cells facilitate pattern completion. *Cell*, *149*(1), 188–201. <https://doi.org/10.1016/j.cell.2012.01.046>
- Nelissen, T. P., Bamford, R. A., Tochitani, S., Akkus, K., Kudzinskas, A., Yokoi, K., Okamoto, H., Yamamoto, Y., Burbach, J. P. H., Matsuzaki, H., & Oguro-Ando, A. (2018). CD38 is Required for Dendritic Organization in Visual Cortex and Hippocampus. *Neuroscience*, *372*, 114–125. <https://doi.org/10.1016/j.neuroscience.2017.12.050>
- Nihon Seikagakkai., T., Ohtsuki, S., Homma, K., & Natori, S. (1998). cDNA Cloning of Mouse Prolyl Endopeptidase and Its Involvement in DNA Synthesis by Swiss 3T3 Cells. *The Journal of Biochemistry*, *123*(3), 540–545. https://www.jstage.jst.go.jp/article/biochemistry1922/123/3/123_3_540/_article
- Nikolaev, A., McLaughlin, T., O’Leary, D. D. M., & Tessier-Lavigne, M. (2009). APP binds DR6 to trigger axon pruning and neuron death via distinct caspases. *Nature*, *457*(7232), 981–989. <https://doi.org/10.1038/nature07767>
- Nishi, M., Takeshima, H., Hashimoto, K., Kano, M., Hashimoto, K., Kano, M., Kuriyama, K., Komazaki, S., & Shibata, S. (2002). Motor discoordination in mutant mice lacking junctophilin type 3. *Biochemical and Biophysical Research Communications*, *292*(2), 318–324. <https://doi.org/10.1006/bbrc.2002.6649>
- Nishiyama, A., Yang, Z., & Butt, A. (2005). Astrocytes and NG2-glia: what’s in a name? *Journal of Anatomy*, *207*(6), 687–693. <https://www.ncbi.nlm.nih.gov/emedien.ub.uni-muenchen.de/pubmed/?term=Astrocytes+and+NG2-glia%3A+what's+in+a+name%3F>
- Okado, H., Ohtaka-Maruyama, C., Sugitani, Y., Fukuda, Y., Ishida, R., Hirai, S., Miwa, A., Takahashi, A., Aoki, K., Mochida, K., Suzuki, O., Honda, T., Nakajima, K., Ogawa, M., Terashima, T., Matsuda, J., Kawano, H., & Kasai, M. (2009). The transcriptional repressor RP58 is crucial for cell-division patterning and neuronal survival in the developing cortex. *Developmental Biology*, *331*(2), 140–151. <https://doi.org/10.1016/j.ydbio.2009.04.030>
- Park, D., Choi, D., Lee, J., Lim, D. S., & Park, C. (2010). Male-like sexual behavior of female mouse lacking fucose mutarotase. *BMC Genetics*, *11*(1), 62. <https://doi.org/10.1186/1471-2156-11-62>
- Penas, C., Hatten, M. E., & Ayad, N. G. (2015). The APC/C and CK1 in the developing

- brain. *Oncotarget*, 6(19), 16792–16793. <https://doi.org/10.18632/oncotarget.4797>
- Penzes, P., & Rafalovich, I. (2012). Regulation of the actin cytoskeleton in dendritic spines. *Advances in Experimental Medicine and Biology*, 970, 81–95. https://doi.org/10.1007/978-3-7091-0932-8_4
- Pereira, A. C., Huddleston, D. E., Brickman, A. M., Sosunov, A. A., Hen, R., McKhann, G. M., Sloan, R., Gage, F. H., Brown, T. R., & Small, S. A. (2007). An in vivo correlate of exercise-induced neurogenesis in the adult dentate gyrus. *Proceedings of the National Academy of Sciences*, 104(13), 5638–5643. <https://doi.org/10.1073/pnas.0611721104>
- Phillips, C., & Fahimi, A. (2018). Immune and Neuroprotective Effects of Physical Activity on the Brain in Depression. *Frontiers in Neuroscience*, 12(July), 1–22. <https://doi.org/10.3389/fnins.2018.00498>
- Pilo-Boyl, P., Di Nardo, A., Mulle, C., Sassoè-Pognetto, M., Panzanelli, P., Mele, A., Kneussel, M., Costantini, V., Perlas, E., Massimi, M., Vara, H., Giustetto, M., & Witke, W. (2007). Profilin2 contributes to synaptic vesicle exocytosis, neuronal excitability, and novelty-seeking behavior. *EMBO Journal*, 26(12), 2991–3002. <https://doi.org/10.1038/sj.emboj.7601737>
- Piper, M., Moldrich, R. X., Lindwall, C., Little, E., Barry, G., Mason, S., Sunn, N., Kurniawan, N. D., Gronostajski, R. M., & Richards, L. J. (2009). Multiple non-cell-autonomous defects underlie neocortical callosal dysgenesis in Nfib-deficient mice. *Neural Development*, 4(1), 43. <https://doi.org/10.1186/1749-8104-4-43>
- Popper, B., Demleitner, A., Bolivar, V. J., Kusek, G., Snyder-Keller, A., Schieweck, R., Temple, S., & Kiebler, M. A. (2018). Staufen2 deficiency leads to impaired response to novelty in mice. *Neurobiology of Learning and Memory*, 150, 107–115. <https://doi.org/10.1016/j.nlm.2018.02.027>
- Pothuizen, H. H. J., Zhang, W. N., Jongen-Rêlo, A. L., Feldon, J., & Yee, B. K. (2004). Dissociation of function between the dorsal and the ventral hippocampus in spatial learning abilities of the rat: A within-subject, within-task comparison of reference and working spatial memory. *European Journal of Neuroscience*, 19(3), 705–712. <https://doi.org/10.1111/j.0953-816X.2004.03170.x>
- Powell, A. W., Sassa, T., Wu, Y., Tessier-Lavigne, M., & Polleux, F. (2008). Topography of thalamic projections requires attractive and repulsive functions of netrin-1 in the ventral telencephalon. *PLoS Biology*, 6(5), 1047–1068. <https://doi.org/10.1371/journal.pbio.0060116>
- Qin, H., Buckley, J. A., Li, X., Liu, Y., Fox, T. H., Meares, G. P., Yu, H., Yan, Z., Harms, A. S., Li, Y., Standaert, D. G., & Benveniste, E. N. (2016). Inhibition of the JAK/STAT Pathway Protects Against α -Synuclein-Induced Neuroinflammation and Dopaminergic Neurodegeneration. *The Journal of Neuroscience*, 36(18), 5144–5159. <https://doi.org/10.1523/JNEUROSCI.4658-15.2016>
- Raaijmakers, J. H., & Bos, J. L. (2010). Specificity in Ras and Rap Signalling. *The Journal Of Biological Chemistry*, 284(17), 10995–10999. <https://doi.org/10.1074/jbc.R800061200>
- Rangaraju, V., Lauterbach, M., & Schuman, E. M. (2019). Spatially Stable Mitochondrial Compartments Fuel Local Translation during Plasticity. *Cell*, 176(1–2), 73–84.e15. <https://doi.org/10.1016/j.cell.2018.12.013>
- Rao, M. S., & Shetty, A. K. (2004). Efficacy of doublecortin as a marker to analyse the absolute number and dendritic growth of newly generated neurons in the adult dentate gyrus. *European Journal of Neuroscience*, 19(2), 234–246. <https://doi.org/10.1111/j.0953-816X.2003.03123.x>
- Reaume, A. G., Elliott, J. L., Hoffman, E. K., Kowall, N. W., Ferrante, R. J., Siwek, D. F., Wilcox, H. M., Flood, D. G., Beal, M. F., Brown, R. H., Scott, R. W., & Snider, W. D. (1996). Motor neurons in Cu/Zn superoxide dismutase-deficient mice develop

- normally but exhibit enhanced cell death after axonal injury. *Nature Genetics*, *13*(1), 43–47. <https://doi.org/10.1038/ng0596-43>
- Richetin, K., Moulis, M., Millet, A., Arr??zola, M. S., Andraini, T., Hua, J., Davezac, N., Roybon, L., Belenguer, P., Miquel, M. C., & Rampon, C. (2017). Amplifying mitochondrial function rescues adult neurogenesis in a mouse model of Alzheimer’s disease. *Neurobiology of Disease*, *102*, 113–124. <https://doi.org/10.1016/j.nbd.2017.03.002>
- Rodríguez, J. J., Jones, V. C., Tabuchi, M., Allan, S. M., Knight, E. M., LaFerla, F. M., Oddo, S., & Verkhratsky, A. (2008). Impaired adult neurogenesis in the dentate gyrus of a triple transgenic mouse model of Alzheimer’s disease. *PloS One*, *3*(8), e2935 1-8. <https://doi.org/10.1371/journal.pone.0002935>
- Rueda, C. B., Traba, J., Amigo, I., Llorente-Folch, I., Gonzalez-Sanchez, P., Pardo, B., Esteban, J. A., del Arco, A., & Satrustegui, J. (2015). Mitochondrial ATP-Mg/Pi Carrier SCA3/Slc25a3 Counteracts PARP-1-Dependent Fall in Mitochondrial ATP Caused by Excitotoxic Insults in Neurons. *Journal of Neuroscience*, *35*(8), 3566–3581. <https://doi.org/10.1523/JNEUROSCI.2702-14.2015>
- Ruest, L. B., Marcotte, R., & Wang, E. (2002). Peptide elongation factor eEF1A-2/S1 expression in cultured differentiated myotubes and its protective effect against caspase-3-mediated apoptosis. *Journal of Biological Chemistry*, *277*(7), 5418–5425. <https://doi.org/10.1074/jbc.M110685200>
- Sadakata, T., & Furuichi, T. (2006). Identification and mRNA expression of Ogdh, QP-C, and two predicted genes in the postnatal mouse brain. *Neuroscience Letters*, *405*(3), 217–222. <https://doi.org/10.1016/j.neulet.2006.07.008>
- Sala, C., & Segal, M. (2014). Dendritic Spines: The Locus of Structural and Functional Plasticity. *Physiological Reviews*, *94*(1), 141–188. <https://doi.org/10.1152/physrev.00012.2013>
- Sano, T., Kim, Y. J., Oshima, E., Shimizu, C., Kiyonari, H., Abe, T., Higashi, H., Yamada, K., & Hirabayashi, Y. (2011). Comparative characterization of GPRC5B and GPRC5C LacZ knockin mice; behavioral abnormalities in GPRC5B-deficient mice. *Biochemical and Biophysical Research Communications*, *412*(3), 460–465. <https://doi.org/10.1016/j.bbrc.2011.07.118>
- Santarelli, L., Saxe, M., Gross, C., Surget, A., Battaglia, F., Dulawa, S., Weisstaub, N., Lee, J., Duman, R., Arancio, O., Belzung, C., & Hen, R. (2003). Requirement of Hippocampal Neurogenesis for the Behavioral Effects of Antidepressants. *Science*, *301*(5634), 805–809. <https://doi.org/10.1126/science.1083328>
- Sato, T., Akasu, H., Shimono, W., Matsu, C., Fujiwara, Y., Shibagaki, Y., Heard, J. J., Tamanoi, F., & Hattori, S. (2015). Rheb protein binds CAD (carbamoyl-phosphate synthetase 2, aspartate transcarbamoylase, and dihydroorotase) protein in a GTP-And effector domain-dependent manner and influences its cellular localization and carbamoylphosphate synthetase (CPSase) activity. *Journal of Biological Chemistry*, *290*(2), 1096–1105. <https://doi.org/10.1074/jbc.M114.592402>
- Scheiffele, P., Fan, J., Choih, J., Fetter, R., & Serafini, T. (2000). Neuroligin expressed in nonneuronal cells triggers presynaptic development in contacting axons. *Cell*, *101*(6), 657–669. [https://doi.org/10.1016/S0092-8674\(00\)80877-6](https://doi.org/10.1016/S0092-8674(00)80877-6)
- Schwanhäusser, B., Busse, D., Li, N., Dittmar, G., Schuchhardt, J., Wolf, J., Chen, W., & Selbach, M. (2011). Global quantification of mammalian gene expression control. *Nature*, *473*(7347), 337–342. <https://doi.org/10.1038/nature10098>
- Seehusen, F., Kiel, K., Jottini, S., Wohlsein, P., Habierski, A., Seibel, K., Vogel, T., Urlaub, H., Kollmar, M., Baumgärtner, W., & Teichmann, U. (2016). Axonopathy in the Central Nervous System Is the Hallmark of Mice with a Novel Intragenic Null Mutation of Dystonin. *Genetics*, *204*(1), 191–203. <https://doi.org/10.1534/genetics.116.186932>

- Shah, S., Lubeck, E., Zhou, W., Cai, L., Beliveau, B. J., Joyce, E. F., Apostolopoulos, N., Yilmaz, F., Fonseka, C. Y., McCole, R. B., Chang, Y., Li, J. B., Senaratne, T. N., Williams, B. R., al., et, Betzig, E., Patterson, G. H., Sougrat, R., Lindwasser, O. W., ... al., et. (2016). In Situ Transcription Profiling of Single Cells Reveals Spatial Organization of Cells in the Mouse Hippocampus. *Neuron*, *92*(2), 342–357. <https://doi.org/10.1016/j.neuron.2016.10.001>
- Sharangdhar, T., Sugimoto, Y., Heraud-Farlow, J., Fernández-Moya, S. M., Ehses, J., Ruiz de los Mozos, I., Ule, J., & Kiebler, M. A. (2017). A retained intron in the 3'-UTR of *Calm3* mRNA mediates its Staufen2- and activity-dependent localization to neuronal dendrites. *EMBO Reports*, *18*(10), 1762–1774. <https://doi.org/10.15252/embr.201744334>
- Shi, P., Ström, A. L., Gal, J., & Zhu, H. (2010). Effects of ALS-related SOD1 mutants on dynein- and KIF5-mediated retrograde and anterograde axonal transport. *Biochimica et Biophysica Acta - Molecular Basis of Disease*, *1802*(9), 707–716. <https://doi.org/10.1016/j.bbadis.2010.05.008>
- Shibutani, S., Okazaki, H., & Iwata, H. (2017). Dynamin-dependent amino acid endocytosis activates mechanistic target of rapamycin complex 1 (mTORC1). *Journal of Biological Chemistry*, *292*(44), 18052–18061. <https://doi.org/10.1074/jbc.M117.776443>
- Shmelkov, S. V., Hormigo, A., Jing, D., Proenca, C. C., Bath, K. G., Milde, T., Shmelkov, E., Kushner, J. S., Baljevic, M., Dincheva, I., Murphy, A. J., Valenzuela, D. M., Gale, N. W., Yancopoulos, G. D., Ninan, I., Lee, F. S., & Rafii, S. (2010). *Slitrk5* deficiency impairs corticostriatal circuitry and leads to obsessive-compulsive-like behaviors in mice. *Nature Medicine*, *16*(5), 598–602. <https://doi.org/10.1038/nm.2125>
- Siemen, H., Colas, D., Heller, H. C., Brustle, O., & Reijo Pera, R. A. (2011). *Pumilio-2* Function in the Mouse Nervous System. *PLoS One*, *6*(10), 1–14. <https://doi.org/10.1371/Citation>
- Snyder, J. S., Choe, J. S., Clifford, M. A., Jeurling, S. I., Hurley, P., Brown, A., Kamhi, J. F., & Cameron, H. A. (2009). Adult-Born Hippocampal Neurons Are More Numerous, Faster Maturing, and More Involved in Behavior in Rats than in Mice. *Journal of Neuroscience*, *29*(46), 14484–14495. <https://doi.org/10.1523/JNEUROSCI.1768-09.2009>
- Snyder, J. S., Soumier, A., Brewer, M., Pickel, J., & Cameron, H. A. (2011). Adult hippocampal neurogenesis buffers stress responses and depressive behavior. *Nature*, *476*(7361), 458–461. <https://doi.org/10.1038/nature10287>. Adult
- Song, H., Stevens, C. F., & Gage, F. H. (2002). Astroglia induce neurogenesis from adult neural stem cells. *Nature*, *417*(6884), 39–44. <https://doi.org/10.1038/417039a>
- Sorrells, S. F., Paredes, M. F., Cebrian-Silla, A., Sandoval, K., Qi, D., Kelley, K. W., James, D., Mayer, S., Chang, J., Auguste, K. I., Chang, E. F., Gutierrez, A. J., Kriegstein, A. R., Mathern, G. W., Oldham, M. C., Huang, E. J., Garcia-Verdugo, J. M., Yang, Z., & Alvarez-Buylla, A. (2018). Human hippocampal neurogenesis drops sharply in children to undetectable levels in adults. *Nature*, *555*(7696), 377–381. <https://doi.org/10.1038/nature25975>
- Spalding, K. L., Bergmann, O., Alkass, K., Bernard, S., Salehpour, M., Huttner, H. B., Boström, E., Westerlund, I., Vial, C., Buchholz, B. A., Possnert, G., Mash, D. C., Druid, H., & Frisén, J. (2013). Dynamics of Hippocampal Neurogenesis in Adult Humans. *Cell*, *153*(6), 1219–1227. <https://doi.org/10.1016/j.cell.2013.05.002>
- Spassov, D. S., & Jurecic, R. (2002). Cloning and comparative sequence analysis of PUM1 and PUM2 genes, human members of the *Pumilio* family of RNA-binding proteins. *Gene*, *299*(1–2), 195–204. [https://doi.org/10.1016/S0378-1119\(02\)01060-0](https://doi.org/10.1016/S0378-1119(02)01060-0)

- Stolt, C. C., Rehberg, S., Ader, M., Lommes, P., Riethmacher, D., Schachner, M., Bartsch, U., & Wegner, M. (2002). Terminal differentiation of myelin-forming oligodendrocytes depends on the transcription factor Sox10. *Genes and Development*, *16*(2), 165–170. <https://doi.org/10.1101/gad.215802>
- Stornetta, R. L., & Zhu, J. J. (2011). Ras and Rap signaling in synaptic plasticity and mental disorders. *Neuroscientist*, *17*(1), 54–78. <https://doi.org/10.1177/1073858410365562>
- Strange, B. A., Witter, M. P., Lein, E. S., & Moser, E. I. (2014). Functional organization of the hippocampal longitudinal axis. *Nature Reviews Neuroscience*, *15*(10), 655–669. <https://doi.org/10.1038/nrn3785>
- Subramanian, J., Dye, L., & Morozov, A. (2013). Rap1 Signaling Prevents L-Type Calcium Channel-Dependent Neurotransmitter Release. *Journal of Neuroscience*, *33*(17), 7245–7252. <https://doi.org/10.1523/JNEUROSCI.5963-11.2013>
- Sultan, S., Li, L., Moss, J., Petrelli, F., Cassé, F., Gebara, E., Lopatar, J., Pfrieger, F. W., Bezzi, P., Bischofberger, J., & Toni, N. (2015). Synaptic Integration of Adult-Born Hippocampal Neurons Is Locally Controlled by Astrocytes. *Neuron*, *88*(5), 957–972. <https://doi.org/10.1016/j.neuron.2015.10.037>
- Takagi, Y., Mitsui, A., Nishiyama, A., Nozaki, K., Sono, H., Gon, Y., Hashimoto, N., & Yodoi, J. (1999). Overexpression of thioredoxin in transgenic mice attenuates focal ischemic brain damage. *Proceedings of the National Academy of Sciences*, *96*(7), 4131–4136. <https://doi.org/10.1073/pnas.96.7.4131>
- Tanaka, M., Kamo, T., Ota, S., & Sugimura, H. (2003). Association of dishevelled with Eph tyrosine kinase receptor and ephrin mediates cell repulsion. *EMBO Journal*, *22*(4), 847–858. <https://doi.org/10.1093/emboj/cdg088>
- Tang, S. J., Meulemans, D., Vazquez, L., Colaco, N., & Schuman, E. (2001). A role for a rat homolog of stau68 in the transport of RNA to neuronal dendrites. *Neuron*, *32*(3), 463–475. [https://doi.org/10.1016/S0896-6273\(01\)00493-7](https://doi.org/10.1016/S0896-6273(01)00493-7)
- Taniguchi, T., Tanaka, S., Ishii, A., Watanabe, M., Fujitani, N., Sugeo, A., Gotoh, S., Ohta, T., Hiyoshi, M., Matsuzaki, H., Sakai, N., & Konishi, H. (2013). A brain-specific Grb2-associated regulator of extracellular signal-regulated kinase (Erk)/mitogen-activated protein kinase (MAPK) (GAREM) subtype, GAREM2, contributes to neurite outgrowth of neuroblastoma cells by regulating erk signaling. *Journal of Biological Chemistry*, *288*(41), 29934–29942. <https://doi.org/10.1074/jbc.M113.492520>
- Tasaki, T., Sohr, R., Xia, Z., Hellweg, R., Hörtnagl, H., Varshavsky, A., & Yong, T. K. (2007). Biochemical and genetic studies of UBR3, a ubiquitin ligase with a function in olfactory and other sensory systems. *Journal of Biological Chemistry*, *282*(25), 18510–18520. <https://doi.org/10.1074/jbc.M701894200>
- Taylor Clelland, C. L., Craciun, L., Bancroft, C., & Lufkin, T. (2000). Mapping and developmental expression analysis of the WD-repeat gene Preb. *Genomics*, *63*(3), 391–399. <https://doi.org/10.1006/geno.1999.6089>
- Tobin, M. K., Musaraca, K., Disouky, A., Shetti, A., Bheri, A., Honer, W. G., Kim, N., Dawe, R. J., Bennett, D. A., Arfanakis, K., & Lazarov, O. (2019). Human Hippocampal Neurogenesis Persists in Aged Adults and Alzheimer’s Disease Patients. *Cell Stem Cell*, *24*(6), 974–982.e3. <https://doi.org/10.1016/j.stem.2019.05.003>
- Toni, N., Laplagne, D. A., Zhao, C., Lombardi, G., Ribak, C. E., Gage, F. H., & Schinder, A. F. (2008). Neurons born in the adult dentate gyrus form functional synapses with target cells. *Nature Neuroscience*, *11*(8), 901–907. <https://doi.org/10.1038/nn.2156>
- Toni, N., Teng, E. M., Bushong, E. A., Aimone, J. B., Zhao, C., Consiglio, A., Van Praag,

- H., Martone, M. E., Ellisman, M. H., & Gage, F. H. (2007). Synapse formation on neurons born in the adult hippocampus. *Nature Neuroscience*, *10*(6), 727–734. <https://doi.org/10.1038/nn1908>
- Vaccari, I., Dina, G., Tronchère, H., Kaufman, E., Chicanne, G., Cerri, F., Wrabetz, L., Payraastre, B., Quattrini, A., Weisman, L. S., Meisler, M. H., & Bolino, A. (2011). Genetic interaction between MTMR2 and FIG4 phospholipid phosphatases involved in Charcot-Marie-Tooth neuropathies. *PLoS Genetics*, *7*(10). <https://doi.org/10.1371/journal.pgen.1002319>
- Vaghi, V., Pennucci, R., Talpo, F., Corbetta, S., Montinaro, V., Barone, C., Croci, L., Spaiardi, P., Consalez, G. G., Biella, G., & De Curtis, I. (2014). Rac1 and Rac3 GTPases control synergistically the development of cortical and hippocampal GABAergic interneurons. *Cerebral Cortex*, *24*(5), 1247–1258. <https://doi.org/10.1093/cercor/bhs402>
- Vallejo, A., Perurena, N., Guruceaga, E., Mazur, P. K., Martinez-Canarias, S., Zanduetta, C., Valencia, K., Arricibita, A., Gwinn, D., Sayles, L. C., Chuang, C. H., Guembe, L., Bailey, P., Chang, D. K., Biankin, A., Ponz-Sarvisé, M., Andersen, J. B., Khatri, P., Bozec, A., ... Vicent, S. (2017). An integrative approach unveils FOSL1 as an oncogene vulnerability in KRAS-driven lung and pancreatic cancer. *Nature Communications*, *8*. <https://doi.org/10.1038/ncomms14294>
- Van Bokhoven, P., Oomen, C. A., Hoogendijk, W. J. G., Smit, A. B., Lucassen, P. J., & Spijker, S. (2011). Reduction in hippocampal neurogenesis after social defeat is long-lasting and responsive to late antidepressant treatment. *European Journal of Neuroscience*, *33*(10), 1833–1840. <https://doi.org/10.1111/j.1460-9568.2011.07668.x>
- van Heesch, S., Witte, F., Schneider-Lunitz, V., Schulz, J. F., Adami, E., Faber, A. B., Kirchner, M., Maatz, H., Blachut, S., Sandmann, C. L., Kanda, M., Worth, C. L., Schafer, S., Calviello, L., Merriott, R., Patone, G., Hummel, O., Wyler, E., Obermayer, B., ... Hubner, N. (2019). The Translational Landscape of the Human Heart. *Cell*. <https://doi.org/10.1016/j.cell.2019.05.010>
- Van Praag, H., Kempermann, G., & Gage, F. (1999). Running increases cell proliferation and neurogenesis in the adult mouse dentate gyrus. *Nature Neuroscience*, *2*(3), 266–270. <https://doi.org/10.1038/6368>
- Vaynman, S., Ying, Z., Wu, A., & Gomez-Pinilla, F. (2006). Coupling energy metabolism with a mechanism to support brain-derived neurotrophic factor-mediated synaptic plasticity. *Neuroscience*, *139*(4), 1221–1234. <https://doi.org/10.1016/j.neuroscience.2006.01.062>
- Vazdarjanova, A., & Guzowski, J. F. (2004). Differences in hippocampal neuronal population responses to modifications of an environmental context: Evidence for distinct, yet complementary, functions of CA3 and CA1 ensembles. *Journal of Neuroscience*, *24*(29), 6489–6496. <https://doi.org/10.1523/JNEUROSCI.0350-04.2004>
- Vessey, J. P., Amadei, G., Burns, S. E., Kiebler, M. A., Kaplan, D. R., & Miller, F. D. (2012). An asymmetrically localized Staufen2-dependent RNA complex regulates maintenance of mammalian neural stem cells. *Cell Stem Cell*, *11*(4), 517–528. <https://doi.org/10.1016/j.stem.2012.06.010>
- Vessey, J. P., Macchi, P., Stein, J. M., Mikl, M., Hawker, K. N., Vogelsang, P., Wiczorek, K., Vendra, G., Riefler, J., Tubing, F., Aparicio, S. A. J., Abel, T., & Kiebler, M. A. (2008). A loss of function allele for murine Staufen1 leads to impairment of dendritic Staufen1-RNP delivery and dendritic spine morphogenesis. *Proceedings of the National Academy of Sciences*, *105*(42), 16374–16379. <https://doi.org/10.1073/pnas.0804583105>
- Vessey, J. P., Vaccani, A., Xie, Y., Dahm, R., Karra, D., Kiebler, M. A., & Macchi, P.

- (2006). Dendritic Localization of the Translational Repressor Pumilio 2 and Its Contribution to Dendritic Stress Granules. *Journal of Neuroscience*, 26(24), 6496–6508. <https://doi.org/10.1523/JNEUROSCI.0649-06.2006>
- Vivar, C., Peterson, B. D., & van Praag, H. (2016). Running rewires the neuronal network of adult-born dentate granule cells. *NeuroImage*, 131, 29–41. <https://doi.org/10.1016/j.neuroimage.2015.11.031>
- Vivar, C., Potter, M. C., Choi, J., Lee, J. Y., Stringer, T. P., Callaway, E. M., Gage, F. H., Suh, H., & Van Praag, H. (2012). Monosynaptic inputs to new neurons in the dentate gyrus. *Nature Communications*, 3(2012). <https://doi.org/10.1038/ncomms2101>
- Walter, J. T., Alviña, K., Womack, M. D., Chevez, C., & Khodakhah, K. (2006). Decreases in the precision of Purkinje cell pacemaking cause cerebellar dysfunction and ataxia. *Nature Neuroscience*, 9(3), 389–397. <https://doi.org/10.1038/nn1648>
- Wang, M., Bianchi, R., Chuang, S. C., Zhao, W., & Wong, R. K. S. (2007). Group I metabotropic glutamate receptor-dependent TRPC channel trafficking in hippocampal neurons. *Journal of Neurochemistry*, 101(2), 411–421. <https://doi.org/10.1111/j.1471-4159.2006.04377.x>
- Wang, Y., Chang, C.-F., Morales, M., Chiang, Y.-H., Harvey, B. K., Su, T.-P., Tsao, L.-I., Chen, S., & Thiernemann, C. (2003). Diadenosine tetraphosphate protects against injuries induced by ischemia and 6-hydroxydopamine in rat brain. *The Journal of Neuroscience*, 23(21), 7958–7965. <https://doi.org/10.1523/JNEUROSCI.2321-03.2003> [pii]
- Weigel, M. T., & Dowsett, M. (2010). Current and emerging biomarkers in breast cancer: Prognosis and prediction. *Endocrine-Related Cancer*, 17(4), 245–262. <https://doi.org/10.1677/ERC-10-0136>
- Weiss, R., Bitton, A., Ben Shimon, M., Elhaik Goldman, S., Nahary, L., Cooper, I., Benhar, I., Pick, C. G., & Chapman, J. (2016). Annexin A2, autoimmunity, anxiety and depression. *Journal of Autoimmunity*, 73, 92–99. <https://doi.org/10.1016/j.jaut.2016.06.011>
- Wickham, L., Duchaine, T., Luo, M., Nabi, I. R., & DesGroseillers, L. (1999). Mammalian Staufen Is a Double-Stranded-RNA- and Tubulin-Binding Protein Which Localizes to the Rough Endoplasmic Reticulum. *Molecular and Cellular Biology*, 19(3), 2220–2230. <https://doi.org/10.1128/MCB.19.3.2220>
- Winner, B., Regensburger, M., Schreglmann, S., Boyer, L., Prots, I., Rockenstein, E., Mante, M., Zhao, C., Winkler, J., Masliah, E., & Gage, F. H. (2012). Role of α -Synuclein in Adult Neurogenesis and Neuronal Maturation in the Dentate Gyrus. *Journal of Neuroscience*, 32(47), 16906–16916. <https://doi.org/10.1523/JNEUROSCI.2723-12.2012>
- Wong, K., Ren, X. R., Huang, Y. Z., Xie, Y., Liu, G., Saito, H., Tang, H., Wen, L., Brady-Kalnay, S. M., Mei, L., Wu, J. Y., Xiong, W. C., & Rao, Y. (2001). Signal transduction in neuronal migration: Roles of GTPase activating proteins and the small GTPase Cdc42 in the Slit-Robo pathway. *Cell*, 107(2), 209–221. [https://doi.org/10.1016/S0092-8674\(01\)00530-X](https://doi.org/10.1016/S0092-8674(01)00530-X)
- Wong, S. T., Athos, J., Figueroa, X. A., Pineda, V. V., Schaefer, M. L., Chavkin, C. C., Muglia, L. J., & Storm, D. R. (1999). Calcium-stimulated adenylyl cyclase activity is critical for hippocampus-dependent long-term memory and late phase LTP. *Neuron*, 23(4), 787–798. [https://doi.org/10.1016/S0896-6273\(01\)80036-2](https://doi.org/10.1016/S0896-6273(01)80036-2)
- Wong, S. T., Trinh, K., Hacker, B., Chan, G. C. K., Lowe, G., Gaggar, A., Xia, Z., Gold, G. H., & Storm, D. R. (2000). Disruption of the type III adenylyl cyclase gene leads to peripheral and behavioral anosmia in transgenic mice. *Neuron*, 27(3), 487–497. [https://doi.org/10.1016/S0896-6273\(00\)00060-X](https://doi.org/10.1016/S0896-6273(00)00060-X)
- Wu, C. L., & Melton, D. W. (1993). Production of a model for Lesch–Nyhan syndrome in hypoxanthine phosphoribosyltransferase-deficient mice. *Nature Genetics*, 3(3), 235–240. <https://doi.org/10.1038/ng0393-235>

- Wu, K. Y., Hengst, U., Cox, L. J., Macosko, E. Z., Jeromin, A., Urquhart, E. R., & Jaffrey, S. R. (2005). Local translation of RhoA regulates growth cone collapse. *Nature*, *436*(7053), 1020–1024. <https://doi.org/10.1038/nature03885>
- Xiao, C., Shim, J. H., Klüppel, M., Zhang, S. S. M., Dong, C., Flavell, R. A., Fu, X. Y., Wrana, J. L., Hogan, B. L. M., & Ghosh, S. (2003). Ecsit is required for Bmp signaling and mesoderm formation during mouse embryogenesis. *Genes and Development*, *17*(23), 2933–2949. <https://doi.org/10.1101/gad.1145603>
- Xie, Z., Moy, L. Y., Sanada, K., Zhou, Y., Buchman, J. J., & Tsai, L. H. (2007). Cep120 and TACCs Control Interkinetic Nuclear Migration and the Neural Progenitor Pool. *Neuron*, *56*(1), 79–93. <https://doi.org/10.1016/j.neuron.2007.08.026>
- Yadav, R., Gupta, S. C., Hillman, B. G., Bhatt, J. M., Stairs, D. J., & Dravid, S. M. (2012). Deletion of glutamate delta-1 receptor in mouse leads to aberrant emotional and social behaviors. *PLoS ONE*, *7*(3). <https://doi.org/10.1371/journal.pone.0032969>
- Yang, S., Lee, Y. J., Kim, J.-M., Park, S., Peris, J., Laipis, P., Park, Y. S., Chung, J. H., & Oh, S. P. (2006). A murine model for human sepiapterin-reductase deficiency. *American Journal of Human Genetics*, *78*(4), 575–587. <https://doi.org/10.1086/501372>
- Yang, Y., Cheng, X. R., Zhang, G. R., Zhou, W. X., & Zhang, Y. X. (2012). Autocrine motility factor receptor is involved in the process of learning and memory in the central nervous system. *Behavioural Brain Research*, *229*(2), 412–418. <https://doi.org/10.1016/j.bbr.2012.01.043>
- Yau, J. L. W., Rasmuson, S., Andrew, R., Graham, M., Noble, J., Olsson, T., Fuchs, E., Lathe, R., & Seckl, J. R. (2003). Dehydroepiandrosterone 7-hydroxylase CYP7B: Predominant expression in primate hippocampus and reduced expression in Alzheimer's disease. *Neuroscience*, *121*(2), 307–314. [https://doi.org/10.1016/S0306-4522\(03\)00438-X](https://doi.org/10.1016/S0306-4522(03)00438-X)
- Zhang, D., Qi, Y., Klyubin, I., Ondrejcek, T., Sarell, C. J., Cuello, A. C., Collinge, J., & Rowan, M. J. (2017). Targeting glutamatergic and cellular prion protein mechanisms of amyloid β -mediated persistent synaptic plasticity disruption: Longitudinal studies. *Neuropharmacology*, *121*, 231–246. <https://doi.org/10.1016/j.neuropharm.2017.03.036>
- Zhang, Q., Nishimura, D., Seo, S., Vogel, T., Morgan, D. A., Searby, C., Bugge, K., Stone, E. M., Rahmouni, K., & Sheffield, V. C. (2011). Bardet-Biedl syndrome 3 (Bbs3) knockout mouse model reveals common BBS-associated phenotypes and Bbs3 unique phenotypes. *Proceedings of the National Academy of Sciences*, *108*(51), 20678–20683. <https://doi.org/10.1073/pnas.1113220108>
- Zhao, C., Teng, E., Summers, R. J., Ming, G., & Gage, F. H. (2006). Distinct Morphological Stages of Dentate Granule Neuron Maturation in the Adult Mouse Hippocampus. *Journal of Neuroscience*, *26*(1), 3–11. <https://doi.org/10.1523/JNEUROSCI.3648-05.2006>
- Zhao, Y., Wang, Y., Yang, J., Wang, X., Zhao, Y., Zhang, X., & Zhang, Y. W. (2012). Sorting nexin 12 interacts with BACE1 and regulates BACE1-mediated APP processing. *Molecular Neurodegeneration*, *7*(1), 1–10. <https://doi.org/10.1186/1750-1326-7-30>
- Zheng, X., Boyer, L., Jin, M., Mertens, J., Kim, Y., Ma, L., Ma, L., Hamm, M., Gage, F. H., & Hunter, T. (2016). Metabolic reprogramming during neuronal differentiation from aerobic glycolysis to neuronal oxidative phosphorylation. *eLife*, *5*(JUN2016). <https://doi.org/10.7554/eLife.13374>
- Zhong, Y., Morris, D. H., Jin, L., Patel, M. S., Karunakaran, S. K., Fu, Y.-J., Matuszak, E. A., Weiss, H. L., Chait, B. T., & Wang, Q. J. (2014). Nrbf2 protein suppresses autophagy by modulating Atg14L protein-containing Beclin 1-Vps34 complex architecture and reducing intracellular phosphatidylinositol-3 phosphate levels. *The*

- Journal of Biological Chemistry*, 289(38), 26021–26037.
<https://doi.org/10.1074/jbc.M114.561134>
- Zhou, F., Liu, P. P., Ying, G. Y., Zhu, X. D., Shen, H., & Chen, G. (2013). Effects of Thioredoxin-1 on neurogenesis after brain ischemia/reperfusion injury. In *CNS Neuroscience and Therapeutics* (Vol. 19, Issue 3, pp. 204–205).
<https://doi.org/10.1111/cns.12051>
- Zhou, J. H., Zhang, T. T., Song, D. D., Xia, Y. F., Qin, Z. H., & Sheng, R. (2016). TIGAR contributes to ischemic tolerance induced by cerebral preconditioning through scavenging of reactive oxygen species and inhibition of apoptosis. *Scientific Reports*, 6(1), 27096. <https://doi.org/10.1038/srep27096>
- Zou, Y., Jiang, W., Wang, J., Li, Z., Zhang, J., Bu, J., Zou, J., Zhou, L., Yu, S., Cui, Y., Yang, W., Luo, L., Lu, Q. R., Liu, Y., Chen, M., Worley, P. F., & Xiao, B. (2014). Oligodendrocyte Precursor Cell-Intrinsic Effect of Rheb1 Controls Differentiation and Mediates mTORC1-Dependent Myelination in Brain. *Journal of Neuroscience*, 34(47), 15764–15778. <https://doi.org/10.1523/JNEUROSCI.2267-14.2014>
- Zou, Yixiao, Stagi, M., Wang, X., Yigitkanli, K., Siegel, C. S., Nakatsu, F., Cafferty, W. B. J., & Strittmatter, S. M. (2015). Gene-Silencing Screen for Mammalian Axon Regeneration Identifies Inpp5f (Sac2) as an Endogenous Suppressor of Repair after Spinal Cord Injury. *Journal of Neuroscience*, 35(29), 10429–10439. <https://doi.org/10.1523/JNEUROSCI.1718-15.2015>

List of abbreviations

AD	<i>Alzheimer's disease</i>	LTP	<i>Long-term potentiation</i>
AF	<i>Alexa Fluor</i>	MAP2	<i>Microtubule-associated protein 2</i>
Aldh1l1	<i>Aldehyde dehydrogenase 1 family member L1</i>	mTOR	<i>mammalian target of rapamycin</i>
BMC	<i>Biomedical Center Munich</i>	NeuN	<i>Neuronal nuclei</i>
CA	<i>Cornu ammonis</i>	NG2	<i>Neural/glial antigen 2</i>
Cy	<i>Cyanine</i>	NSCs	<i>Neural stem cells</i>
DAPI	<i>4',6-Diamidino-2-Phenylindole</i>	PBS	<i>Phosphate buffered saline</i>
DCX	<i>Doublecortin</i>	PD	<i>Parkinson's disease</i>
ddH ₂ O	<i>Double-distilled water</i>	PFA	<i>Paraformaldehyde</i>
DG	<i>Dentate gyrus</i>	Pum1	<i>Pumilio 1</i>
EtOH	<i>Ethanol</i>	Pum2	<i>Pumilio 2</i>
EPA	<i>Enhanced physical activity</i>	RBP	<i>RNA-binding protein</i>
GFAP	<i>Glial fibrillary acidic protein</i>	RGC	<i>Radial glial cell</i>
GFP	<i>Green fluorescent protein</i>	Rgs4	<i>Regulator of G protein signaling 4</i>
GO	<i>Gene ontology</i>	RhoA	<i>Ras homolog family member A</i>
GT	<i>Gene trap</i>	RMS	<i>Rostral migratory stream</i>
HD	<i>Huntington's disease</i>	RNP	<i>ribonucleoparticles</i>
HPA	<i>Hypothalamic-pituitary-adrenal</i>	RT	<i>Room temperature</i>
IPC	<i>Intermediate progenitor cells</i>	SGZ	<i>Subgranular zone</i>
KEGG	<i>Kyoto encyclopedia of genes and genomes</i>	Stau2	<i>Staufen 2</i>
LTD	<i>Long-term depression</i>	SVZ	<i>Subventricular zone</i>
		YFP	<i>Yellow fluorescent protein</i>

List of figures

Figure 1: Adult neurogenesis in mice. Sagittal sections showing a mouse brain including two regions with adult neurogenesis: the dentate gyrus (DG) and the subventricular zone (SVZ). Upper part: magnification of the DG; lower part: five distinct stages of adult hippocampal neurogenesis (see text for details). Abbreviations: ML, molecular layer; GZ, granular zone; SGZ, subgranular zone; CA, cornu ammonis. Own illustration, figure inset based on Ming et al., 2011.	8
Figure 2: Five stages of adult hippocampal neurogenesis including DCX + stages (see text for details). Abbrev.: GZ, granular zone; SGZ, subgranular zone; DCX, doublecortin. Own illustration, based on Ming et al., 2011.	9
Figure 3: Experimental outline. Mice without (10W, n=5) or with (13W, n=5) exposure to running wheel. Abbrev.: W, weeks; (Figure modified from Frey et al., 2020)..	17
Figure 4: Schematic representation showing the experimental workflow for immunohistochemistry performed on WT and <i>Stau2^{GT}</i> mice. Abbrev.: W, weeks.	18
Figure 5: Schematic representation showing the experimental workflow for microdissection followed by mass spectrometry performed on WT mice. Abbrev.: W, weeks.	18
Figure 6: Experimental scheme indicating the chosen subdivision of the hippocampus into dorsal and ventral sections.	19
Figure 7: Ventral and dorsal mice brain slices mounted on one microscope slide for immunostaining. Abbrev.: DH, dorsal hippocampus; VH, ventral hippocampus (Figure modified from Frey et al., 2020).....	21
Figure 8: Confocal microscopy imaging an entire dorsal dentate gyrus by selecting each time six tile scans. Abbrev.: DG, dentate gyrus. (Figure modified from Frey et al., 2020).....	21
Figure 9: Representative example of a DCX-positive (DCX+) cell body and its dendritic arbor in the subgranular zone of the DG. (Figure modified from Frey et al., 2020).	22
Figure 10: Tissue preparation of brain slices for microdissection. In total, five slices were mounted per microscope slide, every second one was processed for microdissection (indicated as systematic sampling in the figure; Figure modified from Frey et al., 2020).....	23
Figure 11: Manual selection of either dorsal (top) or ventral (bottom) hippocampal brain slices. All brain slices between these representative sections were collected and processed for microdissection of either the dorsal (top) or ventral hippocampus (bottom). Representative pictures of the brain slices taken with a Leica DM2500	

bright-field microscope equipped with a DMC2900 CMOS camera (Bioimaging Facility BMC, Munich, Germany). Abbrev.: DH, dorsal hippocampus; VH, ventral hippocampus. (Figure modified from Frey et al., 2020). 23

Figure 12: Microdissection and collection of hippocampal subregions (DG, CA3, CA1) from either the dorsal or the ventral hippocampus. Abbrev.: DH, dorsal hippocampus; VH, ventral hippocampus, DG, dentate gyrus; CA, cornu ammonis; (Figure modified from Frey et al., 2020)..... 24

Figure 13: Experimental outline defining either the upregulation (**A**) or the downregulation (**B**) of low abundant proteins in test mice upon running compared to control mice (each group n=5). Abbrev.: W, weeks. 25

Figure 14: Immunostaining of the ventral DG of a WT control mouse using DAPI (nuclear marker), Ki-67 (proliferation marker) and DCX (marking immature neurons).... 28

Figure 15: Absolute number of Ki-67+ cells in the dorsal (left panel) or ventral (right panel) dentate gyrus of either 10-week-old WT or *Stau2^{GT}* mice. Ki-67+ cell bodies located in the dentate gyrus subgranular and granular zone were counted; n=3 for both dorsal or ventral hippocampus, ns (not significant). 29

Figure 16: Number of revolutions of running wheel and day/night distribution of its use. In total, five WT mice used two wheels for a time period of three weeks. ***P < 0.001. 30

Figure 17: DCX staining of the dorsal dentate gyrus of WT mice with (13 weeks) or without running (10 weeks). Immunostaining shows intensive staining pattern of DCX+ cells and dendrites upon running (indicated as post-running). Magnified confocal images highlight DCX+ adult-born neurons in the SGZ. Black-white image conversion of the original data. Abbrev.: W, weeks; Hil, hilus; DG, dentate gyrus; SM, stratum moleculare; SGZ, subgranular zone; GZ, granular zone; Scale bar 150µm, 15µm (inset); (Figure modified from Frey et al., 2020)..... 31

Figure 18: Quantification of DCX+ stained neurons and their dendrites in the dorsal dentate gyrus of WT aged 10 weeks (10W) and 13 weeks (13W) post-running (Figure modified from Frey et al., 2020)..... 32

Figure 19: Comparison of absolute numbers of DCX+ cell bodies and dendrites from the dorsal dentate gyrus of either 10 week (10W, n=5) old or 13 week old mice that have not been exposed to the running wheel (13W-RW, n=2). Abbrev.: W, weeks; RW, running wheel. (Figure modified from Frey et al., 2020)..... 33

Figure 20: DCX staining of the ventral dentate gyrus of WT mice with (13 weeks) or without access to running wheels (10 weeks). Immunostaining shows an intensive staining pattern of DCX+ cells and dendrites upon running (indicated as post-running). Magnified confocal images highlight DCX+ adult-born neurons in the subgranular zone. Black-white image conversion. Abbrev.: W, weeks; Hil, hilus;

DG, dentate gyrus; SM, stratum moleculare; SGZ, subgranular zone; GZ, granular zone; Scale bar 150 μ m, 15 μ m (inset); (Figure modified from Frey et al., 2020).. 34

Figure 21: Quantification of DCX+ stained neurons and their dendrites in the ventral dentate gyrus of WT aged 10 weeks (10W) and 13 weeks (13W) post-running (Figure modified from Frey et al., 2020)..... 35

Figure 22: Comparison of absolute numbers of DCX+ cell bodies and dendrites from the ventral dentate gyrus of either 10 week (n=5) old or 13 week old mice (n=2) that have not been exposed to the running wheel. Abbrev.: W, weeks; RW, running wheel. (Figure modified from Frey et al., 2020). 36

Figure 23: Immunostaining of a representative hippocampal section of glial-labeled mouse brains with GFP and Stau2..... 38

Figure 24: DCX staining of the dorsal DG of Stau2^{GT} mice with (13 weeks) or without access to running wheels (10 weeks). Immunostaining shows no increase in either DCX+ cells nor dendrites upon running. Magnified confocal images highlight DCX+ adult-born neurons in the SGZ. Black-white image conversion..... 39

Figure 25: Quantification of DCX+ stained neurons and their dendrites in the dorsal dentate gyrus of Stau2^{GT} mice aged 10 weeks (10W) and 13 weeks (13W) upon running..... 40

Figure 26: DCX staining of the ventral dentate gyrus of Stau2^{GT} mice with (13 weeks) or without running (10 weeks). Immunostaining shows no difference in the amount of DCX+ cells upon running, with a slight increase in dendritic branching. Magnified confocal images highlight DCX+ adult-born neurons in the SGZ. Black-white image conversion..... 42

Figure 27: Quantification of DCX immunostaining in the ventral DG of Stau2^{GT} mice aged 10W and 13W post-running;..... 43

Figure 28: Venn diagram representation of the proteins identified in the DG, CA3 and CA1 region, respectively, of either the dorsal or ventral hippocampus of control and test mice. This diagram only includes proteins that were detected in all 57 samples (3 subregions per hippocampus, one dorsal and one ventral hippocampus per mice, 2 experimental groups including each 5 mice leading to 60 samples in total, excluding 3 samples that could not be detected by mass spectrometry). The number of proteins with an adjusted p value lower than 0.20 were considered to be significantly changed after EPA. (Figure modified from Frey et al., 2020). 45

Figure 29: Volcano plot to visualize the proteomic change upon EPA. Mostly, proteins were found to be upregulated upon voluntary running. The plot shows $-\log_2 p$ values versus the \log_2 fold change. Proteins in black indicate those with an adjusted p value < 0.20 (n=70); individually selected proteins are shown in red (n=20, see text for details); (Figure modified from Frey et al., 2020)..... 45

Figure 30: KEGG pathways that are significantly enriched in the upregulated proteome (n=62) of mice upon running. Abbrev.: FDR, false discovery rate; (Figure modified from Frey et al., 2020). 47

Figure 31: Differential distribution of low abundant proteins in either the DG, CA3 or CA1 of the dorsal hippocampus: light-grey bars mark the number of downregulated proteins (left part), dark-grey bars reflect the number of upregulated proteins (right part). Abbrev.: DG, dentate gyrus; CA, cornu ammonis. 51

Figure 32: Venn diagram showing the subregion-specific distribution of upregulated proteins with minimal overlap in the dorsal hippocampus. Abbrev.: DG, dentate gyrus; CA, cornu ammonis. 52

Figure 33: Differential distribution of proteins in either the DG, CA3 or CA1 of the ventral hippocampus: light-grey bars mark the number of downregulated proteins (left part, negative absolute numbers), dark-grey bars reflect the number of upregulated proteins (right part, positive absolute numbers). Abbrev.: DG, dentate gyrus; CA, cornu ammonis. 56

Figure 34: Venn diagram showing the subregion-specific distribution of upregulated proteins with minimal overlap in the ventral hippocampus. 57

Figure 35: Venn diagrams showing differentially expressed upregulated proteins of either the dorsal (DH) or ventral hippocampus (VH) in the different subregions: DG, CA3 and CA1. First, the regions vary regarding the number of upregulated proteins. Second, an overlap can only be found in the CA regions, however, this effect is small (n=3 and n=5). 62

Figure 36: Simplified scheme showing the candidate protein RhoA during cytoskeleton remodeling. Interestingly, RhoA and its downstream effector Profilin-2, of the indicated signaling proteins were detected by mass spectrometry, indicated by bold arrows. 66

List of tables

Table 1: List of buffers and solutions.....	14
Table 2: List of primary and secondary antibodies and nuclear staining used for immunohistochemistry, Abbrev.: AF, Alexa Fluor.....	14
Table 3: Cellular component analysis of significantly upregulated proteins (n=62) in test mice upon EPA. Abbrev.: FDR, false discovery rate.....	46
Table 4: Significantly downregulated proteins in test mice upon running. Fold change <1 implies downregulation. Abbrev.: FC, fold change; Adj.P, adjusted p value.	47
Table 5: Manual selection of upregulated proteins with implication in neuronal, growth or apoptotic processes (n=17). Specific functional implication was individually researched; Fold change >1 indicates an upregulation.....	48
Table 6: Biological processes of significantly upregulated proteins (n=146) in the dorsal hippocampus upon EPA. Abbrev.: FDR, false discovery rate.	50
Table 7: KEGG pathways of significantly upregulated proteins (n=146) in the dorsal hippocampus of test mice upon EPA. Abbrev.: FDR, false discovery rate.....	51
Table 8: Manual selection of upregulated proteins in the DG of the dorsal hippocampus with implications in growth, apoptotic or neuronal processes or locomotory behavior (n=11).	52
Table 9: Manual selection of upregulated proteins in the CA3 region of the dorsal hippocampus with implications in growth, apoptotic or neuronal processes or locomotory behavior (n=18).....	53
Table 10: Manual selection of upregulated proteins in the CA1 region of the dorsal hippocampus with implications in growth, apoptotic or neuronal processes or locomotory behavior (n=18).....	54
Table 11: Biological processes of significantly upregulated proteins (n=87) in the ventral hippocampus upon EPA. Abbrev.: FDR, false discovery rate.	55
Table 12: KEGG pathways of significantly upregulated proteins (n=87) in the ventral hippocampus of test mice upon running. Abbrev.: FDR, false discovery rate.....	56
Table 13: Manual selection of upregulated proteins in the DG of the ventral hippocampus with implications in growth, apoptotic or neuronal processes or locomotory behavior (n=9).	57
Table 14: Manual selection of upregulated proteins in the CA3 region of the ventral hippocampus with implications in growth, apoptotic or neuronal processes or locomotory behavior (n=13).....	58
Table 15: Manual selection of upregulated proteins in the CA1 region of the ventral hippocampus with implications in growth, apoptotic or neuronal processes or locomotory behavior (n=13).....	59

Danksagung

Mein Dank gilt zu allererst Herrn Prof. Dr. Kiebler für die engagierte fachliche Betreuung und Beratung und die Überlassung des Themas dieser Arbeit.

Von Herzen danke ich Herrn Dr. Bastian Popper und Herrn Rico Schieweck für die allumfassende Betreuung, Motivationsgabe und unendliche Geduld.

Ich bedanke mich zudem bei allen Mitarbeitern der Arbeitsgruppe sowie den kooperierenden Arbeitsgruppen am BMC für die sehr gute Zusammenarbeit und den wertvollen interdisziplinären Austausch.

Zuletzt gilt mein besonderer Dank meinen Eltern und meinem Bruder, die mich stets inspirieren, motivieren und ohne die ich nicht die wäre, die ich bin.

Eidesstattliche Erklärung

Ich, Surina Alisha Louisa Frey, erkläre hiermit an Eides statt, dass ich die vorliegende Dissertation mit dem Titel

The role of the RNA-binding protein Staufen2 and the effects of physical activity on adult hippocampal neurogenesis

selbständig verfasst, mich außer der angegebenen keiner weiteren Hilfsmittel bedient und alle Erkenntnisse, die aus dem Schrifttum ganz oder annähernd übernommen sind, als solche kenntlich gemacht und nach ihrer Herkunft unter Bezeichnung der Fundstelle einzeln nachgewiesen habe.

Ich erkläre des Weiteren, dass die hier vorgelegte Dissertation nicht in gleicher oder in ähnlicher Form bei einer anderen Stelle zur Erlangung eines akademischen Grades eingereicht wurde.

München, den 11.05.2021

.....

Ort, Datum

Surina Alisha Louisa Frey

.....

Surina Alisha Louisa Frey